ELEMENTA
Science of the Anthropocene

Ishino, S, et al. 2026. The biogenic sulfur cycle in the coupled ocean–sea ice–atmosphere system. *Elem Sci Anth*, 14: 1.
DOI: https://doi.org/10.1525/elementa.2025.00067

REVIEW

The biogenic sulfur cycle in the coupled ocean—sea ice—atmosphere system

Sakiko Ishino[1,*], Megan D. Willis[2,*], Hélène Angot[3], Thorsten Bartels-Rausch[4], Odile Crabeck[5], Bruno Delille[5], Erin Dunne[6], Emily Franklin[6], Antoine Haddon[7], Hakase Hayashida[8], Sankirna D. Joge[9,10], Rémy Lapere[3,11], Hyung-Gyu Lim[12], Anoop S. Mahajan[9], Marc D. Mallet[13], George Manville[14], Louis Marelle[11], Daiki Nomura[15], Kerri A. Pratt[16], Ilka Peeken[17], Ruth Price[3], Rafel Simó[18], Jacqueline Stefels[19], Jennie L. Thomas[3], Cort L. Zang[2], and Nadja Steiner[7,20,*]

Polar oceans and sea-ice regions are global hot spots for the production of biogenic volatile methylated sulfur (VMS) compounds: dimethyl sulfide (DMS) and methanethiol (MeSH). VMS compounds make important contributions to atmospheric particle formation and cloud property modulation, especially when polar atmospheres are pristine. As a result, the polar biogenic sulfur cycle may induce significant climate feedback in response to ongoing sea ice decline. However, polar VMS production, emission, and atmospheric oxidation processes remain poorly represented in current numerical models, hampering assessments of their radiative impacts and, in turn, implementation of targeted observations necessary for providing predictive understanding of changes in the ocean–sea ice–atmosphere (OIA) system. We synthesize current knowledge of the polar biogenic sulfur cycle and its representation in models. To untangle the existing gaps and provide a roadmap toward predictive understanding, we identify key features of sea ice habitats for biological VMS production, sea ice physical features that enhance or suppress VMS emissions, and atmospheric VMS oxidation at low temperatures that controls the contribution of oxidation products to particle formation or growth. These features are tightly coupled, emphasizing the need for coordinated efforts across disciplines that span the OIA interface, and among observational, experimental, and modeling communities. We recommend 4 priority research areas: (1) model representation of biological VMS production at the sea ice bottom and surface; (2) improved quantification of cloud condensation nuclei (CCN) sensitivity to VMS emissions with updated gas phase and multiphase oxidation chemistry at low temperatures; (3) better spatial and seasonal quantification of MeSH abundance

[1] Institute of Nature and Environmental Technology, Kanazawa University, Japan
[2] Department of Chemistry, Colorado State University, Fort Collins, CO, USA
[3] Université Grenoble Alpes, CNRS, INRAE, IRD, Grenoble INP, IGE, Grenoble, France
[4] Laboratory of Atmospheric Chemistry, Paul Scherrer Institut, Villigen PSI, Switzerland
[5] Chemical Oceanography Unit, FOCUS, University of Liege, Liege, Belgium
[6] Environment Research Unit, Commonwealth Scientific and Industrial Research Organization, Victoria, Australia
[7] School of Earth and Ocean Sciences, University of Victoria, Victoria, BC, Canada
[8] Application Laboratory, Japan Agency for Marine-Earth Science and Technology, Yokohama, Japan
[9] Indian Institute of Tropical Meteorology, Ministry of Earth Sciences, Pune, India
[10] Department of Atmospheric and Space Sciences, Savitribai Phule Pune University, Pune, India
[11] LATMOS/IPSL, Sorbonne Université, UVSQ, CNRS, Paris, France
[12] Korea Institute of Ocean Science and Technology, Busan, South Korea
[13] Australian Antarctic Program Partnership, Institute for Marine and Antarctic Studies, University of Tasmania, Hobart, Tasmania, Australia
[14] Program in Atmospheric and Oceanic Sciences, Princeton University, Princeton, NJ, USA
[15] Hokkaido University, Hakodate, Hokkaido, Japan
[16] Department of Chemistry and Department of Earth & Environmental Sciences, University of Michigan, Ann Arbor, MI, USA
[17] Alfred Wegener Institute Helmholtz-Zentrum für Polar- und Meeresforschung, Bremerhaven, Germany
[18] Institut de Ciències del Mar, ICM-CSIC, Barcelona, Catalonia, Spain
[19] The Groningen Institute of Evolutionary Life Sciences, University of Groningen, Groningen, the Netherlands
[20] Institute of Ocean Sciences, Fisheries and Oceans Canada, Sidney, BC, Canada

* Corresponding authors:
Emails: ishino-sakiko@se.kanazawa-u.ac.jp; megan.willis@colostate.edu; nadja.steiner@dfo-mpo.gc.ca

and its biological and chemical controls in sea-ice environments; and (4) assessment of the contribution of episodic extreme VMS emissions during sea ice breakup for the polar CCN budget.

Keywords: Volatile methylated sulfur (VMS), Dimethyl sulfide (DMS), Methanethiol (MeSH), Biogeochemistry, Arctic Ocean, Southern Ocean, Sea ice, Aerosol and clouds

1. Introduction

Biogenic volatile methylated sulfur (VMS) compounds, largely dimethyl sulfide (DMS) and methanethiol (MeSH), are key contributors to the polar aerosol population during biologically active seasons (Leaitch et al., 2013; Quinn et al., 2017; Fossum et al., 2018; McCoy et al., 2021; Wohl et al., 2024). The specific conditions existing in polar regions drive strong VMS production compared to global oceans (e.g., Levasseur, 2013; Wohl et al., 2024). In particular, sea ice plays an important dual role in the biogenic sulfur cycle: on the one hand, it provides a habitat for prolific VMS-producing microorganisms and, on the other, it can exert a capping effect on sea-to-air VMS emissions. Specific microbial communities thrive in and around sea ice, leading to blooms within, beneath, and at the edge of sea ice (Trevena and Jones, 2006; Levasseur, 2013; Stefels et al., 2018), as well as accumulations in Arctic melt ponds (Abbatt et al., 2019; Park et al., 2019) and Antarctic surface slush layers (Zemmelink et al., 2008a; Nomura et al., 2012; van Leeuwe et al., 2022) during the spring and summer. This results in elevated seawater biogenic sulfur concentrations (Levasseur, 2013; Jarníková and Tortell, 2016; Stefels et al., 2018; Webb et al., 2019; Lizotte et al., 2020; Wohl et al., 2024) compared to the global average. DMS concentrations more than twice as high as the most frequently used climatology (i.e., Lana et al., 2011) are often observed in polar regions, particularly in the marginal ice zone (MIZ) of coastal Antarctica (Jarníková and Tortell, 2016; Webb et al., 2019) and the Canadian Arctic Archipelago (Abbatt et al., 2019; Lizotte et al., 2020). In addition to these episodes and local patches of elevated DMS, emerging global understanding of biogenic sulfur cycling through both DMS and MeSH (e.g., Lawson et al., 2020; Novak et al., 2022; Wohl et al., 2024) points to a potentially key contribution of MeSH to VMS in polar regions (e.g., Gros et al., 2023), with important implications for polar atmospheric oxidizing capacity and the aerosol population (Wohl et al., 2024). However, MeSH is not yet considered in most models.

Critically, polar atmospheres are frequently characterized by low background atmospheric particle concentrations and low air temperatures, which together provide favorable conditions for new particle formation (NPF; the conversion of gases into nanometer-sized particles) (Kerminen et al., 2018). Notably, NPF events and subsequent particle growth associated with VMS oxidation products are frequently observed over the MIZ in both Arctic (Park et al., 2017; Beck et al., 2021) and Antarctic (Jokinen et al., 2018; Baccarini et al., 2021; Brean et al., 2021) regions, during biologically active seasons. These studies underscore the substantial role of VMS emissions from sea-ice environments in influencing the polar cloud condensation nuclei (CCN) budget. However, the relative importance of VMS compared to non-biogenic-sulfur (e.g., Ghahreman et al., 2016; Jongebloed et al., 2023a; Jongebloed et al., 2023b), and non-sulfur (e.g., Schmale and Baccarini, 2021; Tatzelt et al., 2022; Kojoj et al., 2024), particle sources remains unquantified due to limitations in our process-level understanding of VMS production, emission and atmospheric fate, and associated challenges in numerical model representation (Schmale et al., 2021; Mallet et al., 2023; Mallet et al., 2025).

The polar biogenic sulfur cycle is poised to undergo significant changes in response to ongoing anthropogenic warming. As the Arctic experiences rapid sea-ice retreat, the biologically active and VMS-rich sea ice margins are expected to shift poleward and significantly increase the biogenic sulfur supply to the atmosphere, as the summer season lengthens and becomes ice-free (Galí et al., 2019; Rolph et al., 2020). Sea-ice retreat and associated biological shifts (Hayward et al., 2025) are also emerging in Antarctica since 2015 (World Meteorological Organization, 2025). Given that Antarctic sea ice is approximately 85% first-year ice, this implies a reduction in spatial coverage of the MIZ with yet unknown consequences for VMS emissions. However, the complexity of VMS production processes and emissions from sea-ice environments, together with their fine spatial and temporal scales, presents significant challenges in incorporating these processes into Earth System Models (ESMs) and understanding the potential climate feedbacks. Even the latest ESMs treat sea ice simply as a barrier for sea-to-air DMS emissions and do not account for biological DMS production within sea ice (e.g., Bock et al., 2021; Fung et al., 2022) nor do they account for oceanic or sea-ice MeSH production, emission and subsequent impacts on the atmospheric aerosol population and oxidizing capacity (Wohl et al., 2024; Tashmim et al., 2025). The regional climatic consequences of a shift in atmospheric VMS emission, whether it acts as a positive or negative feedback, remain largely uncertain due to our poor knowledge of the CCN formation potential of DMS and MeSH in conjunction with other aerosol sources and removal processes (Browse et al., 2014; Ridley et al., 2016; Gilgen et al., 2018; Mahmood et al., 2019). This range of challenges complicates the development of fully coupled models that include biogenic sulfur across the ocean–sea ice–atmosphere (OIA) system.

Motivated by both the sensitivity of polar cloud properties to available aerosol (e.g., Mauritsen et al., 2011; Leaitch et al., 2013; Mallet et al., 2023; Mallet et al., 2025) and the large potential of sea ice and polar oceans

for VMS production, we review current knowledge of the polar biogenic sulfur cycle and explore potential approaches for adequately incorporating it into large-scale models. Throughout, we highlight key features that must be represented in models across scales (Section 2, **Figure 1**, and **Table 1**). Building on current knowledge,

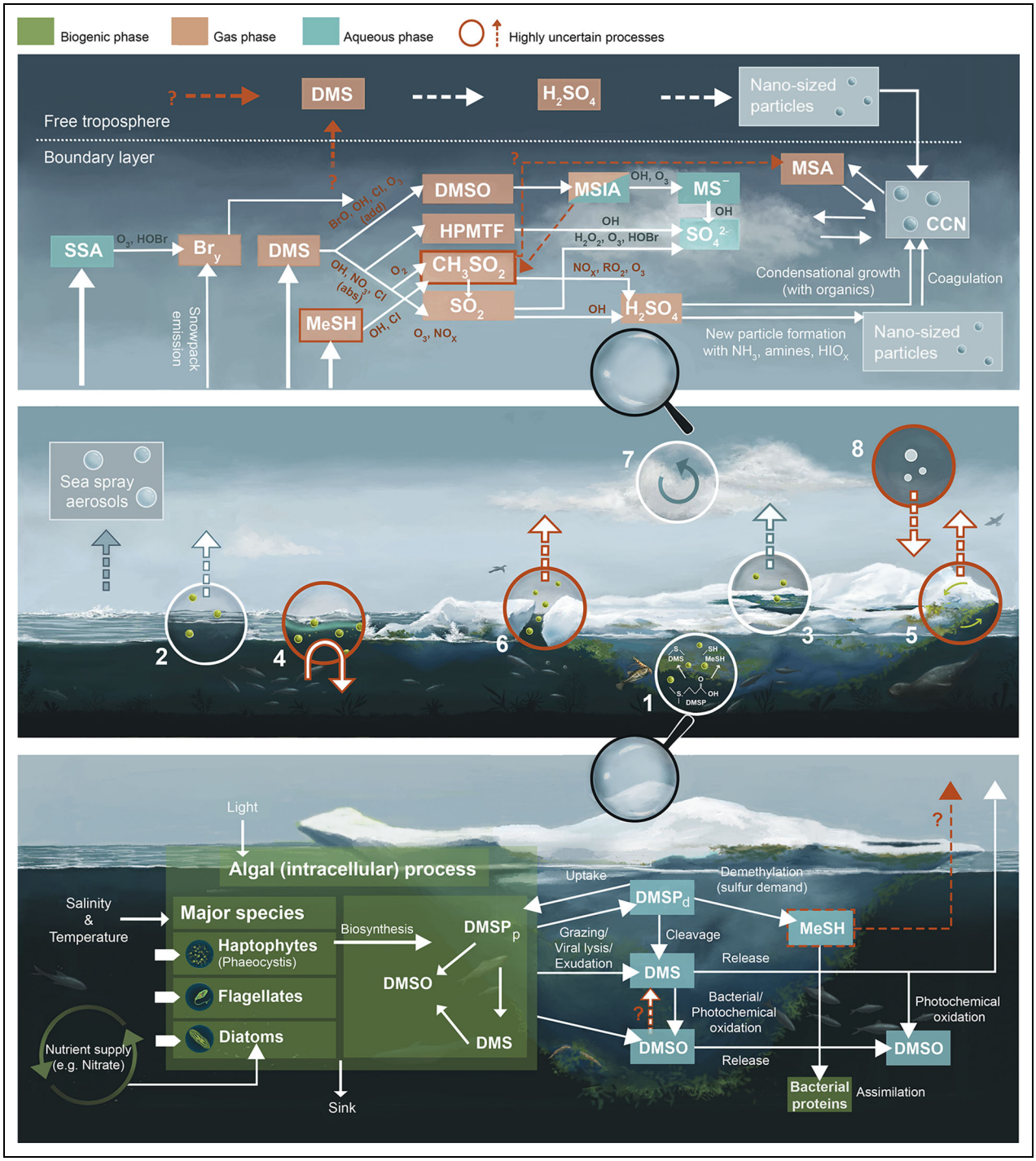

Figure 1. Summary of the biogenic sulfur cycle in the coupled ocean–sea ice–atmosphere (OIA) system. The middle panel shows the overview of key processes: (1) Biological production of DMSP and subsequent conversion into VMS at the top, bottom, or under sea ice, (2) sea-to-air emission of VMS, (3) production and emission of VMS through melt ponds, (4) inhibition or delay of VMS emission by meltwater layers, (5) release of VMS from surface slush layer to ocean or atmosphere (ice-to-air emission), (6) episodic VMS emission from leads or at the edge of sea ice, (7) atmospheric VMS oxidation through different gas- and multiphase pathways and subsequent new particle formation and growth, and (8) new particle formation in the free troposphere and subsequent intrusion to the boundary layer. Bottom and top panels expand (1) and (7), respectively, for the detailed biological and chemical processes. Green, red, and blue boxes indicate the species in biogenic-, gas-, and aqueous-phase, respectively. Red arrows indicate highly uncertain processes or species.

Table 1. Potential future changes in VMS production, emission, and aerosol number concentrations in polar regions

# in Figure 1	Process	Potential change (+/–)	Key Uncertainties	Section
1	Biological production of DMSP and conversion to VMS at the bottom or surface, or under, sea ice	***Production:*** +/– Higher temperature, enhanced light due to thinner, less sea ice, and changes in nutrient supply will impact the whole community structure.	• Bipolar differences and changes in seasonality. • Drivers of MeSH versus DMS yields. • Compensating effects of thinning and retreat of sea ice. • Potential for abrupt shifts in plankton communities.	2.1
2	Sea-to-air flux of VMS	***Emission:*** + Higher temperature, wind speed, and open water area as a result of sea ice loss will enhance fluxes.	• Realistic sea ice projection. • Damping or enhancing effects of sea ice on sea-to-air fluxes.	2.1, 2.2
3	Production and emission of VMS through melt ponds	***Production and emission:*** +/– Higher temperature will lead to more melt ponds while reduction of multiyear ice may decrease melt pond area. Thinner ice and increased melt may allow for bottom intrusions of salt water, increasing production.	• Relative importance of this source. • Variability of melt ponds that enhance and suppress biological activity.	2.1
4	Inhibition or delay of sea-to-air VMS fluxes by meltwater layers	***Emission:*** +/– Higher temperature will induce more meltwater input to the ocean surface which can suppress emissions.	• Outcome as temporal delay, regional change or overall suppression.	2.1, 2.2
5	Release of VMS from surface slush layers into ocean or atmosphere (ice-to-air emissions)	***Production and emission:*** +/– Thinner, more fragile ice cover and higher wind/wave states may make surface intrusions of seawater more likely and increase abundance of slush layers.	• Importance of ice surface communities to seawater VMS compared to bottom- and under-ice communities. • Magnitude of potential ice-to-air VMS emission fluxes.	2.1, 2.2
6	Sporadic emission of VMS from leads and marginal ice zones	***Emission:*** + The increase of first-year ice, higher wind speeds and thinner sea ice will increase leads/crack coverage.	• Relative importance of sporadic versus sustained emissions. • Impact on the CCN budget.	2.2, 2.4
7	Atmospheric VMS oxidation through competing gas phase and multiphase pathways	***VMS-driven aerosol number production:*** +/– Potential increase in low cloud and fog fraction, and duration of open water area, may lead to enhanced multiphase chemical processing.	• Accurate multiphase reaction rates of multiphase competing gas phase reactions, and their dependence on environmental conditions.	2.3

Table 1. *(continued)*

# in Figure 1	Process	Potential change (+/−)	Key Uncertainties	Section
			• Impact of supercooled liquid and cloud ice on multiphase reactions. • Outcome of multiphase reactions for VMS-to-CCN sensitivity. • Impact of potentially enhanced condensation sink from increased sea spray aerosol production. • Shift in seasonality of VMS emission and overlap with reactive halogen production in response to earlier sea ice and snow melt.	
8	New particle formation in the free troposphere and subsequent intrusion to the polar marine boundary layer	***VMS-driven aerosol number production:*** +/− Potential enhancement of extratropical cyclones may enhance transport of NPF precursors to the free troposphere, and subsequently the importance of this process for boundary layer aerosol.	• Contribution of sea-ice-sourced VMS to free troposphere NPF and growth. • Relative importance of free troposphere and boundary layer NPF and growth. • Changes in boundary layer meteorology (e.g., stability, wind speed, precipitation) in response to warming.	2.4
9 (Figure 3)	Autumn phytoplankton blooms in sea-ice regions	***Production and emission:?***	• Magnitude of autumn VMS emissions from accumulated biomass. • Importance relative to other freeze-up related aerosol precursor emissions (e.g., iodine).	2.1
10 (Figure 3)	Biological production in platelet ice	***Production and emission:?***	• Efficiency of VMS production (i.e., DMSP/Chl-*a* ratio) from platelet ice communities.	2.1

we outline key difficulties and prospective approaches for representing the sulfur cycle in coupled OIA models (Section 3) and provide recommendations for future work (Section 4). We note that the marine biogenic sulfur cycle has been reviewed by Hopkins et al. (2023) from a global perspective. However, their work does not provide a complete and accurate analysis of atmospheric VMS contribution to aerosol formation and growth, the radiative effects (REs) of VMS-sourced aerosols relative to that of anthropogenic aerosols, and their global and regional impacts on climate. We address this gap through a focus on polar-specific processes in the biogenic sulfur cycle and synthesis of current knowledge on atmospheric processes and impacts.

2. Key features of marine biogenic sulfur cycle in polar regions

2.1. Production and fate of biogenic sulfur in polar oceans and sea ice

2.1.1. Dissolved VMS production and loss processes

The main origin of VMS in the pelagic ocean is dimethylsulfoniopropionate (DMSP), a cellular compatible solute

produced by micro- and macroalgae, bacteria, and corals, where it plays important ecophysiological roles such as osmoregulant, cryoprotectant, antioxidant and energy overflow buffer (Stefels et al., 2007; Li et al., 2024a). Quantitatively and according to current knowledge, phytoplankton are the main global DMSP producers, resulting in intracellular concentrations ranging from a few µmol L^{-1} to hundreds of mmol L^{-1} (Stefels et al., 2007). DMSP is ubiquitously distributed across the global surface ocean, with the highest regional concentrations occurring in the polar regions (Galí et al., 2015). The production of DMSP is highly species-specific, whereby the Haptophytes and Dinoflagellates are major producers, and diatoms are minor producers (Stefels et al., 2007). But under circumstances in which very high diatom biomasses are created, such as at the underside of sea ice in spring and summer, the DMSP concentration can also become extremely high, even though these concentrations normalized to chlorophyll-*a* are not particularly high (Kirst et al., 1991; Levasseur et al., 1994; Tison et al., 2010; **Figure 1**). High DMSP/Chl-*a* ratios are often found in surface-ice communities around Antarctica, where ratios of several hundred mmol g^{-1} are associated with haptophyte communities as determined by pigment compositions (Tison et al., 2010; Stefels et al., 2012).

Although the species composition is the main driver of the DMSP distribution, abiotic conditions within the ice may also favor the production of DMSP. The role of DMSP as an osmoregulator is especially important in a habitat where brine salinities vary from almost zero, when snow and ice melt in spring, to 3 times seawater salinity during winter. However, direct field data are very limited. During time-series measurements in the western Weddell Sea, a correlation was observed between the DMSP/Chl-*a* ratio and the calculated brine salinity in the upper 12.5 cm of the ice cover where *Phaeocystis* (Haptophytes) were dominant, suggesting a role as osmoregulator or cryoprotectant (Tison et al., 2010). Additionally, laboratory experiments on selected species show that DMSP content increases with increasing salinity (e.g., Stefels, 2000; Lyon et al., 2011). Other stress factors like light have not been investigated in great detail. In general, light levels in and at the underside of ice are lower than in open surface water and DMSP production is expected to respond similarly to growth. On the other hand, Galindo et al. (2016) showed a strong reduction of DMSP production due to UV radiation when samples were exposed to surface-level irradiance, although this also may have been the result of an overall reduction in growth (Bach et al., 2025).

The role of algae within the sulfur cycle is not limited to the production of DMSP. Some are capable of converting DMSP to DMS. Haptophytes and Dinophytes are well known for their DMSP-lyase activity, which may facilitate the release of DMS or DMSP from the cell when physiological conditions require it to do so (Stefels, 2000). DMSP inside the cell may also function as a radical scavenger for reactive oxygen species, which would among others result in the production of dimethyl sulfoxide (DMSO). Likewise, DMS inside the cell may be readily converted to DMSO by oxygen radicals under oxidative stress conditions. However, this is very difficult to prove since both compounds, DMS and DMSO, are highly membrane permeable. In addition, algae may take up DMSP from their surroundings (Vila-Costa et al., 2006), which was suggested to support autotrophs in the energy-poor polar winter (Ruiz-González et al., 2012). The exact function of this mechanism is still unclear. In experiments with the diatom *Thalassiosira weissflogii*, the DMSP uptake rate rather appeared to be related to the growth rate than to the salinity applied (Petrou and Nielsen, 2018).

DMSP inside algal cells ($DMSP_p$) can be released to the environment through sloppy feeding by zooplankton, cell lysis or excretion (**Figure 1**). By convention, once released, this DMSP is called dissolved DMSP ($DMSP_d$). Zooplankton grazing in sea ice mainly occurs at the underside where algal biomass is highest and $DMSP_p$ may be released depending on the grazer (Kasamatsu et al., 2004). However, during the spring melt, when brine channels open, few copepod species are capable of invading brine channels (Schnack-Schiel et al., 2008), where they graze on sympagic algae and also potentially release $DMSP_d$ into the brine. Cell lysis can be either the result of viral attack or autolysis due to extreme stress conditions, such as salinity changes. There is limited experimental evidence of the salinity range that sea-ice algae can withstand. Generally, a range between 5‰ and 100‰ is considered (Arrigo, 2014), but many ice diatoms appear incapable of growing at salinities above 60‰–70 ‰ (Grant and Horner, 1976). When algae are subject to downshifts of salinity due to ice melt, an active excretion of DMSP has been observed (A Webb, personal communication, 25/05/2025).

Another key role in sea ice is played by bacteria, which are known to be larger and more abundant compared to those in the water column, likely caused by the high concentrations of labile dissolved organic substances in the brine channels (Boetius et al., 2015). Similar to algae, bacteria are also capable of producing ice-binding or antifreeze proteins, allowing them to survive the extreme and varying temperature and salinity changes throughout the annual cycle of sea ice (see Boetius et al., 2015, for more details). In these environments, $DMSP_d$ is readily available for uptake, whereby DMSP is used as carbon or reduced sulfur sources, especially in oligotrophic environments, where a lack of energy favors the use of already reduced compounds for assimilation into cellular constituents. There are 2 major biotic pathways: (1) cleavage by phytoplankton and bacteria, to facilitate carbon assimilation and production of DMS, which can then be converted in various ways (see below); and (2) demethylation by bacteria, which facilitates sulfur assimilation and produces MeSH through an intermediate demethiolation process (e.g., Moran and Durham, 2019; Kiene et al., 2000; Kiene and Linn, 2000; Lawson et al., 2020; Shaw et al., 2022; Hopkins et al., 2023). The efficiency of the DMSP-to-DMS cleavage pathway is highly variable and depends both on the available $DMSP_d$ concentration and the activity of the consumers. Due to the energetic benefits and the relatively economic way to assimilate reduced sulfur, Kiene et al. (2000) proposed that bacterioplankton may derive

their total sulfur demand from the demethylation pathway, leaving only the leftover $DMSP_d$ for conversion to DMS. In this scenario, the fraction of $DMSP_d$ converted to DMS depends on the biomass and activity of the bacterial community.

The majority of $DMSP_d$ is converted in the demethylation/demethiolation pathway, with exceptions found in bloom situations and under high UV regimes, when bacterial activity is reduced (Simó, 2001). Although the intermediate compound of the demethylation pathway, MeSH, is rapidly consumed through assimilation into cells (i.e., in sulfur-containing amino acids; Kiene et al., 1999; Sun et al., 2016), some fraction may be released into the environment (Wohl et al., 2024) and subsequently either converted through abiotic reactions with dissolved organic matter and mineral particles (Flöck and Andreae, 1996; Kiene, 1996) or emitted to the atmosphere (Novak et al., 2022). Overall, the MeSH consumption rate is likely higher than for DMS, resulting in a shorter lifetime for MeSH (minutes to hours) than DMS (hours to days; Kiene, 1996; Kiene and Linn, 2000). Several functional groups of polar and sea ice phytoplankton and bacteria possess the enzymatic ability to convert DMSP to both DMS and MeSH (Bowman et al., 2014; Teng et al., 2021), but there is no data on actual conversion rates in sea-ice ecosystems. We lack experimental studies measuring both DMS and MeSH cycling process rates with polar-relevant species and communities under polar conditions (i.e., within sea ice brines at in situ conditions). This hinders our ability to predict the distribution of dissolved VMS compounds in sympagic environments, though key information may be alternatively obtained by measurements of concentration ratios (i.e., DMS/DMSP, MeSH/DMSP, MeSH/DMS) in sea ice brines. Although a genetic study has suggested that plankton in polar waters are particularly prone to VMS production (Teng et al., 2021), the question of which biogeochemical processes control the apparent spatial and sea surface temperature (SST) dependence of MeSH/VMS (**Figure 2a**) remains open.

DMSP can also be intracellularly oxidized to dimethylsulfoxonium propionate (DMSOP) by both microalgal and bacterial DMSP producers (Thume et al., 2018), yet this is estimated to contribute to only a small proportion of DMSP degradation. Released DMSOP is subsequently metabolized by bacteria to DMSO. The majority of DMSO is, however, derived from the bacterial oxidation of DMS by widespread monooxygenases (Hopkins et al., 2023) and from photooxidation of DMS, with high rates of photooxidation observed in high-nitrate Antarctic waters (Toole and Siegel, 2004). DMSO is a major pool of dissolved methylated sulfur in the ocean (Simó and Vila-Costa, 2006) and can be regarded as a sink for DMS: in temperate coastal waters, >94% of DMSO is dissimilated to CO_2 (Dixon et al., 2020). The conversion of DMSO to DMS by algal, bacterial, and archaeal DMSO reductases (McCrindle et al., 2005; Spiese et al., 2009) is an important pathway in anoxic sediments, when DMSO competes with oxygen as an electron acceptor. However, in oxygenated surface waters, this process is estimated to account for a minor proportion of DMS production (Dixon et al., 2020). High DMSO reduction rates were observed in brine and slush samples from Antarctic sea ice that contained extremely high concentrations of DMSO (Asher et al., 2011). The similar DMS consumption rates in these samples—including photooxidation that yields DMSO—are somewhat puzzling, and there might be methodological issues. Whether or not low oxygen concentrations due to potentially deteriorated organic material in brines play a role might be worth investigating. Asher et al. (2011) suggest that a rapid redox cycling between DMS and DMSO plays a role in photoprotective mechanisms of Antarctic microbes, but evidence is still lacking.

2.1.2. Spatial and temporal variability of VMS in polar oceans and sea ice

Owing to differences in geography and seasonal meteorological characteristics, the distribution of primary producers and the associated sulfur cycling in sea-ice environments differ substantially between the Arctic and Antarctic (**Figure 3**). In general, the return of sunlight after winter triggers the production of DMSP-producing microalgae, mainly at the underside of sea ice (**Figure 1**; Levasseur, 2013). In autumn, algae can get encapsulated in newly formed ice and get frozen-in over winter. Sea-ice melt during summertime results in the release of algae and their sulfur compounds to the surrounding seawater, often triggering under-ice and/or ice-edge blooms with DMS concentrations 1 or 2 orders of magnitude higher compared to the global annual mean surface seawater DMS of 2–3 nmol L^{-1} (Zemmelink et al., 2005; Galí and Simó, 2010; Levasseur, 2013; Webb et al., 2019; Galí et al., 2021; section 3.2 in Hulswar et al., 2022). The timing of the blooming phase, the distribution of algae and associated sulfur compounds in the ice, and the magnitude of the pools and processes, however, vary substantially between the Arctic and Antarctic.

In the Arctic, high-latitude winter darkness results in ice growth containing almost no primary producers, followed in early spring by growth of ice algal biomass, mainly diatom species, in the bottom-layer ice (e.g. Levasseur et al., 1994; Galindo et al., 2014). This bottom-ice algal growth results in an L-shaped chlorophyll-*a* and DMS(P) distribution through the sea-ice column over spring and summer (**Figure 3**), which is well characterized in Canadian Arctic Archipelago landfast ice (Levasseur, 2013). Release of these bottom-ice communities in melt periods can trigger development of under-ice pelagic blooms (Galindo et al., 2014) that are accompanied by elevated seawater $DMSP_p$ concentrations up to approximately 200 nmol L^{-1}. This is higher than those observed in the ice-free zone over the shallow continental shelves during summer, ranging from 10 to 80 nmol L^{-1} $DMSP_p$ (Matrai et al., 2007; Li et al., 2017). However, the spatial distributions and seasonality in the Central Arctic differ widely from coastal regions with shallow continental shelves as reviewed in Levasseur (2013). In general, DMS and DMSP concentrations in the Central Arctic Ocean are low, typically <1 nmol L^{-1} and <10 nmol L^{-1}, respectively (Uhlig et al., 2019), even in summertime. Elevated DMS and DMSP concentrations in the Central Arctic Ocean are

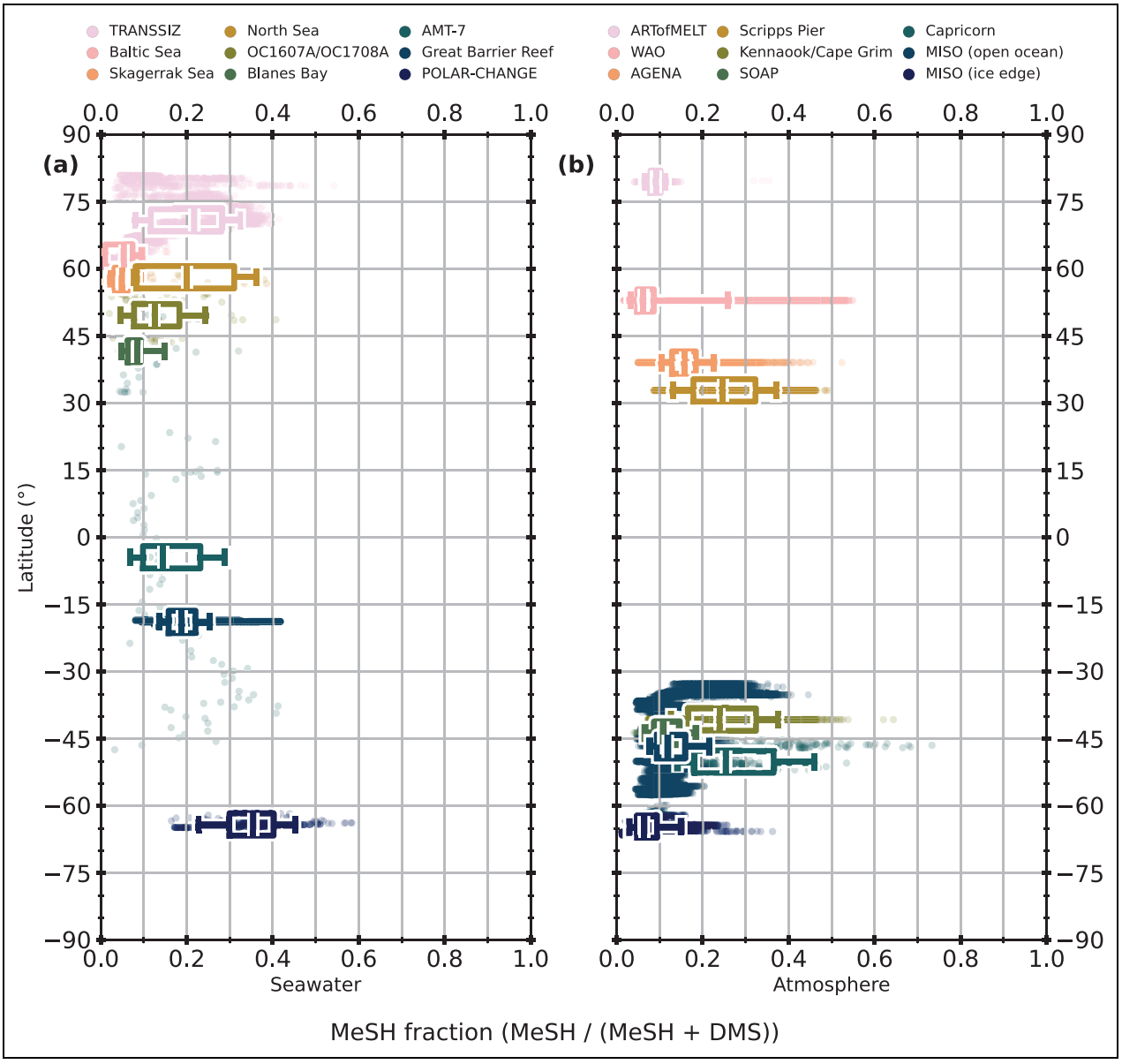

Figure 2. Compilation of fractional MeSH contribution to VMS (DMS + MeSH) in available simultaneous (a) seawater and (b) atmospheric measurements. (a) Seawater measurements include TRANSSIZ (Norwegian Sea and Svalbard Archipelago, May 2015, R/V *Polarstern*), OC1607A (sub-Arctic Northeast Pacific, July 2016, R/V *Oceanus*), OC1708A (sub-Arctic Northeast Pacific, August 2017, R/V *Oceanus*), AMT-7 (Atlantic Ocean spanning from England to Falkland Islands, September–October 1998, RRS *James Clark Ross*), Blanes Bay (Mediterranean Catalan Coast, 2022, Blanes Bay Microbial Observatory), Great Barrier Reef (Central Great Barrier Reef, December 2021, R/V *Guardian* and February 2022, R/V *Guardian* & R/V *Magnetic*), POLAR-CHANGE (Antarctic Peninsula and Weddell Sea, February–March 2023, BIO R/V *Hesperides* A-33), and Baltic, Kattegat/Skagerrak, and North Seas (July 1988, Helicopter Sampling). (b) For comparison between observations with a range of detection limits, atmospheric measurements include observations with DMS > 25 ppt_v and MeSH > 15 ppt_v, representing the upper limit for reported detection limits. Datasets include WAO (Norfolk, England, United Kingdom, May–June 2024, Weybourne Atmospheric Observatory), AGENA (Graciosa Island, Azores, Portugal, June–July 2022, ENA ARM Research Facility), SOAP (Chatham Rise, Pacific Ocean, February–March 2012, R/V *Tangaroa*), CAPRICORN (Southern Ocean south of Tasmania, March–April 2016, R/V *Investigator*), Scripps Pier (San Diego, California, USA, September 2019, Ellen Browning Scripps Memorial Pier), Kennaook/Cape Grim (Northwestern Tasmania, August–December 2023, April–May 2024, Kennaook/Cape Grim Baseline Air Pollution Station), MISO (Southern Ocean and Antarctic ice edge, January–March 2024, R/V *Investigator*), and ARTofMELT (Arctic Ocean in the Fram Strait, May–June 2023, I/B *Oden*). The latitude of the box plot is the median latitude of the corresponding dataset. Whiskers are at 10th and 90th percentiles. Box extents and line represent the 25th, 50th, and 75th percentiles. Corresponding latitudinal distribution in absolute DMS and MeSH concentrations are shown in Figure S1.

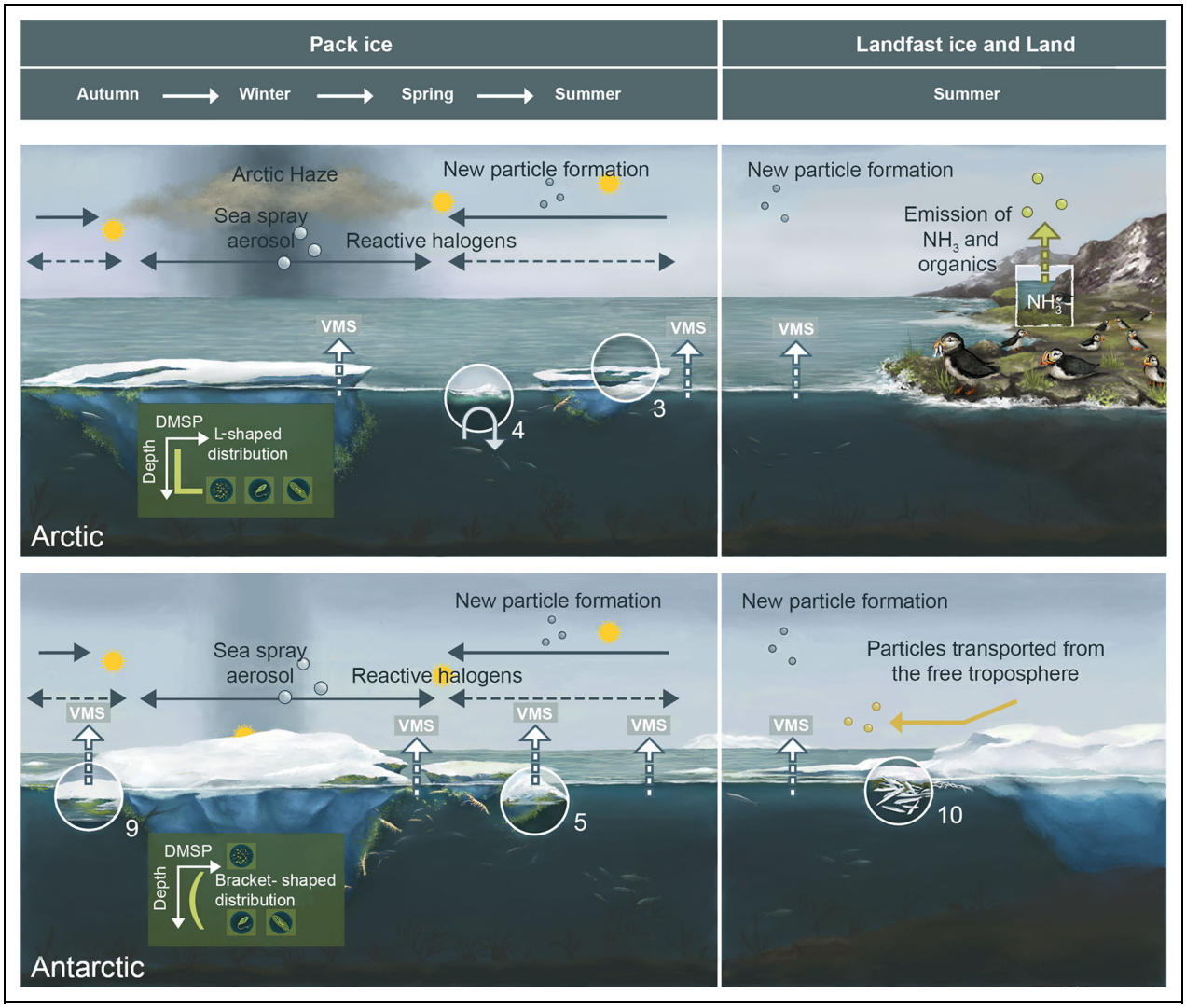

Figure 3. Differences in biogenic sulfur cycles in the Arctic (top) and Antarctic (bottom). The vertical white line distinguishes between the pack ice (left) and the landfast ice (right). Two key processes of polar biogenic sulfur cycle in addition to those in **Figure 1** are described: biological production associated with (9) autumn blooms and (10) platelet ice under glacial ice. The horizontal arrows in the left panel indicate the approximate seasons of features exhibiting significant contribution to atmospheric particle number concentrations. The dotted line for sea spray aerosol indicates its persistent contribution throughout the year but with decreased magnitude during summer compared to winter. Note that the figure is to emphasize the features dominant in one pole compared to the other, and most of the features illustrated in the figure commonly exist in both poles. See texts in Sections 2.1 and 2.4 for the description of each process of sea-ice biogeochemistry and atmospheric particle formation, respectively.

associated with Atlantic water inflow or with the breakup of sea ice in the MIZ of the Eurasian basin (Uhlig et al., 2019). In particular, the development of blooms of the haptophyte *Phaeocystis* sp. results in significantly increased DMS(P) concentrations (Matrai et al., 2008; Uhlig et al., 2019).

Melt ponds are a key feature of Arctic sea ice in the melt season (**Figures 1** and **3**). Although there have been a few reports of modestly elevated DMS(P) concentrations in melt ponds around the Canadian Arctic Archipelago (Gourdal et al., 2018), this observation was associated with rare seawater intrusion, and therefore brackish conditions, introducing the necessary cells to form DMS(P). In contrast, melt ponds in the Central Arctic harbored fresh or strongly stratified waters with reduced DMS(P) levels near the surface due to a dilution effect with snow and sea-ice meltwater (Smith et al., 2023). In freshwater melt ponds, primary production is extremely low due to nutrient limitation and a lack of seeding phytoplankton cells. Stratified waters within leads and along the ice edge impacted by meltwater also showed reduced DMS(P) concentrations relative to the underlying waters (**Figures 1** and **3**; Galí and Simó, 2010; Smith et al., 2023). During the MOSAiC campaign in the Central Arctic Ocean, high accumulation of biomass was observed at the interface between surface meltwater and seawater in melt ponds and leads, with relatively high DMS(P) concentrations (Smith et al., 2023) suggesting a potential to release DMS to the

atmosphere when the stratification is broken by mixing through wind-induced ice floe drift. However, since the DMSO pool made up approximately two-thirds of the total DMS(O+P) pool, (photo-)oxidation might be an important sink for DMS in these high-Arctic regions (A Webb, personal communication, 25/05/2025).

In Antarctic sea ice, considerable ice algal growth is often observed at the surface, in between snow and ice, in addition to the predominant bottom-ice communities. This arises from high snow loading on Antarctic sea ice, which can result in negative freeboard leading to flooding and consequent saline slush layers including infiltration of nutrients and phytoplankton from the seawater. Widespread surface communities in both Antarctic landfast and pack ice (Meiners et al., 2012; Meiners et al., 2018) are dominated by Haptophyte flagellate species with notoriously strong DMS(P) production (van Leeuwe et al., 2018; van Leeuwe et al., 2022; **Figure 3**). In addition, when the physical conditions allow, the twilight of Antarctic winter, due to the presence of sea ice at lower latitudes than that in the Arctic, can drive early growth of surface-layer communities. Together with bottom-ice communities, these surface-slush communities result in a C-shaped vertical distribution of algal biomass and DMS(P) throughout the sea-ice column (Tison et al., 2010; Vancoppenolle et al., 2013; **Figure 3**). During ice breakup and melt, large amounts of these surface communities are released to the surrounding seawater and seed subsequent pelagic blooms (Trevena and Jones, 2006; Stefels et al., 2018; Webb et al., 2019). This can result in a surface microlayer with strongly elevated algal biomass and more than 10 times higher DMS(P) concentrations (Zemmelink et al., 2005; Zemmelink et al., 2008b) than the underlying ocean. During a 5-year time series of DMS(P) in Ryder Bay, West Antarctic Peninsula, extreme peaks of DMS up to 100 nmol L^{-1} were observed during spring ice melt, when the aerial coverage of sea ice was 20%–40% (Webb et al., 2019). In addition, direct measurements of high DMS emission fluxes from the sea ice in the Weddell Sea suggest that these surface communities can lead to DMS emission through the snow above, not only through the release to seawater (Zemmelink et al., 2008a; Section 2.2).

An important feature of the biogenic sulfur cycle around Antarctica is the ice-associated phytoplankton blooms in autumn, with extremely high biomass consisting of *Fragilariopsis* (diatoms) and *Phaeocystis* (Haptophytes) species (Lieser et al., 2015). Late summer and autumn blooms in pack ice have been described for the Weddell and the Ross Sea (Fritsen et al., 1994; Fritsen et al., 2001). A similar bloom was observed by DeJong et al. (2017) in Terra Bay in the Ross Sea with up to 6 times higher particulate organic carbon (POC) concentrations in the slush ice compared to the water column. They observed band-like structures of frazil ice with actively growing algae over time, which were even visible from satellites. They attribute these late autumn blooms to strong katabatic winds, which prevent the formation of consolidated ice and allow phytoplankton to concentrate in newly forming frazil ice at the ocean surface, and also enhance the nutrient input from deeper waters (DeJong et al., 2017). DeJong et al. (2018) further showed that this colored frazil ice is present in 11 of the 13 sea ice producing polynyas, pointing out a major importance of this phenomenon in biogeochemical cycles across coastal Antarctica. Importantly, dominance of the strong DMS producer *Phaeocystis* was found in surface pancake blooms during a cruise to the Eastern Weddell Sea in March 2021 (Hellmer and Holtappels, 2021). Given that time series of atmospheric DMS concentration show a second peak in March at several Antarctic measurement stations (Preunkert et al., 2007; Read et al., 2008; see Section 2.4.2 for more details), the phenomenon of sea-ice-associated, DMSP-producing algal blooms in autumn deserves focused observations.

A hidden, and largely understudied, pool of sulfur compounds is found in the highly concentrated biomass observed within platelet ice. Platelet ice is derived from basal melt of ice shelves, when frazil-ice crystals form due to super cooling, rise toward the surface and become trapped at the underside of the adjacent sea-ice cover. There, the platelets become incorporated into growing sea ice, or form dense layers of platelet ice, sometimes many meters thick, with important impact on physical, biological, and biogeochemical properties (Hoppmann et al., 2020). High algal biomass can be formed in the sub-ice platelet layers just under the sea ice and in the bottom section of the sea ice itself. Although light levels are low in this habitat, the ample supply of nutrients from the underlying seawater and the protection against large grazers provide an environment in which low-light adapted algae can grow excessively. Peak accumulation of >6,000 mg chlorophyll-*a* m^{-3} has been reported for sub-ice platelet layers in McMurdo Sound (Arrigo et al., 1995) and of 1,000–3,000 mg chlorophyll-*a* m^{-3} in Atka Bay (I Peeken, personal communication, 14/01/2026). When using a DMSP/Chl-*a* conversion factor of 4 (mmol g^{-1}) for diatoms (Stefels et al., 2007), this would correspond to $DMSP_p$ concentrations of 24 and 4–12 μmol L^{-1}, respectively, which would be the highest concentration ever observed in any habitat. In another study in McMurdo Sound—and in the absence of sub-ice platelet layers—incorporated platelets appeared to impact the distribution of algal species and hence the DMSP vertical profile of sea ice (Carnat et al., 2014). DMSP maxima in the ice interior were observed, associated with the occurrence of dinoflagellates that were assumed to be incorporated with the platelet crystals. These layers had typical DMSP/Chl-*a* ratios of >100 mmol g^{-1}. Given the potential importance of these high-biomass platelet ecosystems as a source of DMS upon ice breakup, these systems need urgent attention.

A final remark in this section concerns the limited dissolved MeSH measurements, with orders of magnitude less data than for DMS, both globally and in polar regions (**Figure 2**). These data show higher contribution of MeSH to total VMS (MeSH + DMS) at lower sea surface temperatures (SST < 8°C) and toward higher latitudes (Kettle et al., 2001; Gros et al., 2023; Wohl et al., 2024), though observations are severely limited in sea-ice covered regions. For

example, in the Atlantic Arctic, MeSH concentrations north of 60°N were 22% (median) of total VMS, with contributions up to 50% at the highest latitudes near sea-ice covered regions (Gros et al., 2023). Around the Antarctic Peninsula and the Weddell Sea, MeSH concentrations were 35% (median) of total VMS (Wohl et al., 2024). While dissolved MeSH/VMS from the limited available measurements fall into a relatively narrow range (<0.1 to ~0.35; **Figure 2a**), these fractional abundances of MeSH arise from widely variable absolute concentrations of MeSH and DMS (Figure S1). Using the limited available data (see Figure S2 for data coverage), constructions of global ocean fields of MeSH concentrations and emissions revealed important contributions of MeSH to the VMS flux to the atmosphere, especially over the Southern Ocean, south of 40°S (**Figure 2**; Wohl et al., 2024). Given the challenges of quantifying MeSH, owing to its conversion to dimethyl disulfide (DMDS) on metal surfaces (e.g., Perraud et al., 2016; Kilgour et al., 2022), the frequent lack of direct calibration standards (e.g., Gros et al., 2023), use of unit mass resolution proton-transfer reaction mass spectrometers (PTR-MS; Kilgour et al., 2022), and potential for rapid production rates from damaged cells in unfiltered samples and through on-board pumping systems, existing MeSH measurements should still be considered with some caution. Despite these measurement uncertainties, available observations in surface oceans point to a potentially important contribution of MeSH to the polar reduced sulfur budget, even though it lacks sufficient spatial and seasonal constraint, especially in sea-ice influenced environments.

In summary, to comprehensively model the polar marine biogenic sulfur cycle in numerical models, several key features must be represented, including bottom-ice, under-ice, and surface-slush microbial communities, as well as ice-associated pelagic phytoplankton blooms in the MIZ, and their consequences for VMS formation. Further, characterization of algal assemblages in terms of at least functional groups will facilitate more accurate representations of VMS production processes. Some specific features including platelet ice production and secondary autumn blooms require further observational evidence before incorporation into models. Finally, while existing measurements highlight the potentially significant contribution of MeSH to VMS in polar regions, very little is known about MeSH consumption and production by sea ice communities, which limits our ability to implement MeSH production and exchange into models and fully predict the impact of biogenic sulfur cycling on polar atmospheres. The status and difficulties of representing this polar specific sulfur biogeochemistry in ESMs are further detailed in Section 3.1.

2.2. Ice-sea-air fluxes of VMS

Both DMS and MeSH are persistently supersaturated across the global ocean, driving a sea-to-air flux (Lawson et al., 2020; Novak et al., 2022; **Figure 1**). Sea-to-air DMS fluxes are typically estimated using (i) a gas transfer velocity and (ii) the air-sea concentration gradient (Nightingale et al., 2000; Lana et al., 2011; Stanley and Bell, 2025). The gas transfer velocity is affected by various chemical and physical factors, including gas diffusivity, wind speed, breaking waves, bubble formation, mixed layer depth, and the presence of sea surface surfactants (Goldman et al., 1988; Bell et al., 2017; Stanley and Bell, 2025). In general, higher fluxes occur at higher wind speeds (e.g., Joge et al., 2024b); however, direct DMS flux measurements have revealed a less enhanced gas transfer, relative to CO_2, at medium to high wind speeds (>10 m s^{-1}; Bell et al., 2017). This phenomenon is attributed to differences in bubble-mediated transport (highly soluble DMS being less affected by bubbles compared to CO_2), as well as the influence of surfactants (Zavarsky et al., 2018), aspects now accounted for in recent representations of the air–sea flux (Stanley and Bell, 2025). The air-sea concentration gradient is often simply approximated by the concentration of DMS in near-surface seawater (Lana et al., 2011; see details in Section 3.2 for data-based seawater DMS concentration estimates). This approximation considers a negligible atmospheric concentration of DMS, or very small compared to that in equilibrium with the aqueous concentration, assuming rapid dispersion once emitted. It should be noted, however, this approximation may be inadequate for high DMS emissions and shallow atmospheric boundary layers, such as in polar regions, and will lead to an overestimation of the flux (Steiner and Denman, 2008).

DMS and MeSH have similar diffusion coefficients (1.22×10^{-5} cm^2 s^{-1} and 1.56×10^{-5} cm^2 s^{-1}, respectively; Gharagheizi, 2012) and Henry's law solubilities at 298 K (0.39 M atm^{-1} and 0.54 M atm^{-1}, respectively; Przyjazny et al., 1983; Burkholder et al., 2019; Sander, 2023) such that their dissolved concentration ratio may be indicative of the sea-air flux ratio (Johnson, 2010; Bange et al., 2024). However, owing to the applicable temperature range of the recommended Henry's law solubility for MeSH (i.e., 298–368 K; Burkholder et al., 2019), it is currently unclear whether the ratio of DMS and MeSH Henry's law constants remains constant at temperatures relevant to polar ocean sea-air exchange. Uncertainties in both DMS and MeSH recommended Henry's law constants are significant (i.e., a factor of 10 to a factor of 100, according to Burkholder et al., 2019), such that improved solubility measurements will be beneficial to improved flux estimates. Concentrations of MeSH in near-surface seawater have been estimated globally with a SST-dependent scaling to a DMS climatology (Section 3.2; Wohl et al., 2024), with potentially significant uncertainty in sea-ice environments. Still, applying this scaling yields the highest predicted fluxes of MeSH from sub-Arctic, Arctic, and Southern Oceans regions, together with high DMS fluxes (Wohl et al., 2024).

In polar regions, sea ice plays important roles for modulating air-sea gas exchange processes (e.g., Willis et al., 2023). In the ocean partly covered with sea ice, VMS emission is often scaled to the fraction of open water (Watts et al., 2022), assuming that sea ice acts as a complete barrier to gas exchange (i.e., a "capping" effect). In approximations of fluxes based on data-based or modeled seawater DMS concentration fields, a common practice involves using a mask that aligns with the sea-ice zone to eliminate

DMS emissions or concentrations in sea-ice regions (e.g., Wang et al., 2020; Hulswar et al., 2022; Wohl et al., 2024; Section 3.3). However, this assumption contains uncertainty because sea ice can also participate in gas exchange in 3 key ways: (1) suppression or enhancement of sea-to-air gas transfer velocity due to the presence of sea ice (e.g., Loose et al., 2017; Prytherch and Yelland 2021; No. 2 of **Figure 1**); (2) inhibition or enhancement of sea-to-air gas emissions by surface meltwater layers (Zemmelink et al., 2005; Smith et al., 2023; No. 5 of **Figure 1**); and (3) direct gas emissions from ice-atmosphere interface (e.g., Zemmelink et al., 2008a; Nomura et al., 2012; Delille et al., 2014; No. 6 of **Figure 1**).

First, sea ice can affect the gas transfer velocity (e.g., Willis et al., 2023). Briefly, the presence of sea ice can produce unique turbulence due to shear in the ice-water boundary layer (McPhee and Martinson, 1994), buoyant convection (Loose et al., 2017; Prytherch and Yelland, 2021), and/or modifications to the wave field by fetch reduction and the dampening action of sea ice (Loose et al., 2017; Loose et al., 2024), resulting in either suppression or enhancement of gas transfer velocity. Prytherch and Yelland (2021) conducted eddy covariance CO_2 flux measurements at a large lead in the Arctic to find an average decrease of gas transfer velocity by 30%, with some increase observed at wind speeds between 2 and 6 m s^{-1}. Loose et al. (2024) evaluated numerical model estimates of gas transfer velocity for long-lived compounds such as CO_2 during the MOSAiC campaign by in situ measurements of turbulent kinetic energy, and these estimates reasonably reproduced this trend of sea-air exchange suppression with enhancement only at low wind speeds. These effects are governed by dampened wave activity due to fetch reduction, with relatively weak effects of additional turbulence induced by sea ice at low winds speeds (Prytherch and Yelland, 2021). However, the localized effect of turbulence could be important for air–sea exchange of short-lived compounds such as DMS given the heterogeneity of its concentration both in the ocean and atmosphere. In addition, the mechanisms and response of DMS gas transfer velocity could be different from that of CO_2 given their different wind dependency (Bell et al., 2017; Blomquist et al., 2017). These effects require validation through direct sea-air flux measurements of DMS, preferably together with MeSH, both of which are notably scarce in sea-ice regions.

Second, meltwater layers can have a strong effect on air-sea gas exchange. Sea ice and snow melt in spring to summer provides low-salinity meltwater to the ocean surface. This meltwater influx may be localized, for example, associated with melt ponds, in leads, or at the sea-ice edge (Zemmelink et al., 2005; Smith et al., 2023), and may cause either enhancement or inhibition of sea-to-air gas emission. In the Central Arctic, Smith et al. (2023) found significantly lower salinity water (<10‰ compared to 34‰ in seawater) at the surfaces of melt ponds and leads, associated with significantly lower DMS(P) concentrations (<5 nmol L^{-1}) than in the underlying water, implying a potential role of meltwater inhibiting DMS emission. However, this remains a hypothesis to be tested because Smith et al. (2023) also observed high accumulation of biomass at the interface between surface meltwater and seawater, which supports high DMS(P) concentrations and a potential release of DMS to the atmosphere when stratification is broken (see Section 2.1.2). On the other hand, in 2 different leads in the Weddell Sea, Antarctica, Zemmelink et al. (2005) found strong stratification at the top surface (0.2 cm) due to the meltwater with low salinity (ca. 27‰), which was associated with high DMS concentration up to 50 nmol L^{-1} due to in situ production and supply from sea ice, indicating enhanced DMS emission from meltwater. This suggests that there may be key differences based on the origin and release process of the DMSP or DMS: if produced by ice algae and released with the low-salinity meltwater, the incurring stratification may concentrate high DMS within the melt layer and cause higher emissions; if produced by pelagic phytoplankton or released from ice algae before formation of the meltwater layer, DMS may remain trapped below (Galí and Simó, 2010; Haddon et al., 2025).

Third, ice-to-air direct emissions may be important for VMS emission. While sea ice is often referred to as a barrier for air–sea exchange, it is a porous medium characterized by a network of brine channels and inclusions forming an exchange pathway to the atmosphere and the underlying seawater. Studies on CO_2 fluxes (e.g., Delille et al., 2014; Nomura et al., 2018; Prytherch et al., 2024) showed that the sea ice is often permeable to gas exchange during the spring, coinciding with algal blooms and peak concentration of sulfur compounds in sea ice. The DMS produced in sea ice can either be transported downward to underlying seawater by brine convection and flushing or move upward into the ice column by diffusion and bubble buoyancy (Gourdal et al., 2019). Once the DMS reaches the upper surface layers of sea ice, it can be directly exchanged with the atmosphere depending on the ice surface conditions. While the milder temperatures in the spring favor the permeability to gas, the presence of superimposed ice (Delille et al., 2014), snow ice, or snow cover can significantly alter the emission of gases. So far, observations of air-ice DMS fluxes are scarce, only 3 studies directly or indirectly quantified DMS fluxes from sea ice, and all reported emissions of DMS. In Weddell Sea, Antarctica, Zemmelink et al. (2008a)used the relaxed eddy accumulation (REA) technique to report rather high DMS fluxes over biologically productive brown slush sea ice, with a mean of 11 μmol m^{-2} d^{-1}. Nomura et al. (2012) used the closed chamber flux technique to report fluxes over productive sea ice and slush ranging from 0.1 to 5.3 μmol m^{-2} d^{-1}, off Syowa Station, East Antarctica. Finally, in the western Baffin Bay, Arctic, Gourdal et al. (2019) indirectly estimated potential diffusive fluxes from the ice to the atmosphere ranging from 0.4 to 10.4 μmol m^{-2} d^{-1}. The ice surface blooms associated with slush layers commonly observed for Antarctic sea ice are most likely hot spots for DMS emission given the close contact between atmosphere and the production source. Efforts should be made to include diffusive fluxes from slush to the atmosphere into budgeting and model approaches.

These 3 processes are key features of VMS fluxes in the sea-ice environment that must be considered in models, including ESMs, in order to adequately represent the polar biogenic sulfur cycle. In particular, modulations of sea-to-air emissions by turbulence and meltwater layers may trigger sporadic extreme VMS emissions from the sea-ice edge and leads (Levasseur et al., 1994; Koga et al., 2014; see details in Section 2.4.3). However, these processes are completely missing in current ESMs (Section 3.3), mainly because of the severely limited understanding of their mechanisms and spatial heterogeneity to develop generalized parameterizations and in part due to the general ignorance of sea-ice biogeochemical processes in ESMs. This highlights a large need for in situ measurements of VMS flux in different sea-ice environments, for example, around leads with different width and fetch, different salinity in meltwater layers, or on sea ice with different slush layer and snow properties. Whereas the eddy covariance flux measurement is a promising tool for capturing overall effects of sea ice on gas fluxes, it must be combined with more local flux chamber measurements to capture the high surface heterogeneity as well as simultaneous measurements of surface ocean turbulence around sea ice. In addition, the ice-to-air MeSH flux through snow on sea ice may not be linearly scaled to DMS due to potential differential oxidation of the 2 compounds in the highly oxidative interstitial air in snow (e.g., Grannas et al., 2007). To compensate for the difficulties in executing such extensive field observations, possible approaches in representing these processes in ESMs are discussed in Section 3.3.

2.3. Atmospheric oxidation processes

Accurate representation of atmospheric VMS oxidation processes is essential for evaluating how VMS emissions modulate atmospheric chemistry, aerosol, and cloud properties. Atmospheric VMS oxidation occurs through both gas phase and multiphase reactions (i.e., within, or at the interface of, cloud droplets and liquid aerosol particles; Abbatt and Ravishankara, 2023) (**Figure 1**; e.g., Davis et al., 1999; Sciare and Mihalopoulos, 2000; Legrand et al., 2001; Barnes et al., 2006). The gas phase product H_2SO_4 contributes to NPF and subsequent growth of particles to a few tens of nanometers in diameter (**Figure 1**; e.g., Kulmala et al., 2000). Another gaseous product, methanesulfonic acid (MSA), contributes to the growth of preexisting particles (Willis et al., 2017; Dall´Osto et al., 2018; Beck et al., 2021) and possibly also to nucleation (Bork et al., 2014; Chen and Finlayson-Pitts, 2017; Johnson and Jen, 2023); however, its contribution to NPF is not evident from available ambient observations (e.g., Beck et al., 2021). Sulfate (SO_4^{2-}) and methanesulfonate (MS^-) are also formed directly through multiphase processes on preexisting particles (e.g., Hoffmann et al., 2016), where they contribute to the aerosol growth but their direct condensed phase formation does not increase total particle number concentrations. In addition, unlike SO_4^{2-} that remains in the condensed phase, MS^- can partition back to gas phase MSA at low relative humidities (Hodshire et al., 2019; Baccarini et al., 2021), possibly allowing MSA to be recycled for the growth of other particles (e.g., Kecorius et al., 2023). Overall, stable VMS oxidation products (H_2SO_4, SO_4^{2-}, MSA, and MS^-) can drive both NPF and subsequent growth to CCN sizes (e.g., Giamarelou et al., 2016; Willis et al., 2016; Jokinen et al., 2018; Beck et al., 2021). Thus, the balance of gas phase and multiphase reactions exerts an important, but challenging to quantify, control on the contribution of VMS to the CCN population (e.g., Andreae and Rosenfeld, 2008; Woodhouse et al., 2013).

Here we describe the major chemical oxidation mechanisms and environmental factors that control VMS fate in the atmosphere: the presence of clouds and aerosol liquid water, temperature, and available oxidants. In Section 3.4.2, we provide a more quantitative explanation of VMS fate based on atmospheric modeling literature. We note that a recent review on the global relevance of DMS biogeochemistry features a dedicated section on DMS oxidation pathways (Hopkins et al., 2023); however, it offers an insufficient account of key reaction pathways and their impact on the atmospheric CCN population. We present a summary of current knowledge and most recent findings, with a focus on mechanisms most relevant in polar regions and the environmental factors that control the impact of biogenic sulfur on cloud albedo through CCN formation.

2.3.1. Overview of major VMS atmospheric oxidation mechanisms

The first step of DMS oxidation occurs through 2 parallel gas phase reaction pathways: "Hydrogen (H)-abstraction" and "Oxygen (O)-addition" (**Figure 1**; Turnipseed et al., 1996; Ravishankara et al., 1997). Both the relative importance and outcome of each pathway are controlled by the atmospheric conditions, including temperature, relative humidity, cloud presence, main oxidant (·OH, HO_2·, O_3, NO_3·, reactive halogens) and nitrogen oxide ($NO_x \equiv NO$· + NO_2·) concentrations. Importantly, oxidant and NO_x abundance partly reflect the level of anthropogenic pollution influence and can therefore differ significantly between the poles (**Figure 3**). However, photochemistry of halides, organic matter, and nitrate in snow are an important polar source of reactive halogens, HO_x ($HO_x \equiv$ ·OH + HO_2·), and NO_x (e.g., Honrath et al., 1999; Sumner and Shepson, 1999; Beine et al., 2002; Grannas et al., 2007; Pratt et al., 2013; Ahmed et al., 2022), which are expected to perturb the fate of VMS (Section 2.3.2.3).

The DMS H-abstraction pathway is initiated by oxidants including ·OH, NO_3·, and Cl· radicals. While all 3 of these oxidants drive H-abstraction, their reaction rates and relative importance vary diurnally, seasonally, and spatially (Section 2.3.2); for example, NO_3· forms in the dark and can drive rapid H-abstraction especially under elevated NO_x (polluted) conditions (e.g., Stark et al., 2007). Regardless of the initiating oxidant, the H-abstraction pathway produces a peroxy radical (i.e., CH_3SCH_2OO·, or "RO_2·") whose fate depends on the rate of its reaction with other atmospheric radicals (i.e., NO·, HO_2·, or other RO_2·; e.g., Hoffmann et al., 2016; Berndt et al., 2019; Veres et al., 2020). Two main RO_2· fates are important. First, bimolecular reaction with NO·, HO_2·, or RO_2· leads to production

of the $CH_3S\cdot$ radical (e.g., Barnes et al., 2006). The fate of $CH_3S\cdot$ also depends on available bimolecular reaction partners (i.e., O_3, $NO_2\cdot$, O_2), with predominant formation of the $CH_3SO_2\cdot$ radical (e.g., Hoffmann et al., 2016; Berndt et al., 2020; Chen et al., 2021; Berndt et al., 2023). $CH_3SO_2\cdot$ can form SO_2 through decomposition, or MSA (via $CH_3SO_2OO\cdot$ and $CH_3SO_3\cdot$) and SO_3 with strongly temperature-dependent yields (e.g., Lin and Chameides, 1993; Barnes et al., 2006; Chen et al., 2021; Ye et al., 2022; Chen et al., 2023) that enhance the importance of non-SO_2 products at low temperatures (see Section 2.3.2.2). SO_3 formation is important because it reacts rapidly with water vapor in the gas phase to form $H_2SO_{4(g)}$ (e.g., Berndt et al., 2023). Overall, bimolecular reactions of the first DMS-derived $RO_2\cdot$, such as in the presence of elevated NO_x, likely produce a temperature-dependent combination of SO_2, H_2SO_4, and MSA (**Figure 1**, Section 2.3.2.3; e.g., Hoffmann et al., 2016; Berndt et al., 2023; Chen et al., 2023). Second, under pristine marine boundary layer conditions (i.e., at background NO_x levels with <1 to 10's of ppt_v NO), the rate of $RO_2\cdot$ bimolecular reactions is slow enough that hydrogen-shift reactions become competitive (Wu et al., 2015; Berndt et al., 2019; Veres et al., 2020; Ye et al., 2022). These unimolecular reactions lead to strongly temperature-dependent formation of a stable intermediate compound: hydroperoxymethyl thioformate (HPMTF; $HOOCH_2SCHO$; **Figure 1**; Berndt et al., 2019; Veres et al., 2020; Jernigan et al., 2022; Assaf et al., 2023). While pristine conditions are relevant to polar regions, the hydrogen-shift reactions required to form HPMTF are likely to slow significantly at low temperatures (Assaf et al., 2023), which limits the importance of HPMTF formation in polar regions (Section 2.3.2.2). Once formed, HPMTF can react with the ·OH radical in the gas phase to form SO_2 and carbonyl sulfide (OCS) as end products (Jernigan et al., 2022).

The DMS O-addition pathway is driven by ·OH, BrO·, Cl· (with O_2), and O_3 and involves the addition of an oxygen atom to the central sulfur atom of DMS to form primarily DMSO (e.g., Ingham et al., 1999; Barnes et al., 2006). DMS oxidation by BrO· can be an important and potentially even dominant oxidation pathway in polar regions under some conditions (see Section 2.3.2.3). DMSO is then oxidized by ·OH in the gas phase to produce methanesulfinic acid (MSIA, CH_3SO_2H). MSIA is further oxidized by ·OH to form $CH_3SO_2\cdot$ and subsequently SO_2, SO_3 (H_2SO_4), and MSA (e.g., Shen et al., 2022; Chen et al., 2023; Goss and Kroll, 2024). Recent laboratory studies demonstrate that the gas phase fate of DMSO is likely impacted by the presence of NO_x, where elevated NO· concentrations led to a higher yield of SO_2 from ·OH-driven DMSO oxidation (Goss and Kroll, 2024). This observation is in contrast to established mechanisms and suggests NO_x-dependent pathways in the fate of MSIA and $CH_3SO_2\cdot$ that require further study (Chen et al., 2023; Goss and Kroll, 2024). Gas phase ·OH oxidation of DMSO and MSIA represents a "crossover" point between O-addition and H-abstraction pathways; branching toward this gas phase pathway controls the potential for DMS-driven NPF at low temperatures (see Section 2.3.2.2).

The rate constant of MeSH reaction with the ·OH radical is 3–4 times larger than DMS (at 273 K), and $CH_3SO_2\cdot$ radicals are produced in high yield (**Figure 1**; Tyndall and Ravishankara, 1991; Atkinson et al., 2004; Mai et al., 2020). As a result, MeSH gas phase oxidation produces a NO_x and temperature-dependent combination of SO_2, SO_3 (H_2SO_4), and MSA (e.g., Chen et al., 2021; Berndt et al., 2023; Chen et al., 2023; Tashmim et al., 2025; Section 2.3.2.2). As a result, model representation of MeSH emission and oxidation that assume conversion of MeSH to SO_2 with unity yield (Section 3.4; e.g., Novak et al., 2022; Wohl et al., 2024) may overestimate MeSH contributions to SO_2 at low temperatures. Additionally, limited laboratory evidence suggests that MeSH reacts efficiently with Br·, BrO·, and Cl· (Figure S3) to produce $CH_3S\cdot$ in pathways that could be competitive with ·OH oxidation; however, significant uncertainties in relevant laboratory kinetic data exist (Nesbitt and Leone, 1981; Nicovich et al., 1992; Nicovich et al., 1995; Aranda et al., 2002; Burkholder et al., 2019). Omission of halogen initiated oxidation could lead to an overestimate in the atmospheric lifetime of MeSH, but additional laboratory studies quantifying MeSH reaction rates at atmospherically relevant temperatures and pressures are needed before these pathways can be reliably evaluated in atmospheric models.

Gas phase reactions compete with multiphase reactions in the presence of clouds and aerosol. The DMS O-addition pathway to form DMSO can occur directly in the aqueous phase with O_3, which may be important in polar regions where gas phase ·OH concentrations are relatively low and low altitude, liquid-cloud coverage can be significant (e.g., Chen et al., 2018; Fung et al., 2022; Section 3.4). DMSO loss by multiphase ·OH oxidation to condensed phase MSIA (i.e., MSI^-) is likely competitive with gas phase reaction under typical atmospheric conditions (e.g., Zhu et al., 2003), directing sulfur away from gas phase end products. Aqueous phase MSI^- oxidation forms MS^- through competing reactions with ·OH or O_3 (e.g., Hoffmann et al., 2016; Chen et al., 2018; Liu et al., 2023), which can be further converted to SO_4^{2-} by multiphase ·OH oxidation (Kwong et al., 2018; Mungall et al., 2018). HPMTF is rapidly lost through cloud uptake and subsequent aqueous phase oxidation to form SO_4^{2-}, likely through hydrolysis and O_3 reactions (Novak et al., 2021; Jernigan et al., 2022; Jernigan et al., 2024; Kilgour et al., 2025). These multiphase pathways effectively reduce the fraction of biogenic sulfur contributing to OCS production (Jernigan et al., 2022; Kilgour et al., 2025) and NPF through gas phase production of H_2SO_4 (e.g., Chen et al., 2018; Fung et al., 2022; Tashmim et al., 2024).

SO_2 oxidation also occurs through both gas phase and multiphase pathways. Gas phase SO_2 oxidation by ·OH is a dominant pathway to produce gaseous H_2SO_4. On the other hand, SO_2 dissolves into clouds, fog, and aerosol liquid water to form aqueous S(IV) ($=SO_2{\cdot}H_2O + HSO_3^- + SO_3^{2-}$; e.g., Liu et al., 2021b). Depending on the liquid phase pH, S(IV) compounds are oxidized to SO_4^{2-} by H_2O_2, O_3, or hypohalous acids (HOBr and HOCl; e.g., von Glasow and Crutzen, 2004; Chen and Finlayson-Pitts, 2017;

Tilgner et al., 2021). In addition, multiphase reaction of S(IV) with dissolved aldehydes promotes production of hydroxyalkylsulfonates, including hydroxymethanesulfonate (HMS), which can become particularly important in polluted and cold atmospheric conditions (e.g., Liu et al., 2021a; Campbell et al., 2022; Campbell et al., 2024; Dingilian et al., 2024). Overall, the competition between gas and multiphase oxidation is active across the entire VMS oxidation mechanism (e.g., Hoffmann et al., 2016).

2.3.2. Factors controlling VMS abundance and oxidation pathways in polar atmospheres

Both emissions (Sections 2.1–2.2) and subsequent atmospheric oxidation chemistry (Section 2.3.1) control atmospheric VMS speciation and burden. Observed DMS concentrations are typically higher in the polar marine boundary layer (i.e., from ship-based measurements) compared to lower latitudes during biologically active seasons. Arctic (>60°N) median DMS concentrations from available surface-based measurements in May to September are 169 ppt_v (IQR: 43–243 ppt_v), compared to 112 ppt_v (IQR: 39–196 ppt_v) during the same months at lower latitudes (0–60°N) (G Manville, personal communication, 09/10/2025). Similarly, high-latitude Southern Ocean (>60°S) DMS concentrations in October to March are 208 ppt_v (IQR: 114–446 ppt_v), compared to 127 ppt_v (IQR: 81–211 ppt_v) at lower latitudes (0–60°S) (G Manville, personal communication, 09/10/2025).

Dissolved VMS observations in the surface ocean reveal an important contribution of MeSH to potential VMS emissions especially in sub-Arctic, Arctic (elevated MeSH/VMS >50°N), and Southern Ocean (elevated MeSH/VMS ∼40 to >60°S) regions (**Figure 2a**; Sections 2.1–2.2; Wohl et al., 2024; Mynard et al., 2025). Consistent with dissolved concentrations, the limited available atmospheric VMS observations consistently demonstrate an important contribution of MeSH (**Figure 2b**). Atmospheric MeSH concentrations in the marine boundary layer are closely coupled with but typically an order of magnitude lower than DMS (Figure S1; median 12 ppt_v, IQR: 7–23 ppt_v), with corresponding MeSH/VMS ratio of approximately 0.1–0.4 (**Figure 2b**). While illustrative of existing measured MeSH atmospheric concentrations, these values should be interpreted with caution, especially given the current bias in available datasets toward the Southern Ocean and coastal regions (**Figures 2a** and S2), and in comparison to median atmospheric DMS concentrations that arise from significantly more observations (G Manville, personal communication, 09/10/2025). Over the Southern Ocean, the largest atmospheric MeSH concentrations are observed over biologically productive regions between 45°S and 52°S at the Subantarctic Front and near the Antarctic sea-ice edge (>62°S; Chapman et al., 2020; Mynard et al., 2025) in general agreement with predictions from the first global MeSH seawater data product (Wohl et al., 2024). However, available observations at the Antarctic sea-ice edge show that atmospheric MeSH/VMS decreases to below 0.1 and the coupling between MeSH and DMS becomes less coherent (**Figure 2b**; Mynard et al., 2025). Measured atmospheric MeSH/VMS depends not only on marine biological controls and emission fluxes but also on available atmospheric oxidants and the time elapsed since emission, especially because MeSH reacts more rapidly with ·OH radical than DMS (Section 2.3.1). As a result of its short atmospheric lifetime, the contribution of MeSH at emission will be larger than the observed ambient MeSH/VMS (Section 2.2).

Together, the sparse available atmospheric and dissolved MeSH/VMS appear to suggest an opposing global latitudinal dependence (**Figure 2**); however, any apparent spatial trend must be interpreted with extreme caution because the available ocean and atmospheric MeSH/VMS measurements are largely unmatched in season and location even within common latitude bands (Figure S1). Lower atmospheric MeSH/VMS in regions where high dissolved MeSH/VMS has been observed could arise from a combination of factors: spatial and temporal variability in the relative atmospheric reactivity of MeSH and DMS, such as in the presence of reactive halogens (Section 2.3.1); potentially limited emissions of MeSH in sea-ice regions arising from its short lifetime in seawater (Section 2.1); or sparse data coverage, especially in sea-ice regions where atmospheric VMS concentrations are characterized by episodically elevated concentrations on a low background and frequent extremes in DMS concentration (Figure S1). Overall, both the abundance of MeSH and DMS and their chemical fate through gas phase and multiphase processes control the impact of VMS on atmospheric oxidizing capacity, the aerosol population, and resulting cloud properties (e.g., Fung et al., 2022; Wohl et al., 2024). Three major environmental factors control the relative importance of gas phase and multiphase VMS fates: (1) the availability of atmospheric condensed phases, (2) temperature effects on both gas phase and multiphase chemistry, and (3) the abundance of atmospheric oxidants.

2.3.2.1. The availability of atmospheric condensed phases

First, the volume, surface area and phase state of atmospheric condensed phases—clouds and aerosol—are a dominant control on competing VMS gas phase and multiphase fate. In liquid clouds, predominant oxidation pathways can transition from gas to aqueous phase. This shift in chemical regime occurs due to both multiphase uptake processes and reflection of solar radiation that results in decreased gas phase oxidant concentrations (e.g., Hoffmann et al., 2016). Global chemical transport models show that multiphase pathways may play a dominant role in DMS oxidation over the Arctic Ocean and coastal Antarctica (Chen et al., 2018; Fung et al., 2022; Tashmim et al., 2024). However, many atmospheric models do not resolve clouds, leading to biases in predicted reaction rates, which can be remedied by applying entrainment-limited multiphase reaction for very soluble reactants (Holmes et al., 2019; Holmes, 2022). In addition, satellite-derived cloud coverage products can significantly underestimate cloud fractions (e.g., Kilgour et al., 2025) and models persistently struggle to accurately represent cloud microphysics and phase in polar regions (e.g., Mallet

et al., 2023; McCluskey et al., 2023; Sokol and Storelvmo, 2024). Mixed-phase clouds are persistent in Arctic regions throughout the year, with elevated liquid fractions especially in low-level clouds (e.g., Cesana et al., 2012; Morrison et al., 2012; Sokol and Storelvmo 2024; Wex et al., 2025; Yang et al., 2025). In contrast, summertime Southern Ocean clouds are often dominated by supercooled liquid water, except when conditions approach homogeneous freezing (i.e., below −38°C; Koop et al., 2000; Knopf and Alpert, 2023), probably because of extremely low concentrations of ice nucleating particles (e.g., McCluskey et al., 2018; Mace et al., 2021; McCluskey et al., 2023; Sokol and Storelvmo, 2024). While cloud ice formation may not completely shutoff multiphase reactivity (e.g., Clegg and Abbatt, 2001a; Clegg and Abbatt, 2001b; Bartels-Rausch et al., 2014), significant uncertainties exist in the rates and mechanisms of multiphase VMS oxidation in both cloud and aerosol liquid water and on cloud ice (e.g., Chen et al., 2018; Fung et al., 2022; Kilgour et al., 2025; Section 2.3.1, **Figure 1**).

Even in clear sky conditions, multiphase reactions in aerosol liquid water, and at aerosol interfaces, can play an important role for controlling the fate of VMS and its oxidation products (e.g., Davis et al., 1999; Hoffmann et al., 2016; Mungall et al., 2018). Importantly, multiphase chemical regimes differ between dilute cloud conditions and more concentrated aerosol (e.g., Hoffmann et al., 2016; Su et al., 2020; Hoffmann et al., 2021; Liu et al., 2023). For example, the rate of SO_2 oxidation by H_2O_2 in aerosols can be enhanced by approximately 50 times when increasing the ionic strength from dilute cloudlike conditions to aerosol conditions (Liu et al., 2020). This change in chemical regime can occur in part because liquid water content differs significantly, and thus high solute concentrations in aerosols (up to ~ 10 mol kg^{-1}) lead to chemistry that is distinct from more dilute cloud water ($\sim 10^{-4}$ mol kg^{-1} ionic strength; e.g., Tilgner et al., 2021; Liu et al., 2021b). However, and most importantly, such acceleration in the reaction rate cannot always be attributed to increased concentrations in atmospheric aerosol (e.g., Liu et al., 2020; Liu et al., 2021b). Secondary effects of the high solute concentrations and confined reaction environments may also contribute to the distinct chemical regimes in aerosol multiphase processes that can lead to reaction rate enhancement or suppression (e.g., Limmer et al., 2024; Wilson and Prophet, 2024). These include effects on reactant solubility (e.g., Bartels-Rausch et al., 2014; Edebeli et al., 2019), particle phase and viscosity (e.g., Shiraiwa et al., 2011; Shiraiwa et al., 2017), acid–base equilibria (e.g., Zheng et al., 2023; Campbell et al., 2024), surface to volume ratio of particles and the fraction of molecules present at an interface (e.g., Liu and Abbatt, 2021; Ammann and Artiglia, 2022; Limmer et al., 2024; Wilson and Prophet, 2024; Judd et al., 2025), phase separation, and the magnitude of rate constants (e.g., Liu et al., 2021b; Limmer et al., 2024). A detailed knowledge of biogenic sulfur multiphase and interfacial chemistry at high solute strength, atmospherically relevant temperatures, aerosol acidity and composition, must be developed to accurately represent the atmospheric fate of sulfur in models (Section 3). New robust laboratory studies are urgently needed (e.g., Rovelli et al., 2020; Bartels-Rausch et al., 2025).

2.3.2.2. Temperature effects on both gas phase and multiphase chemistry

Second, temperature exerts an important control on both the gas phase and multiphase chemical fate of VMS and its stable oxidation products. In the gas phase, lower temperatures favor O-addition pathways (**Figures 1** and **4**; Hynes et al., 1986; Williams et al., 2001; Albu et al., 2006; Williams et al., 2007; Williams et al., 2009; Burkholder et al., 2019), and slow peroxy radical hydrogen-shift reactions (Assaf et al., 2023). Together, these additive effects can lead to a smaller branching of sulfur into HPMTF compared to lower latitudes (Veres et al., 2020; Novak et al., 2021; Siegel et al., 2023). Beyond the first step of DMS oxidation, temperature is a key control on rates and branching ratios of intermediate oxidation steps ·OH oxidation of MSIA to MSA are likely enhanced at lower temperatures (e.g., Shen et al., 2022; Chen et al., 2023); low-temperature laboratory experiments produced reasonable agreement with existing ambient

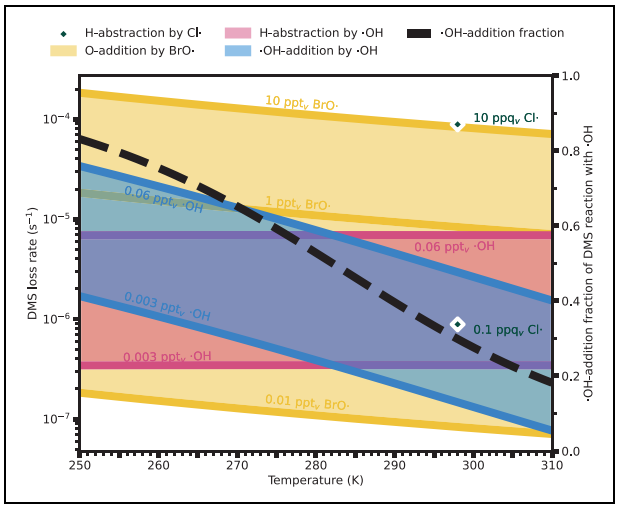

Figure 4. Temperature dependence of initial DMS oxidation pathways by ·OH, BrO·, and Cl·. Rate constants are based on recommended expressions from Burkholder et al. (2019). The ·OH concentration range is estimated using coastal Antarctic data (Kukui et al., 2012). Cl· concentrations are estimated using modeled concentrations based on measurements of Cl_2 and ClO· in Utqiaġvik, Alaska (Custard et al., 2016). BrO· concentrations are based on measurements in Utqiaġvik, Alaska (Wang et al., 2019a). $k_{OH(abstraction)} = 1.2 \times 10^{-11} \times \exp(-280/T)$, $k_{OH(addition)} = (8.2 \times 10^{-39} \times \exp(5376/T) \times [O_2])/(1 + 1.05 \times 10^{-5} \times \exp(3{,}644/T) \times [O_2]/[M])$, $k_{BrO} = 1.4 \times 10^{-14} \times \exp(950/T)$, and $k_{Cl} = 3.5 \times 10^{-10}$ (at 1 atm, 298 K). The right axis (dashed black line) displays the fraction of ·OH-initiated reactions proceeding through the ·OH-addition pathway. ·OH-addition makes up 50% of these reactions at approximately 282 K and becomes more important at temperatures below 282 K.

measurements of gas phase MSA/H_2SO_4 ratios (Berresheim et al., 2002; Jokinen et al., 2018; Beck et al., 2021). Critically, both the production and fate of the CH_3SO_2· radical are likely steeply temperature dependent (e.g., Hoffmann et al., 2016; Chen et al., 2023). At higher temperatures, CH_3SO_2· is formed from DMS at <50% yield and then decomposes to SO_2 at near 100% yield, while at lower temperatures CH_3SO_2· is produced at high yield (∼85%) and predominantly forms CH_3SO_3· (Chen et al., 2023). Theoretical calculations demonstrate that at low temperatures (e.g., 260 K), CH_3SO_2· produces a predominant yield of gas phase MSA (67%–73%), with smaller fractions of SO_3 (7%–8% yield) and to SO_2 (4%–10% yield; Chen et al., 2023). Low-temperature gas phase SO_3 (H_2SO_4) and MSA production could be particularly important in polar regions for supplying precursors for NPF and growth. In addition, MeSH likely produces CH_3SO_2· with high yield (**Figure 1**; Section 2.3.1), and more rapidly than DMS, which could further enhance gas phase H_2SO_4, MSA, and SO_2 production potential in polar atmospheres. However, key uncertainties remain in the temperature-dependent fate of these key radical intermediates (CH_3SO_2·, CH_3SO_3·), with a long-standing and persistent need for measurement of thermal decomposition rates (e.g., Ravishankara et al., 1997; Butkovskaya and Barnes, 2002; Borissenko et al., 2003; Hoffmann et al., 2016; Berndt et al., 2023; Chen et al., 2023).

Temperature is also an important control on multiphase VMS fate through its typically opposing effects on reactant partitioning and bimolecular reaction rate constants. Multiphase pathways can be promoted by the negative temperature dependence of Henry's Law partitioning (i.e., the air-water partition coefficient; Sander, 2023), which likely increases the importance of these pathways in polar regions when atmospheric liquid water is present (e.g., Hoffmann et al., 2016). While the Henry's Law constant for DMS is reasonably well characterized, limited temperature-dependent measurements of the Henry's Law constants exist for MeSH and VMS oxidation products (e.g., Watts and Brimblecombe, 1987; De Bruyn et al., 1995; Burkholder et al., 2019; Sander, 2023). These partition constants can also be predicted with thermodynamic models (e.g., Wollesen de Jonge et al., 2021); however, these estimates should be treated with caution as uncertainties can be very large (e.g., Wang et al., 2017). Further, the vast majority of measured temperature-dependent Henry's Law constants are applicable in a narrow temperature range that approaches 0°C (e.g., Sander, 2023), but limited measurements suggest that their negative temperature dependence may not be applicable in supercooled liquid water (Sieg et al., 2009). However, no measurements of Henry's Law constants for VMS and oxidation products exist in supercooled liquid water, nor for effective Henry's Law constants applicable to highly concentrated aerosols. Further, measurements of temperature-dependent reaction rate constants do not exist over a fully atmospherically relevant range; such measurements are, of course, technically very challenging. Once cloud ice forms in mixed-phase or entirely glaciated clouds, multiphase reactivity likely changes dramatically (e.g., Clegg and Abbatt, 2001a; Clegg and Abbatt, 2001b; Bartels-Rausch et al., 2014). While models often assume that multiphase reactivity shuts off below a set temperature threshold (e.g., −15°C; Alexander et al., 2009), in reality multiphase reactions on and in cloud ice will be controlled by ice surface area, presence of liquid or liquid-like regions at the air-ice interface, location of reactive solutes upon freezing, and gas-ice uptake and partitioning properties (e.g., Roth et al., 2004; Bartels-Rausch et al., 2014; Malley et al., 2018; Chakraborty and Kahan, 2020; Bartels-Rausch et al., 2021). Overall, our understanding of biogenic sulfur multiphase fate at low temperatures is extremely limited.

2.3.2.3. The abundance of atmospheric oxidants

Third, available oxidants are a key control on VMS atmospheric fate. The initial step of VMS oxidation chemistry is often controlled by the ·OH radical (e.g., Hoffmann et al., 2016; Novak et al., 2022). ·OH formation in the troposphere is driven by solar radiation, O_3, and water vapor (Stone et al., 2012), leading to efficient atmospheric oxidation and frequent NPF events in polar summertime (e.g., Dall´Osto et al., 2017; Willis et al., 2018; Lachlan-Cope et al., 2020; Schmale and Baccarini, 2021). The abundance of ·OH radicals will impact not only initial H-abstraction and O-addition pathways but also the fate and lifetime of stable DMS oxidation products (e.g., DMSO, HPMTF, MSIA/MSI^-, MS^-) through both their gas and multiphase chemistry (**Figure 1**). For example, lower ·OH concentrations in polar regions compared to lower latitudes (e.g., Wolfe et al., 2019; Lelieveld et al., 2002) may lead to a longer MS^- lifetime in aerosol and thus contribute to higher observed MS^-/SO_4^{2-} ratios. However, large uncertainty exists in the abundance of ·OH in cloud and aerosol water, with indirect observations in cloud water ranging 2 orders of magnitude from 10^{-16} to 10^{-14} M (Arakaki et al., 2013; Kaur and Anastasio, 2017) while box models estimate 10^{-14} to 10^{-12} M (Herrmann et al., 2000). A single study has measured ·OH photoformation from extracts of ambient Arctic aerosols collected at Alert, NU in spring (March–April, 1995), demonstrating significant midday production rates for April of approximately 1 mM h^{-1} (at 248 K; Anastasio and Jordan, 2004). Such high production rates could lead to elevated condensed phase ·OH concentrations at steady state, depending on the magnitude of ·OH sinks; however, the prevalence and seasonality of strong aerosol ·OH photoproduction is essentially unknown. Large uncertainty arises from the fast and complex organic chemistry in the condensed phase, which is a major sink for $\cdot OH_{(aq)}$ (Ervens, 2015). Improved estimates of atmospheric condensed phase oxidants will support better understanding of the competition between gas and multiphase VMS oxidation.

Oxidant and nitrogen oxide (NO_x) concentrations are interlinked especially in polar regions with prevalent aerosol and snowpack photochemistry that leads to halogen activation, and HO_x and NO_x production (e.g., Honrath et al., 1999; Sumner and Shepson, 1999; Beine et al., 2002; Simpson et al., 2015; Pratt, 2019; Thomas et al., 2019). HO_x and NO_x abundance can be enhanced in the

presence of reactive halogens (e.g., Brough et al., 2019), highlighting the coupled nature of VMS oxidation processes and the importance of detailed chemical representation of snowpack photochemistry for accurately representing polar VMS lifetime and chemical fate in models (e.g., Ahmed et al., 2022). Both HO_2· and NO· can determine the fate of key radical intermediates in VMS oxidation (Section 2.3.1), where the production of the stable intermediate compound HPMTF is favored under marine background HO_2· and NO· concentrations (e.g., Veres et al., 2020). However, depending on the ambient temperature, elevated HO_x and NO_x concentrations will promote partitioning of sulfur into CH_3S· and CH_3SO_2· radicals, whose fate is also dependent on temperature and NO_x abundance (Section 2.3.1; e.g., Chen et al., 2023; Jongebloed et al., 2025). Laboratory studies focused on the VMS H-abstraction pathway suggest that rapid formation of gas phase MSA and H_2SO_4 or particle phase MS^- and SO_4^{2-} is promoted under elevated NO· concentrations (i.e., ppb_v levels of NO·; Ye et al., 2022; Berndt et al., 2023; Goss and Kroll, 2024). The fate of DMS in the O-addition pathway is also dependent on NO· concentrations (Section 2.3.1), with recent work highlighting both enhanced SO_2 production and rapid aerosol formation from DMSO oxidation under conditions of elevated NO· (Goss and Kroll, 2024). Importantly, many NO_x-dependent pathways may not be captured by existing VMS reaction mechanisms (e.g., Goss and Kroll, 2024; Jongebloed et al., 2025). This shortcoming is highlighted by recent attempts to explain preindustrial (PI) to present-day (PD) changes in MS^- and biogenic-SO_4^{2-} observed in ice core records. Although these records strongly suggest that anthropogenic pollution has altered the fate of VMS over the industrial era (e.g., through enhanced NO_3·-driven oxidation that may promote SO_2 and SO_4^{2-} production; Chalif et al., 2024), existing model oxidation mechanisms cannot capture either the magnitude or trends (Jongebloed et al., 2025). These discrepancies highlight important gaps in our knowledge of VMS oxidation pathways.

When halogen activation occurs, the Cl· radical is a potentially important oxidant for VMS (i.e., driving rapid H-abstraction reactions; **Figure 4**); however, important uncertainty exists in its abundance. Models suggest very low polar Cl· radical concentrations (e.g., Chen et al., 2018; Wang et al., 2019b; Fung et al., 2022) in strong contrast to the limited available observational constraints that demonstrate Cl· concentrations on the order of 0.02 ppt_v in Arctic springtime (Tuckermann et al., 1997; Liao et al., 2014; Thompson et al., 2015; Custard et al., 2016; McNamara et al., 2019). Uncertainties in Cl· oxidation are driven not only by its poorly constrained abundance across seasons but also by uncertain temperature dependence of its reaction with DMS; limited available laboratory studies suggest an increasing reaction rate constant at lower temperatures (**Figure 4**; Atkinson et al., 2007).

Reactive bromine radicals (Br·, BrO·) may be key oxidants for VMS globally and in polar regions (e.g., Barnes et al., 2006; Chen et al., 2018; Fung et al., 2022). Incorporating DMS oxidation by BrO· into an atmospheric chemistry transport model led to a global increase in atmospheric DMSO concentrations by 63% (von Glasow and Crutzen, 2004); however, ambient observational constraints on the importance of this pathway are extremely limited. Tropospheric BrO· concentrations are highest in the springtime Arctic and Antarctic (Theys et al., 2011; Seo et al., 2020) due to the photochemical snowpack and aerosol emission of its precursor molecular bromine (Br_2; Pratt et al., 2013), which photolyzes to produce Br· radicals that react with ozone to produce BrO· (Wang et al., 2019a). As a result, reactive bromine chemistry ceases upon snowmelt (Burd et al., 2017; Jeong et al., 2022). If the presence of polar BrO· (e.g., Buys et al., 2013; Seo et al., 2020; Benavent et al., 2022) overlaps in space and time with late-spring VMS emissions, then the BrO-driven O-addition pathway could be an important fate for DMS (**Figure 4**). Available observations provide some limited evidence for this hypothesis. Long-term measurements of particulate MS^- seasonality at Alert, Canada (Leaitch et al., 2013), and Ny-Ålesund, Svalbard (Becagli et al., 2019), demonstrate that concentrations increase beginning in spring (April–May), suggesting a potential role for late-spring DMS oxidation by BrO·. In Utqiaġvik, Alaska, MS^- increases in late spring (April–May; Quinn et al., 2002), just prior to the cessation of reactive bromine chemistry upon snowmelt in mid-May (Jeong et al., 2022). The available measurements at 2 Antarctic coastal stations exhibit increases in DMS and MS^- concentrations from November (Preunkert et al., 2007; Weller et al., 2011b), with BrO· declining through the month from its maximum levels in October (Saiz-Lopez et al., 2007; Seo et al., 2020). Nonetheless, even in summertime Antarctica, BrO· oxidation of VMS needs to be considered to explain oxygen isotope fingerprints in aerosol SO_4^{2-} (Ishino et al., 2021). Despite uncertainties in these mostly indirect observations, global models often predict that BrO· is a key oxidant for DMS in polar regions (Chen et al., 2018; Fung et al., 2022); however, these models persistently struggle to reproduce polar spring tropospheric ozone depletion and thus reactive halogen concentrations (Whaley et al., 2023). Overall, DMS oxidation by BrO· is likely an important pathway that drives DMS rapidly toward O-addition pathways, though the seasonal and spatial importance of this reaction remains an open question.

2.3.2.4. Summary of environmental factors that control polar VMS oxidation

In summary, the combined impact of available atmospheric condensed phases, temperature and oxidants drives the fate of VMS toward growth of existing aerosol (i.e., direct condensed phase formation of MS^- and SO_4^{2-}) or NPF (i.e., gas phase SO_2, H_2SO_4 formation). However, significant uncertainties remain in the dependence of VMS fate on these environmental drivers, challenging our ability to quantify the contribution of gas and multiphase oxidation globally and in polar regions. Key uncertainties in the controls on VMS abundance and oxidation pathways include (1) the importance of halogen-driven sulfur oxidation in gas and condensed phases; (2) the magnitude of SO_2 and SO_3 production from the O-addition pathway through competition between gas

and multiphase DMSO and MSIA (or MSI^-) oxidation; (3) the temperature-dependent fate of $CH_3SO_2\cdot$ and $CH_3SO_3\cdot$ radicals; and (4) the rates of multiphase reactions in liquid clouds, both above and below 273 K, and in the presence of cloud ice. Limited constraints from field and low-temperature laboratory observations suggest the importance of O-addition pathways, and associated $MSA_{(g)}$ and MS^- formation, in polar regions; MS^-/non-sea-salt-SO_4^{2-} ($nssSO_4^{2-}$) ratios in the particle phase and MSA/H_2SO_4 ratios in the gas phase are typically higher at low temperatures and high latitudes (e.g., Chen et al., 2012; Shen et al., 2022), with lower gas phase HPMTF/DMS ratios (Veres et al., 2020). $MS^-/nssSO_4^{2-}$ ratios in the particle phase often exceed 0.5 in Antarctic summer (Legrand et al., 2001; Becagli et al., 2022) and 0.1 in Arctic summer (Chen et al., 2012; Sharma et al., 2019), compared to those well below 0.1 at lower latitudes (Gondwe et al., 2004; Chen et al., 2012). These latitudinal differences in $MS^-/nssSO_4^{2-}$ ratios cannot be entirely explained by either abundant anthropogenic sulfate over the lower latitude oceans or temperature effects on the first steps of DMS oxidation (e.g., Castebrunet et al., 2009). Latitudinal trends in $MS^-/nssSO_4^{2-}$ ratios and HPMTF production are qualitatively captured by global models (Chen et al., 2018; Novak et al., 2021; Fung et al., 2022; Tashmim et al., 2024); however, a quantitative, polar-focused evaluation is needed (Section 3.4) that captures key drivers of gas and multiphase chemistry and that can represent spatial heterogeneity of oxidation pathways (e.g., Pernov et al., 2025). Overall, the contribution of gas and multiphase pathways is not easily distinguishable in observations alone, but insight can be meaningfully gained through combined ambient observations and modeling (e.g., Kilgour et al., 2025).

2.4. Polar VMS contributions to the atmospheric aerosol population: Spatiotemporal context for VMS-driven NPF and growth

A notable role of biogenic VMS emissions for the polar aerosol number budget has often been inferred from the occurrence of NPF events associated with enhanced sulfur oxidation products (gas phase H_2SO_4, MSA, and/or particle-phase MSA (MS^-)) over the marginal sea-ice zone during the biologically active season (e.g., Dall´Osto et al., 2017; Jokinen et al., 2018; Baccarini et al., 2021; Beck et al., 2021; Brean et al., 2021). However, their actual overall importance to the aerosol population compared to non-biogenic-sulfur and non-sulfur particle sources remains highly uncertain (Ghahreman et al., 2016; Schmale and Baccarini, 2021; Jongebloed et al., 2023a; Jongebloed et al., 2023b; Mallet et al., 2023). The general requirements for NPF events to occur are (i) a sufficient supply of low-volatility precursor gases for nucleation and subsequent particle growth and (ii) low concentrations of preexisting particles that scavenge both precursor vapors and nano-size particles before their growth (Kerminen et al., 2018). A key factor in the contribution of biogenic VMS oxidation products to NPF is the copresence of a base (e.g., NH_3), which can be emitted by terrestrial sources (e.g., Wentworth et al., 2016; Croft et al. 2016b; Murphy et al., 2024; Boyer et al., 2025) and potentially marine sources (Brean et al., 2021). This is in addition to meteorological factors, such as temperature, relative humidity, and radiation, that indirectly impact the seasonality of NPF events. Here we outline when and where sea ice and MIZ-sourced VMS can be significant precursors for NPF and growth, based on a compilation of the seasonal and spatial variability of aerosol chemical and microphysical properties from Arctic and Antarctic ground-based stations (**Figure 5**).

The discussion in this section centers on ground-based and shipborne observations; however, the vertical transport of surface-derived aerosols and precursors to cloud level, and their subsequent involvement in aerosol–cloud interactions, is difficult to discern from surface-based observations. Polar low-level clouds are often decoupled from the surface air by a temperature inversion below clouds (e.g., Sotiropoulou et al., 2014; Griesche et al., 2021), though surface-connected fogs can also be present (e.g., Leaitch et al., 2016). Even when coupled with the surface, drizzling from low-level clouds can act as an efficient aerosol sink, highlighting the complex role of boundary layer meteorology in mediating the potential impact on cloud properties (Browse et al., 2014; Croft et al., 2016a; Mahmood et al., 2019). VMS oxidation processes—and thus NPF and growth potential—will also vary with altitude (Section 2.3.2). Nevertheless, a few studies have reported linkages between surface CCN loadings and cloud formation or cloud droplet number concentrations in polar regions (Mauritsen et al., 2011; Mallet et al., 2025). Overall, the extent to which surface-level aerosol and CCN number concentrations translate into cloud impacts remains highly uncertain, as emphasized in several reviews on polar aerosols (e.g., Willis et al., 2018; Schmale et al., 2021; Mallet et al., 2023). Modeling studies have suggested an important role of Arctic DMS in modifying cloud cover and droplet properties including at high altitude (Ghahreman et al., 2021; Lapere et al., n.d.), but more in situ vertical measurements and coupled meteorology-chemistry modeling (e.g., large-eddy simulations) are clearly needed to resolve this open question.

2.4.1. Potential VMS contribution to NPF and growth in the Arctic

Figure 5c and **d** shows the monthly occurrence probability of size-resolved particle number distributions at Zeppelin (Dall´Osto et al., 2017) and Villum (Pernov et al., 2022) stations in the Arctic. Among the aerosol size distribution categories, "Nucleation-Bursting" and "Nascent" are dominated by particles smaller than 50 nm in diameter and are therefore often considered as indicating the occurrence of NPF and subsequent particle growth, in the absence of local combustion influence (Dall´Osto et al., 2017; Lachlan-Cope et al., 2020). Note that this simple assumption is not always valid because primary sea spray aerosols (SSA) down to tens of nanometers in diameter may also contribute to these 2 aerosol modes (e.g., Yang et al., 2019; Myers et al., 2021; Gong et al., 2023; Sellegri et al., 2023). Indeed, observations of

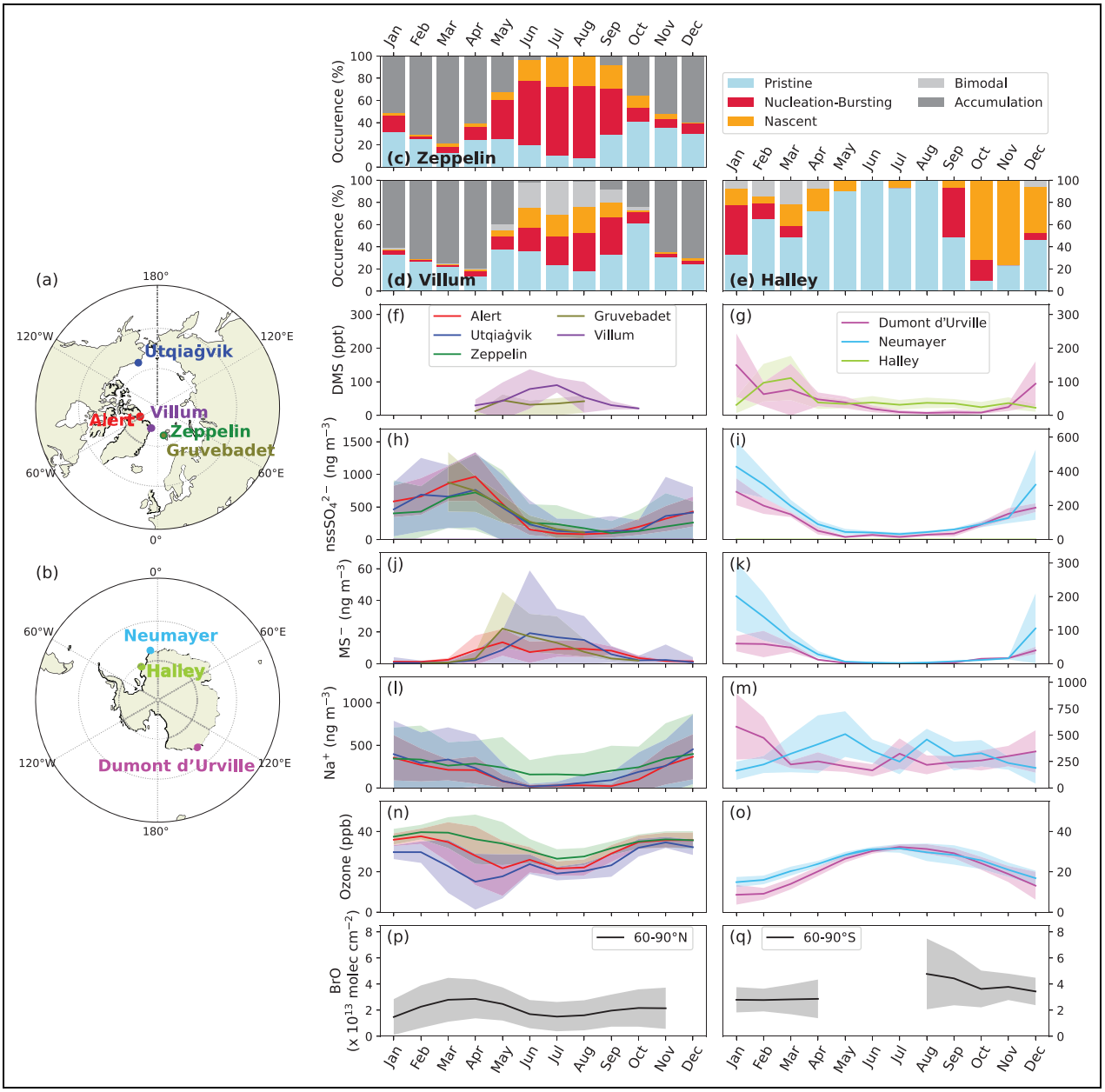

Figure 5. Seasonal variations of aerosol composition and size distributions, DMS, ozone, and BrO at both poles. (a, b) Location of stations. (c–e) Monthly occurrence probability of particle number size distribution (PNSD) types at Zeppelin (c, Dall´Osto et al., 2017), Villum (d, Pernov et al., 2022), and Halley (e, Lachlan-Cope et al., 2020). Note that the classification definitions of PNSD types are not identical among studies (see Table S1). To obtain a simplified view of particle characteristics among different sites, we converted the original PNSD classifications across 3 studies into 5 categories. Pristine: Broad distribution with particle number concentrations lower than 200 cm^{-3} across all size bins; Nucleation-Bursting: Peak below 30 nm; Nascent: Peak at 30–100 nm; Accumulation: Peak above 100 nm; Bimodal: Peaks below and above 100 nm. (f–o) Atmospheric concentrations of DMS (f, g), particulate non-sea-salt sulfate ($nssSO_4^{2-}$) (h, i), particulate MSA (MS^-) (j, k), particulate sodium (l, m), and ozone (n, o), from station-based measurements. Note that the cut-off size for aerosol chemical measurements varies among different sites: total particulate matter (TPM) for Alert (red), Zeppelin (green), and Dumont d'Urville (magenta), PM_{10} for Gruvebadet (khaki) and Neumayer (light blue), and PM_1 for Utqiaġvik (blue). $nssSO_4^{2-}$ (=total-SO_4^{2-} − 0.252 × Na^+) is shown instead of total-SO_4^{2-} concentration because sea-salt-SO_4^{2-} mass dominantly resides in coarse particles (>1 μm) whose contribution to particle number concentration is small (Seguin et al., 2011). (p, q) Tropospheric column BrO levels averaged over 60°–90° of both poles from GOME-2 satellite data (Theys et al., 2011). Lines and shading for (f–q) correspond to means and 1 − σ standard deviations, respectively. Data sources are detailed in the data accessibility statement.

20–60 nm particle composition in the summertime High Arctic show that this size range contains elevated levels of both MSA and sodium during NPF and growth events, pointing to the complexity of ultrafine aerosol chemical composition in the polar regions (Lawler et al., 2021). Although caution must be applied in their interpretation, the sum of the monthly occurrences of "Nucleation-Bursting" and "Nascent" aerosol size distributions exceeds 20% of the time from May to September at both stations, suggesting an increased importance of NPF sourced particles during these months compared to other periods of the year (Dall´Osto et al., 2017; Pernov et al., 2022).

These Arctic summer months generally coincide with the biologically active season and therefore increased atmospheric concentrations of DMS and particulate MSA (i.e., MS^-, **Figure 5f** and **h**) (Leaitch et al., 2013; Jang et al., 2021; Pernov et al., 2024). In contrast to MS^-, non-sea-salt sulfate ($nssSO_4^{2-}$) concentrations tend to be lower in summer months (**Figure 5j**), due to suppressed transport of anthropogenic pollution from lower latitudes (Sharma et al., 2019; Schmale et al., 2022). In addition, relatively low concentrations of sodium (Na^+; **Figure 5l**) likely reflect greater atmospheric boundary layer heights and increased wet scavenging during summer that reduce sea spray aerosol concentrations and further enable NPF due to the reduced condensation sink (Browse et al., 2014). Consequently, in the Arctic, May to September is characterized as the period of coincidence of more frequent NPF events and increased DMS emission, highlighting the potential importance of biogenic sulfur-driven NPF for the aerosol population. However, these coinciding seasonalities are alone insufficient evidence for the role of biogenic sulfur-driven NPF in competition with other particle sources.

In situ observations of particle microphysical properties and composition in the Arctic supply further evidence for the role of biogenic sulfur-driven NPF and growth. Several summertime Arctic studies observed elevated number concentrations of <70 nm diameter particles coincident with elevated DMS and/or MS^- (Leck and Persson, 1996; Chang et al., 2011; Leaitch et al., 2013; Willis et al., 2016). At Zeppelin and Gruvebadet, NPF events are often associated with elevated concentrations of DMS and MS^- on hourly time scales, particularly in spring (Dall´Osto et al., 2017; Park et al., 2021). Notably, molecular cluster observations revealed a dominance of springtime NPF involving sulfuric acid (H_2SO_4) and ammonia (NH_3) at Gruvebadet (Beck et al., 2021). Along with this, high concentrations of gas- or particle-phase MSA coincide with rapid growth of nano-size particles often up to CCN-size particles (Willis et al., 2016; Beck et al., 2021; Park et al., 2021; Kecorius et al., 2023), underscoring the significant role of MSA for particle growth. However, Beck et al. (2021) also revealed that, as the season progresses to summer, highly oxygenated organic molecules (HOMs) may become a dominant contributor to particle growth and possibly even in NPF. Similar NPF mechanisms, involving H_2SO_4-NH_3 nucleation and growth by MSA and/or organic molecules, are also likely at Alert (Croft et al., 2016b) during summertime regional growth events (Tremblay et al. 2019), at other Canadian Archipelago regions in summer (Mungall et al., 2017; Willis et al., 2017; Croft et al., 2019), and at Utqiaġvik, Alaska (Kirpes et al., 2022). Furthermore, limited simultaneous measurements of sulfur isotopic composition ($\delta^{34}S$) of SO_2 and submicron SO_4^{2-} (<0.49 μm) suggest episodic particle growth driven by biogenic SO_2 during the summer months (Seguin et al., 2011; Ghahreman et al., 2016).

On the other hand, a range of observational evidence demonstrates the contribution of non-biogenic-sulfur and non-sulfur particle sources to the Arctic aerosol population and the CCN budget, even from May to September. Importantly, $\delta^{34}S$ measurements demonstrate that non-biogenic sources can account for 30%–70% of $nssSO_4^{2-}$ during July–August, and even more in other months (Norman et al., 1999; Rempillo et al., 2011; Seguin et al., 2011; Leaitch et al., 2013; Ghahreman et al., 2016). This non-biogenic sulfur includes anthropogenic (Ghahreman et al., 2016; Jongebloed et al., 2023b), volcanic sources including noneruptive, passive degassing of H_2S and SO_2 (Jongebloed et al., 2023a), and potentially biomass burning emissions (Mungall et al., 2016; Li et al., 2024b). We note that the $\delta^{34}S$ measurements of SO_4^{2-} from a Greenland ice core by Jongebloed et al. (2023a) and Jongebloed et al. (2023b) provide averaged values over 1–2 years and are not directly applicable to distinguish seasonal SO_4^{2-} sources. Anthropogenic sources of both sulfur-containing and other aerosol types are notably important in Arctic regions. Increasing Arctic development (Schmale et al., 2018) may also contribute to primary emission of CCN-sized aerosol and NPF and growth. Indeed, increased aerosol growth is observed within and downwind of Arctic oil fields in June–September (Kolesar et al., 2017; Gunsch et al., 2020). In addition, limited size-resolved aerosol composition data suggest a minor contribution of sea-salt-SO_4^{2-} to submicron size particles during spring and autumn (Rempillo et al., 2011; Seguin et al., 2011). Important natural non-sulfur aerosol sources include primary marine aerosol and biological particles that can be enhanced in biologically active periods (Kojoj et al., 2024; Pereira Freitas et al., 2024; Creamean et al., n.d.). Iodic acid (HIO_3) is another important driver of NPF, depending on season and region; for example at Villum in spring (Sipilä et al. 2016; Dall´Osto et al., 2018; Beck et al., 2021) and in the Central Arctic in autumn during sea ice freeze up (Baccarini et al., 2020; Price et al., 2023). Modeling studies suggest that the entrainment of particles formed in the free troposphere can make up a dominant contribution to the boundary layer particles at Alert and Zeppelin from fall into spring (Croft et al., 2016a), and even in summer in the Central Arctic (Price et al., 2023). These free-tropospheric-NPF events can involve natural and anthropogenic sulfur and organic molecules originating from lower latitudes outside the Arctic (Gordon et al., 2017; Price et al., 2023), potentially providing further challenges for developing accurate models of the Arctic aerosol budget. Overall, the relative contributions of these various Arctic aerosol sources and the spatial and

temporal contributions of biogenic sulfur NPF precursors must be carefully evaluated.

2.4.2. Potential VMS contribution to NPF and growth in the Antarctic

NPF and growth events in Antarctica are similar to the Arctic, though with some noticeable differences. The occurrence probability of aerosol size distribution types at Halley station (**Figure 5e**; Lachlan-Cope et al., 2020) shows the dominance of "Pristine" aerosol size distributions, particularly in austral winter (May–August), due to the isolation from major anthropogenic sources. This feature is also reflected in $nssSO_4^{2-}$ concentrations (**Figure 5k**) with a winter minimum (May–September) and an increase in summer (December–March) driven by biogenic sulfur sources from ice and ocean (Ishino et al., 2019), unlike in the Arctic where $nssSO_4^{2-}$ aerosols in winter and spring are dominated by anthropogenic sources (e.g., Norman et al., 1999; Willis et al., 2018; **Figure 5j**).

Despite these clean conditions, the occurrence probability of NPF-like features in the aerosol population (**Figure 5e**) shows a different seasonality from that of biogenic sulfur species (**Figure 5g** and **i**). The sum of "Nucleation-Bursting" and "Nascent" aerosol size distribution frequencies exceeds 20% of the time from September to April, that is, the austral spring to autumn (**Figure 5e**), as is also common to the Arctic. However, the highest occurrence appears in spring (September–November) rather than mid-summer (December–January), without significant increases in biogenic sulfur species (**Figure 5g**, **i**, and k). This unique increase of ultrafine particles in early spring is common across the coastal Antarctic (Hara et al., 2011; Weller et al., 2011a; Herenz et al., 2019; Park et al., 2023) and even over sea ice (Humphries et al., 2016). For example, Humphries et al. (2016) have shown approximately 10 times higher concentrations of ultrafine particles at the pole-side compared to the equator-side of the polar front in spring (October), and identified its source as an intrusion from the free troposphere into the boundary layer associated with cyclone activity. Even though a series of studies also suggested the free troposphere as a dominant source of particles in the Antarctic boundary layer (Hara et al., 2011; Lachlan-Cope et al., 2020), the NPF mechanism there remains largely unknown (No. 8 of **Figure 1**). It is commonly believed that, for the case of the remote marine atmosphere, the convective updraft through clouds efficiently transports DMS and other organic vapors to the free troposphere as potential sources of NPF (Kazil et al., 2011; McCoy et al., 2021). However, year-round $\delta^{34}S$ measurements of $nssSO_4^{2-}$ at East Antarctica suggest a significant contribution from non-biogenic SO_4^{2-} (20%–50%) specifically in November (Ishino et al., 2019). In addition, significant iodine oxide (IO) concentrations appear in springtime Antarctica (Saiz-Lopez et al., 2007; Schönhardt et al., 2012) and may be linked to iodine-driven NPF observed at several Antarctic stations around Weddell Sea area (Roscoe et al., 2015; Sipilä et al., 2016).

The rest of the Antarctic frequent NPF period (December–April) coincides with elevated biogenic sulfur species (**Figure 5g**, **i**, and **k**). Notably, $nssSO_4^{2-}$ in this period is dominated (>90%) by biogenic sources based on $\delta^{34}S$ measurements (Ishino et al., 2019; Walters et al., 2019). Molecular cluster measurements during mid-summer (December–January) revealed that NPF events were primarily driven by H_2SO_4 and bases such as NH_3 and amines (Jokinen et al., 2018; Baccarini et al., 2021; Brean et al., 2021). These events are often observed in air masses which have passed over the MIZ, while a scarcity of NPF events has been noted over open ocean areas of the Southern Ocean (Kerminen et al., 2018; Baccarini et al., 2021). This could suggest both an important source of biogenic precursors from sea-ice regions and a suppressed condensation sink from lower sea spray emissions compared to open ocean. Note that free-tropospheric NPF is also identified for this period and a quantitative assessment of the relative contribution of free-tropospheric versus sea-ice-sourced NPF remains a future area of research (Lachlan-Cope et al., 2020; McCoy et al., 2021). Also, NPF frequency is slightly higher in March than in February (**Figure 5e**), which also coincides with March maxima in ultrafine particle number concentrations at Neumayer (Weller et al., 2011a) and Syowa (Hara et al., 2021), but not at King Sejong (Jang et al., 2019). Weller et al. (2011a) pointed out that this March maximum was accompanied by a small secondary maximum in MSA, after the primary peak in January, and proposed a linkage to the enhanced biological productivity during the sea ice minimum. With the recent findings regarding autumn blooms of sea-ice algae in the Weddell Sea (see Section 2.1.2), this March particle formation is worth revisiting in both field and modeling studies.

2.4.3. Knowledge gaps common to the Arctic and Antarctic

In addition to this seasonal picture, episodically extreme emission of VMS at the time of sea ice breakup has been a subject of debate for both poles. Although the initial hypothesis of episodic emission by Levasseur et al. (1994) included a possibility of emission through sea-ice leads and cracks during the entire season, the largest impact is expected when in-sea-ice DMS concentrations are at a maximum. They suggested that, in the Canadian Arctic Archipelago, DMS accumulated at the bottom 2 cm of sea ice during mid-May was suddenly released into the surface seawater (2 m mixed layer depth), leading to estimated seawater DMS concentrations of 3–12 nmol L^{-1} and a flux to the atmosphere of 5–20 μmol m^{-2} day^{-1} continuing for a full day. The potential occurrence of such short-term emissions associated with sea-ice melt was verified by a 1-D model experiment which considers the sea-ice biogenic sulfur cycle and more realistic seawater dynamics, although they obtained a more modest DMS flux up to 8 μmol m^{-2} day^{-1} in mid-June (Hayashida et al., 2017). A subsequent 3-D model study found a maximum contribution of bottom-ice DMS to surface seawater DMS concentrations (>50%) in May, both in the Canadian Arctic Archipelago and central Arctic (Hayashida et al., 2020). Similarly in the Antarctic, extremely high seawater DMS concentrations (>10 nmol L^{-1}) at the onset of sea-ice melt have been observed in seasonal ice areas (Trevena and

Jones, 2006; Webb et al., 2019) and leads (Zemmelink et al., 2005) from late spring to mid-summer (November–January, see Section 2.1). The high concentrations lasted longer than in the Arctic, possibly linked to the dominance of slush-layer communities in sea-ice DMS production in the Antarctic (Stefels et al., 2018). Furthermore, Antarctic shipborne observations in austral spring and summer indicate abrupt increases in atmospheric DMS concentrations from below <100 ppt_v to > 2,000 ppt_v associated with marginal ice regions and ice break-up (Koga et al., 2014; Mynard et al., 2025).

Despite this growing body of knowledge on DMS emission from sea-ice covered regions, limited information on MeSH emissions adds a large and unquantified uncertainty to our understanding of key aerosol precursor gases (Section 2.3). Notably, the existing database of MeSH/VMS at colder SSTs (<8–12°C; Wohl et al., 2024) lacks coverage in undersampled sea-ice regions with extremes in cold SST and likely distinct biological sulfur cycling dynamics (Section 2.1.1; e.g., Teng et al., 2021). For example, because of its short lifetime (Section 2.1) dissolved MeSH may not persist below sea ice long enough for substantial emission to the atmosphere, which could suppress MeSH/VMS in sea-ice regions. Process studies across the OIA interface are required to develop a better understanding of MeSH sources from sea-ice regions. Overall, developing a comprehensive picture of sea-to-air VMS fluxes during episodic emissions is technically challenging, and therefore we lack knowledge of their scale, frequency, and consequent impact on the polar aerosol budget.

In summary, from current knowledge on the spatiotemporal variability in NPF and growth mechanisms and VMS emissions from sea-ice regions, we hypothesize that sea-ice-derived biogenic sulfur could have important impacts on the polar aerosol population. In the Arctic, sea-ice biogenic sulfur is likely most relevant during the onset of biological activity in spring, especially in May to June. Given that this period partly overlaps with prevalent reactive halogen species such as BrO· and Cl· (Saiz-Lopez et al., 2007; McNamara et al., 2019; Benavent et al., 2022) that are important oxidants for DMS and potentially MeSH (Section 2.3), atmospheric models with comprehensive multiphase chemistry and halogen cycling will be necessary to precisely evaluate VMS impact on aerosol formation. In the Antarctic, on the other hand, the importance of sea-ice biogenic sulfur to the aerosol population is persistent to mid-summer (November–January). To represent this extended time period in the Antarctic, slush-layer communities (Section 2.1) must be included in sea-ice biogeochemistry models. Development of parameterizations for localized emissions associated with sea ice breakup is also important for implementation in large-scale models. More atmospheric VMS measurements focusing on fluxes from melt periods, slush layers, and the MIZ are required to better capture the frequency and magnitude of fine-scale emissions. In addition, given that modeling studies point to an importance of free-tropospheric-NPF events at both poles, seasonally and spatially expanded vertical profile measurements of aerosol properties are essential.

3. Current modeling works and limitations

A range of key features must be captured to represent the polar biogenic sulfur cycle in models (Section 2). These include biogenic sulfur production in and around sea ice (Section 2.1), sea ice effects on VMS emission (Section 2.2), and atmospheric VMS oxidation processes (Section 2.3) under the specific oxidant and low temperature environments of the polar atmosphere (**Figures 1** and **3**). Potential future changes in the polar biogenic sulfur cycle through different processes are summarized in **Table 1**, and the inherent complexity emphasizes the call for further developing integrated ESMs to evaluate climate impacts under ongoing warming. However, most of these polar-specific processes are either poorly represented or not considered at all in the current ESMs, owing to different levels of obstacles. Some parameterizations are under development in 1-D or regional-scale models, but others lack observations and laboratory experiments to develop parameterizations. Also, there are several general bottleneck issues in ESMs, such as the reproducibility of the sea ice distribution (Section 3.1), that challenge the precise representation of the sulfur cycle. This section describes the current status of polar sulfur cycle representations in models, ranging from lower dimensional, simplified models to ESMs. We aim to identify possible approaches and concerns for future model development. Although MeSH is increasingly recognized as an important component of the biogenic sulfur cycle (Sections 2.1 and 2.3), it is not yet included in either regional or global models. As a result, assessing its broader impact on the aerosol life cycle remains difficult. Without at least regional-scale model studies that explicitly simulate its oxidation and conversion to aerosol sulfur, the role of MeSH in polar aerosol formation and climate feedback cannot be fully understood. Therefore, this section focuses on DMS using existing literature that identifies gaps in model descriptions.

3.1. Modeling ocean and sea-ice biogeochemistry

3.1.1. General issues in the representation of marine sulfur biogeochemistry

Among the ESMs participating in the sixth phase of the Coupled Model Intercomparison Project (CMIP6), only 4 simulate surface ocean DMS concentrations, with 2 models computing DMS prognostically (CNRM-ESM2-1 and NorESM2-LM) whereas the other 2 are diagnostic (MIROC-ES2L and UKESM1-0-LL) (Table S2). In CNRM-ESM2-1, $DMSP_p$ is computed from the carbon biomass of the 2 phytoplankton groups (diatoms and nanophytoplankton) via group-specific DMSP-to-carbon ratios which further vary with nutrient, light, and temperature stress (Séférian et al., 2019). DMSP is released from phytoplankton to seawater ($DMSP_d$) by exudation, cell lysis or grazing by zooplankton and is then converted to DMS with a yield dependent on nutrient stress to bacterial activity (Section 2.1.1; Belviso et al., 2012). DMS sinks are then bacterial degradation, photooxidation, or emission to the atmosphere. However, CNRM-ESM2-1 does not couple ocean and atmospheric sulfur cycles, and instead a prescribed DMS air–sea flux is used in the aerosol model simulations. In contrast, NorESM2-LM simulates a fully coupled ocean–

atmosphere sulfur cycle but does not consider DMSP. Instead DMS production is computed from the detritus export rate which is used as a proxy for phytoplankton cell destruction from lysis or grazing (Kloster et al., 2006). The same DMS sinks as CNRM-ESM2-1 are considered, and both models use the same air–sea flux parameterization (Wanninkhof, 2014; Section 3.3). The other 2 models consider simpler schemes, with MIROC-ES2L computing DMS concentrations directly from chlorophyll concentration and the mixed layer depth, based on Aranami and Tsunogai (2004), whereas UKESM1-0-LL considers the parametrization of Anderson et al. (2001) which uses chlorophyll concentration, light level, and nitrate concentration. For the air–sea flux, MIROC-ESL2 follows the approach of Aranami and Tsunogai (2004) and UKESM1-0-LL follows Liss and Merlivat (1986), with both models feeding the DMS emissions into the aerosol module. In addition, the CESM v1.2 model also incorporated an atmosphere–ocean coupled sulfur cycle to evaluate the CLAW hypothesis (Wang et al., 2018), but again without representation of the sea-ice sulfur cycle. Overall, the representation of marine sulfur biogeochemistry in ESMs remains simplified and many processes described in Section 2.1.1 (e.g., intracellular conversion of $DMSP_p$ to DMS by algae) have yet to be included. In particular, none of these CMIP6 models simulate the production and emission of MeSH from the ocean, and the production of any VMS in sea ice.

Figure 6 presents both time series and 30-year climatologies of summer mean surface ocean DMS concentrations in polar regions from these 4 CMIP6 models. Focusing on the global historical and SSP585 simulations, Bock et al. (2021) in their CMIP6 evaluation found that there is no agreement on the absolute values nor the sign of the trend of DMS concentration and fluxes, with increasing and decreasing trends found in both prognostic and diagnostic models. In the poles (**Figure 6**), the trend in DMS concentration is weaker than the global trend; in contrast, models predict a sharper rise in DMS flux. This can be explained mainly by a strong decline in sea ice extent, as all models linearly scale DMS emissions on the non-sea ice-covered fraction, in addition to an increase in wind speeds (Joge et al., 2025). The trend in DMS concentration is of secondary importance in polar regions. In the Arctic, this is further supported by the strong correlation between DMS emissions and sea ice free extent found in all models, over both past and future simulations. However, global changes in flux are dominated by trends in DMS surface concentrations, confirming the conclusions of previous work on observation-based seawater DMS estimates that gas transfer parametrization and spatial distribution of DMS is of secondary importance (Tesdal et al., 2015). Nonetheless, the trend in flux is slightly shifted positive, likely due to the dependence on SST of gas exchange parametrizations, which will increase strongly in the SSP585 scenario.

A more comprehensive assessment of performance of these models compared with data-based seawater DMS estimation products from Lana et al. (2011), Galí et al. (2018), and Wang et al. (2020) is given in Bock et al. (2021), and here we briefly describe the polar features. Bock et al. (2021) concluded that, both globally and in polar regions, models don't agree with each other and that none of the models performs better than the others. In particular, they note no significantly better skill for prognostic models. The models underestimate DMS concentrations compared to the global climatologies (Lana et al., 2011), while the multi-model mean is the closest to the "empirical model" type data-based products (Galí et al., 2018; Wang et al., 2020). In the Arctic, models show a large spread in concentrations (**Figure 6**) and fluxes as well as trends. When compared with the recent Arctic-specific satellite-based DMS estimation product (Galí et al., 2019), only MIROC-ES2L simulates higher DMS along the Arctic coasts both in the present and future, as opposed to the other 3 models. Around Antarctica, none of the models reproduce the high levels of DMS shown in Lana et al. (2011) (**Figures 6** and **7d**), whereas we note that Lana dataset may suffer from a positive sampling bias (see Section 3.2). In both hemispheres, the models reproduce a clear seasonal cycle of DMS concentrations, following the timing and duration of the summer maximum observed in data-based DMS estimates (Lana et al., 2011; Galí et al., 2018; Wang et al., 2020), but underestimating the amplitude compared to Lana et al. (2011; Bock et al., 2021). This seasonal cycle is however not seen in the DMS emissions of all models, with only 2 models showing a clear summer maximum (Bock et al., 2021). CNRM-ESM2-1 and UKESM1-0-LL simulate high emissions in the southern ocean but for different reasons: for the latter it is a consequence of high DMS concentrations, whereas in the former it is a combination of year-round high sustained winds and moderate DMS concentrations. Global emission estimates from the 4 models are within the range of previous studies (Tesdal et al., 2015). However, with the current low resolution of ocean models and the lack of specific processes such as DMS enhancement under sea ice and release during breakup, these models do not reproduce short and local episodes of large DMS emissions in polar regions. Moreover, these models likely underestimate DMS concentrations below sea ice as they don't account for production from sea-ice algae (Section 2.1.2). Thus, the simulated DMS emissions, in particular during sea ice breakup, might represent the lower bound of actual fluxes. A machine learning (ML)-based approach may be a promising alternative way to reduce the uncertainty of future projections in seawater DMS concentrations by ESMs (Joge et al., 2025; see Section 3.2 for details).

3.1.2. Difficulty in representations of sea ice physical status

Adequate representation of changes in the sea ice physical status is also an important step toward reasonable representation of the sulfur cycle in models. Both snow and sea ice determine the light availability for DMSP-producing algae that grow within and under sea ice. The timing of sea ice formation, breakup, and retreat is important for correctly simulating the timing of VMS production, accumulation, and emissions. In the Arctic Ocean, uncertainties in the simulated sea ice extent of ESMs have been

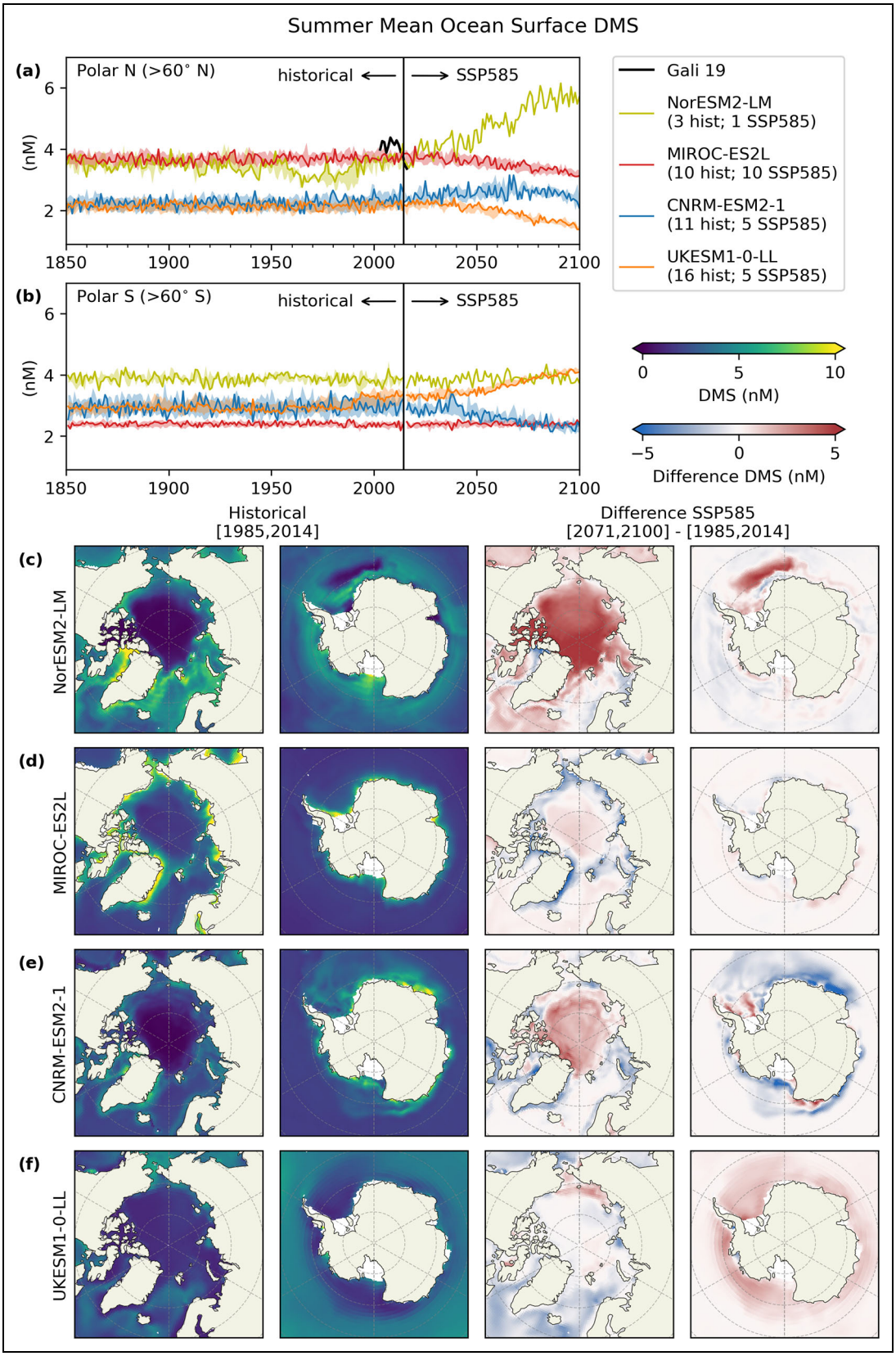

Figure 6. Mean ocean surface DMS concentrations from CMIP6 models for the Historical and SSP585 scenarios. (a, b): Time series of summer mean ocean surface DMS for the polar regions (a) beyond 60°N and (b) beyond 60°S. Lines correspond to a single simulation and shaded areas show the range of values of all simulations of the ensemble, with numbers in legend indicating the size of the ensemble. (c–f): 30-Year climatologies of summer mean ocean surface DMS for (c) NORESM2-LM, (d) MIROC-ES2L, (e) CNRM-ESM2-1, and (f) UKESM1-0-LL, computed from a single simulation for each model. The 2 columns left show the 30-year mean over 1985–2014 and 2 columns right are the difference between the future (2071–2100) and recent past (1985–2014). Summer means are computed over the summer months in the northern (June, July, and August) and southern (December, January, and February) hemispheres.

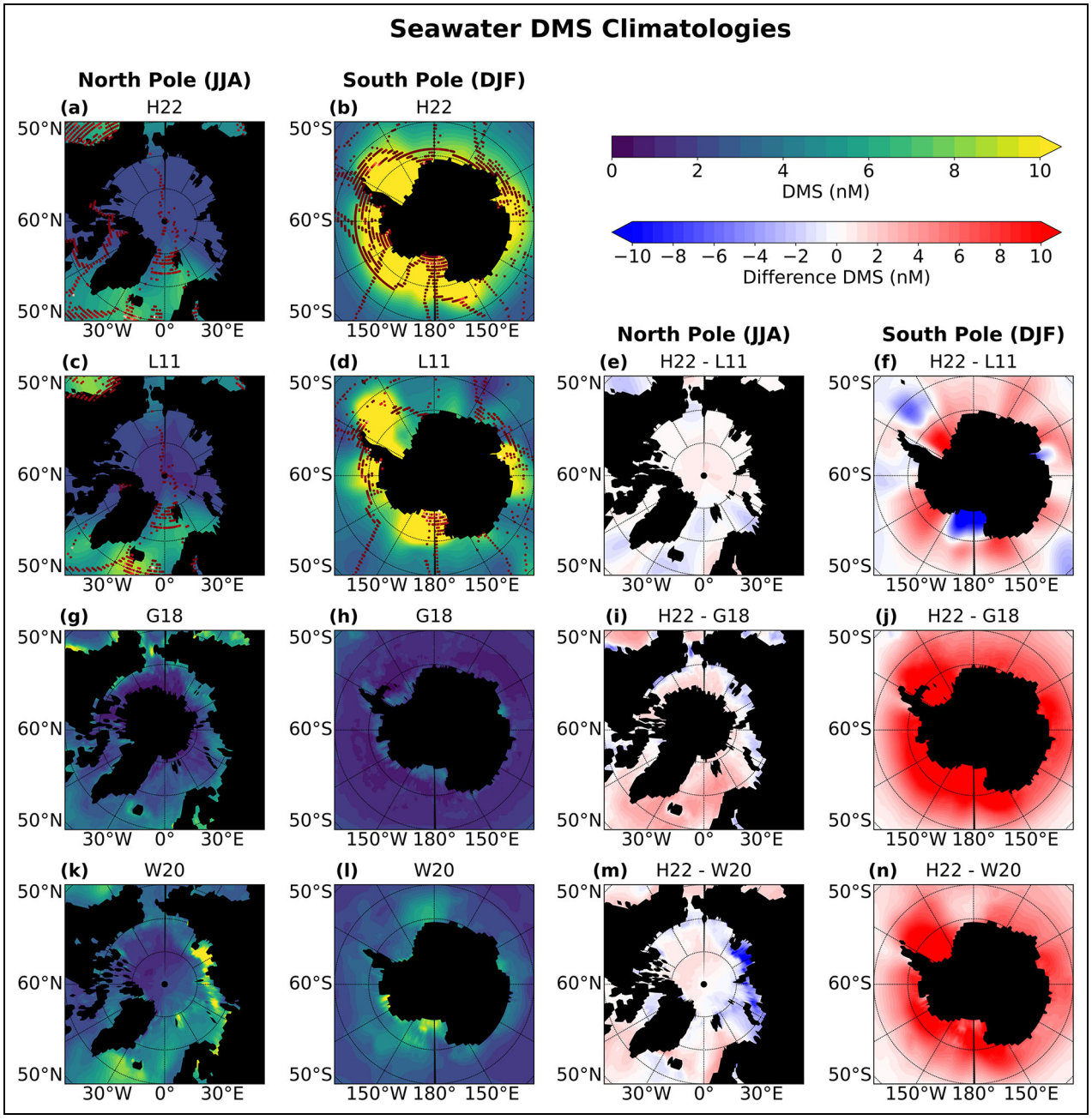

Figure 7. The latest seawater DMS climatologies using different techniques. Data for the summer months in the northern (June, July, and August) and southern (December, January, and February) hemispheres are shown. The top panels show the Hulswar et al. (2022) climatology (H22), which was updated using new observations since the Lana et al. (2011) climatology (L11; second row). The observations in both climatologies are included as red dots in (a)–(d). The third row shows the Gali et al. (2018) (G18) which was created using regression analysis on satellite-based proxies; the bottom row shows the Wang et al. (2020) (W20) climatology predicted using an artificial neural network with satellite-based proxies as inputs. The differences of each climatology with the H22 climatology is shown in the right-hand side columns.

reported for present and future projections of CMIP3, CMIP5 (Stroeve et al., 2012), and CMIP6 (Notz and SIMIP Community 2020). The declining trend of sea ice concentration simulations in Kara-Barents Sea has been shown to follow the strength of the Gulf Stream and its associated ocean heat transport to the Kara-Barents Sea (Yamagami et al., 2022). The subsurface ocean heat content is therefore a critical source of predictability of Arctic sea ice thickness and its extent simulations (Collow et al., 2015; Yeager et al., 2015; Dirkson et al., 2017; Bushuk et al., 2021).

Climate model evaluations have identified low confidence in simulating Antarctic sea ice extent in CMIP5 models, which has been improved for key characteristics of its seasonal cycle in CMIP6 (Turner et al., 2013; Roach et al., 2020). Eddy-permitting or eddy-parameterizing the ocean model embedded in ESMs may play a key role to reduce the warm bias of SST in the Southern Ocean and

simulate Antarctic sea ice extent realistically (Adcroft et al., 2019). Advected upper-oceanic heat content may provide regional Antarctic sea ice prediction and predictability skill (Bushuk et al., 2021). However, realistic representation of Antarctic sea ice minima in the austral summer is still challenging for most climate models (Roach et al., 2020) which may cause biases for modeling DMS seasonal cycles and DMS emissions predictability associated with sea-ice retreat (Haddon et al., 2025). In addition, freshwater discharge into the Southern Ocean resulting from massive loss of Antarctic ice-sheets/shelf has not been included in ESMs. Freshwater discharge into the Southern Ocean may not only play a role of controlling regional (Oh et al., 2020) and global climate (Bronselaer et al., 2018; Park and Latif, 2019) but also drive dynamical changes of various marine biogeochemistry (Bronselaer et al., 2020) and its limiting conditions for phytoplankton (Oh et al., 2022).

3.1.3. Representation of sea-ice-specific biogeochemistry

Despite the observational evidence for the accumulation of DMSP and DMS in sea ice (Section 2.1), only a handful of published studies exist on the development and application of DMS models within sea ice (Elliott et al., 2012; Hayashida et al., 2017; Hayashida et al., 2019; Hayashida et al., 2020; Haddon et al., 2025). These models represent the bottom sea-ice community in the Arctic and have shown the seasonal importance of bottom-ice DMS production to the annual oceanic emission. For example, albeit its small extent (a few centimeters), bottom-ice DMS can dominate the DMS emission at the beginning of the melt season (late spring) and before the onset of the pelagic DMS production following phytoplankton blooms (Hayashida et al., 2020). However, sea-ice and ocean biogeochemical models in general still struggle to reproduce the seasonal cycles of ice algal and pelagic productivity (e.g., Watanabe et al., 2019); improvements in this area remain an active area of research and will aid in creating robust future projections of primary productivity and resulting VMS production.

Existing sea-ice DMS models lack representation of the interior and surface communities that can be important sources especially in Antarctic sea ice (Zemmelink et al., 2008a; Zemmelink et al., 2008b; Nomura et al., 2012; Section 2.1.2). Recently, vertically resolved sea-ice biogeochemistry has been incorporated into an ESM for the first time (Jeffery et al., 2020). This model simulates DMS, but its performance has not been evaluated nor has it been coupled to the atmospheric sulfur cycle. Future modeling efforts should be invested into constraining both the sea-ice algal and VMS processes by incorporating field observations of the intracellular ratio of DMSP to algal biomass (or chlorophyll-*a*) for the interior and surface communities in the Antarctic.

3.2. Data-based seawater VMS estimation products

In this section, we delve into the features of several different global seawater DMS estimation products, and specific considerations for their use in polar regions, which often arise as concerns for ocean and atmospheric modeling of the polar biogenic sulfur cycle (e.g., Bock et al., 2021; Bhatti et al., 2023; Joge et al., 2024a). These data products have played a critical role in evaluating the reliability of ocean DMS models (Bock et al., 2021) and serving as the boundary condition for atmospheric DMS emissions in climate model projections (e.g., Carslaw et al., 2013; Mahajan et al., 2015). The estimated data products include "climatologies," based on informed interpolation of in situ seawater DMS observations by objective analysis (e.g., Kettle et al., 1999 (K99); Lana et al., 2011 (L11); Hulswar et al., 2022 (H22)), and "empirical models," which predict DMS concentration distributions using statistical relationships with other variables with better data coverage (e.g., Galí et al., 2018 (G18); Wang et al., 2020 (W20)). Most of these efforts have focused on using an open-access database of observations (available at: https://saga.pmel.noaa.gov/dms; last accessed on March 29, 2025) to create gridded monthly climatologies representing the average of long-term data, but more recent work focuses on creating empirical models with time-dependent seawater DMS estimations (e.g., Mansour et al., 2023; Mansour et al., 2024; Joge et al., 2025).

DMS climatologies have evolved significantly both in the quantity of observations on which they rely and in their approaches to interpolating observations that remain sparse in many regions. The latest climatology (Hulswar et al., 2022 (H22)) was developed using 18-fold more in situ measurements than the most frequently used climatology (Lana et al., 2011 (L11)) and incorporating a significantly improved interpolation procedure (Manville et al., 2023). **Figure 7a**–**d** highlights better data coverage in H22 for polar regions. In the Arctic, H22 includes in situ measurements in the Davis Strait and the Canadian Arctic Archipelago during boreal summer (**Figure 7a**), which were lacking in L11 (**Figure 7c**). The addition of the new data points in these and other Arctic regions does not change the climatological values significantly (**Figure 7e**), but it does build confidence in the climatology (**Figure 7a**). However, many parts of the Arctic (the Beaufort, East Siberian, Kara, Laptev, and Barents Seas) still have low or no in situ data coverage, due to the difficulty in accessing these regions, limiting the climatology's credibility for large regions of the Arctic. In the Antarctic, data coverage in the latest climatology has improved across the region (**Figure 7b** relative to 7d), which resulted in a larger difference from the earlier climatology compared to the Arctic (**Figure 7f**). Most remarkably, H22 shows about 10 nmol L^{-1} lower DMS concentrations in the Ross Sea and 10 nmol L^{-1} higher DMS concentrations in the Weddell Sea compared to L11. These differences presumably reflect the improvements due to the combination of increased data coverage and improved interpolation methods. However, the Southern Ocean remains poorly sampled for DMS—spatially (e.g., zonally in the Pacific sector), seasonally (particularly during winter), and with few repeat interannual observations (Galí et al., 2018; Hulswar et al., 2022). This persistent sparsity, coupled with highly localized and variable DMS concentrations in sea-ice environments—spanning up to 4 orders of magnitude—introduces substantial uncertainty. Observational data are heavily biased toward the austral summer, and

climatologies omit measurements beneath sea ice (Galí et al., 2018; Hulswar et al., 2022; Zhou et al., 2022). Consequently, the extrapolation of summer DMS hot spots across broad, under sampled regions likely leads to overestimates of Southern Ocean DMS concentrations in L11 and H22 (Galí et al., 2018; Hulswar et al., 2022; Bhatti et al., 2023; **Figure 7f**).

To deal with the challenge in data coverage, DMS "empirical model" products are developed relying on emerging relationships between observed DMS and environmental predictors such as SST, irradiance, chlorophyll-*a*, and the mixed layer depth (e.g., Simó and Dachs, 2002; Belviso et al., 2004). Two of the recent global empirical model products through regression analysis (Galí et al., 2018; G18) and ML approaches (Wang et al., 2020; W20) are shown for comparison with H22 (**Figure 7g**–**n**). These approaches estimate generally lower DMS seawater concentrations than the observation-based climatology in both polar regions (Joge et al., 2024a). This systematic low bias compared to climatologies suggests difficulty in applying the empirical model parameterizations that are presumably heavily reliant on the oceanographic conditions in the extra-polar region. Alternatively, as mentioned above, the extrapolation of existing observations to open water DMS is likely to have resulted in a positive bias in polar regions of the H22 climatology. Each of the available approaches has advantages and limitations, potentially leading to significant differences in the resulting estimates of DMS concentration, particularly at high latitudes (**Figure 7**). Hence, caution must be taken when applying different products and interpreting the results, while quantifying the uncertainties associated with the use of different seawater DMS products.

The evaluation of ocean biogeochemistry models using these DMS data products is discussed in Bock et al. (2021) from a global perspective and in Section 3.1.1 with a focus on polar regions. Most atmospheric chemistry models use the L11 or K99 climatologies and generally capture the seasonality of atmospheric DMS in the 4 limited station-based observations, including 1 from the mid-Northern latitudes, 2 from the mid-latitude Southern Ocean, and 1 from coastal Antarctica (e.g., Castebrunet et al., 2009; Mahajan et al., 2015; Jongebloed et al., 2025). However, Bhatti et al. (2023) showed with the UKESM model that atmospheric DMS concentrations over the Southern Ocean are better reproduced when using their "empirical model" product based on satellite chlorophyll-*a* data, compared with using L11 or H22. Moreover, for the summertime Arctic, Ghahreman et al. (2019) showed that their model (GEM-MACH) underpredicts shipborne atmospheric DMS measurements using either L11 or G18. A comprehensive assessment of the choice of seawater DMS data products for modeling polar aerosols remains lacking.

Note that 2 major issues remain with these climatologies and empirical models in polar regions. First, the existing DMS database lacks under-ice observations, which will result in a negative bias in the climatologies if an ice mask of null concentrations is used, and inaccurate emissions if no ice mask is used as the values result from interpolation of open water measurements. Second, both types of products miss high-frequency variability in seawater DMS concentration and DMS flux spikes associated with some phytoplankton blooms, which may drive episodic emissions inducing NPF and particle growth events in polar regions (see Section 2.4.3).

ML-based empirical models could in theory address these issues subject to the sufficient number of observations (e.g., Wang et al., 2020; McNabb and Tortell, 2022; Zhao et al., 2022; Mansour et al., 2023; McNabb and Tortell, 2023; Mansour et al., 2024). However, they are currently struggling to capture high DMS concentrations (**Figure 7k**–**n** for W20), because predictor-DMS relationships vary across time and location. It is important to identify the exact predictors using sufficiently high-frequency observations across ocean basins. Considering potential high nonlinearity between DMS and its predictors, the choice of the ML algorithm is also crucial. Artificial neural network-based algorithms (e.g., Wang et al., 2020) require a larger number of data and strong correlation between predictors and DMS, while the Gaussian Process Regression (GPR) algorithm (e.g., Mansour et al., 2023; Mansour et al., 2024) can work even with a smaller dataset due to its ability to quantify the uncertainty and prediction confidence. Despite these challenges, ML techniques have already led to major improvements in the estimation of seawater DMS both globally and regionally. For example, Joge et al. (2025) resolved discrepancies in sign and trend among CMIP6 model projections of global seawater DMS concentrations (Bock et al., 2021; Section 3.1.1) using ML algorithms, suggesting a future decline in concentrations but increase in the sea-air flux due to increasing wind speed. Future efforts should focus on the development of ML-based seawater DMS empirical models specifically tailored to polar regions, ideally constructed separately for the Arctic and Antarctic, which will require a sufficient number of high-frequency observations.

Finally, a first empirical estimate of seawater MeSH distribution is now available (Wohl et al., 2024), which applies linear scalings to seawater DMS in "warm" and "cold" SST regimes (above and below 8–12°C), and continental-shelf and open-ocean waters, based on a limited observational dataset (**Figure 2a**). Further development of MeSH distribution data products with expanded observations is a crucial need for future research.

3.3. Modeling VMS fluxes at OIA interface

Currently, global and regional atmospheric models commonly represent VMS emissions (specifically DMS) in sea-ice regions as the open ocean flux weighted by the sea ice fraction in each grid box of the model (Section 2.2). Models generally do not represent specific features in sea-ice environments, such as enhanced turbulence around sea ice, reduced fetch (e.g., Loose et al., 2017; Prytherch and Yelland, 2021) and meltwater layers (e.g., Smith et al., 2023), which may suppress or enhance the sea-to-air gas fluxes, or direct ice-to-air emissions from the surface slush layers (e.g., Zemmelink et al., 2008a). There remains a critical need for in situ observations of VMS fluxes in polar oceans and sea-ice environments to develop

generalized parameterizations. However, the lack of modeling studies evaluating the importance of these characteristics in sea-ice environments in turn hampers the motivation for the large-scale field campaigns required for such flux measurements. To get out of this loop between modelers and observers (Steiner et al., 2016), we discuss possible approaches to quantify uncertainties and limitations in models.

One important example is the ability to simulate episodic extreme VMS emissions from sea-ice leads and their potential importance for regional NPF (Levasseur et al., 1994; Koga et al., 2014; Section 2.4.3). In addition to the difference in emission mechanisms between leads and open ocean, the background aerosol and oxidant fields are different over sea ice and open ocean (Fossum et al., 2018; Jang et al., 2022), potentially causing different effects on NPF mechanisms. To adequately represent VMS fluxes from leads, 2 key pieces of information are needed: (1) where the leads are located and (2) a lead-specific emission parameterization. The location of leads can be informed by satellite products (e.g., Willmes et al., 2023; von Albedyll et al., 2024) at high spatial resolution ($\sim$1 km), although the temporal resolution (typically daily) may be too limited to capture some lead dynamics. Also, as some of these products are based on thermal contrast, they do not have data for the summer months. On the other hand, more recent sea ice models include improved representations of fine-scale sea ice physics, including the opening and closing of leads (e.g., Boutin et al., 2023). Contrary to satellite products, such models can provide high temporal resolution (typically 3- to 6-hourly) and full-year coverage. However, model resolutions of typically 5–10 km remain too coarse to represent most individual leads, but maybe enough to statistically represent lead fraction at the regional scale. Given this fine-scale variability of leads, the first step would be implementation into 1-D to regional-scale atmospheric models, for example, PACT-1D (Ahmed et al., 2022) or WRF-Chem (Marelle et al., 2021), with a reasonable representation of VMS oxidation chemistry (Section 3.4.2).

With respect to flux parameterizations, measurements of VMS flux from leads with a variety of width and fetch (Zemmelink et al., 2005) are inevitably needed. However, preemptive model sensitivity studies could identify the potential importance of lead emissions, for example, a sensitivity study varying the gas transfer velocity within the available range of suppression by 30% (Prytherch and Yelland, 2021) or by 3.5 times (Loose et al., 2024) relative to the equivalent open ocean conditions, with a potential enhancement at low wind conditions. In addition to such sea-ice-specific parameterizations, a reduced sensitivity in DMS gas transfer relative to CO_2 at medium to high wind speeds (>10 m s^{-1}) (Bell et al., 2017; Section 2.2) is an important feature to be considered in the sensitivity studies. Using a linear relationship between DMS gas transfer velocities and wind speed (Goddijn-Murphy et al., 2012; Blomquist et al., 2017), instead of traditionally used power-law relationships (Liss and Merlivat, 1986; Wanninkhof, 2014), reduces atmospheric DMS concentrations and results in a better agreement with observed fluxes (Bhatti et al., 2023). There is a considerable difference in the flux parameterizations proposed based on empirical findings (Joge et al., 2024a; Joge et al., 2024b), which affects the overall uncertainty in computing the DMS fluxes. In some areas, the uncertainty in sea-air DMS parameterizations is larger than the seawater DMS concentration uncertainty (Joge et al., 2024a; Joge et al., 2024b), underscoring the need for more detailed flux parameterization studies in the laboratory and field. Model sensitivity studies should take this effect into account to assess overall uncertainty.

Information on direct ice-to-air VMS emissions is also scarce (Section 2.2). Given the potentially large contribution of emissions from Antarctic surface slush layers (Zemmelink et al., 2008a; Nomura et al., 2012), the spatial distribution and potential impacts of this emission pathway could be tested through implementation in sea-ice biogeochemistry models with vertically resolved sea ice (e.g., Jeffery et al., 2020; Section 3.1.3). A key step would be to develop a parameterization representing the snow properties above sea ice, which regulates emissions to the atmosphere (Nomura et al., 2012). Combined simulations with the oxidant chemistry in the interstitial air within snow (e.g., Thomas et al., 2011) may be worthwhile to represent MeSH emission, given the more rapid oxidation of MeSH than DMS (Section 2.3).

3.4. Modeling atmospheric chemistry, particle formation, and VMS climate impact

3.4.1. Climate impact of DMS estimated in current large-scale models

The climate impact of changes in marine biological production and emission of VMS through modification of aerosols and clouds is consequently estimated by global or regional atmospheric aerosol models. Before delving into the current model representation of VMS oxidation and particle formation, we provide a note of caution on different definitions of climate impacts. Radiative forcing (RF), the most commonly used term, often refers to a change in the net downward radiative flux from preindustrial (PI: 1750 or 1850 depending on study focus) to present-day (PD), due to an imposed perturbation (e.g., changes in greenhouse gas or aerosol concentrations, or in DMS emissions) (Forster et al., 2021). However, RF is not always defined only for the industrial era. Comparison of RFs estimated for different time periods or model experiments is misleading. For example, the effective radiative forcing (ERF) in response to a temporal doubling in DMS emission (i.e., a "2xDMS simulation") is estimated to be -1.02 ± 0.29 W m^{-2} based on the average of ESM estimates in the CMIP6 framework (Thornhill et al., 2021). This ERF from a 2xDMS simulation cannot be directly compared to the better-known ERF values of anthropogenic CO_2 (2.16 [1.90 to 2.41] W m^{-2}) or aerosols (-1.3 [-2.0 to -0.6] W m^{-2}), which represent PI-PD changes (Forster et al., 2021). The PI-PD RF of DMS, on a global scale, is likely smaller than the ERF from a 2xDMS simulation because the PI-PD changes in DMS emissions in current models are much less than doubling (Bock et al., 2021; Section 3.1.1). Similarly, the concept of total RE,

which represents the instantaneous radiative impact of an atmospheric component and is calculated as the difference in radiative flux with and without the component in a model, is sometimes confused with RF (Heald et al., 2014). The REs of DMS estimated by different atmospheric models range from -2.03 to -1.49 W m^{-2} (Thomas et al., 2010; Mahajan et al., 2015; Fiddes et al., 2018); critically, these values are distinct from, and not comparable with, RF calculated in a 2xDMS simulation nor a PI-PD period. Furthermore, REs from short-lived atmospheric components, such as aerosols, usually have large spatial and temporal variability among individual model grid boxes because of their short atmospheric lifetimes relative to well-mixed greenhouse gases. This variability is often orders of magnitude larger than corresponding global annual mean RE. For example, Mahajan et al. (2015) investigated the difference in RE of DMS estimated using different DMS climatologies and derived a modest change of 0.3 W m^{-2} for the global annual mean but with a large regional and seasonal variability of up to ± 10 W m^{-2}. We emphasize that such estimates of seasonal and spatial variability are in no way representative of an uncertainty in the effect of DMS on Earth's radiative balance, as has been suggested in some recent literature (Hopkins et al., 2023).

Using any definition, our quantitative understanding of VMS climate impacts is strictly limited both globally and in polar regions. In the CMIP6 framework, an evaluation of climate feedbacks through changes in DMS emissions, with the abovementioned ERF from 2xDMS simulations, was conducted based on only 3 models, NorESM2-LM, UKESM1, and GISS-E2-1 (Thornhill et al., 2021; see Table S2). The former 2 models have ocean DMS biogeochemistry interactively simulated with climate changes (Section 3.1.1), while GISS-E2-1 uses prescribed seawater DMS concentration (Kettle et al., 1999). The simulations used sea-to-air DMS emissions dependent on wind speed and SST. The results of Thornhill et al. (2021) seemingly suggest a limited climate feedback effect arising from the projected future changes in DMS emission, at least on a global scale. However, this limited subset of models does not reflect the full range of knowledge or uncertainty in atmospheric chemistry, particularly regarding DMS oxidation pathways (see Section 3.4.2) and aerosol formation processes. Furthermore, in polar regions, the regional climate feedback effect of DMS may be more significant than on a global scale because DMS emissions are expected to increase substantially due to reductions in sea-ice cover (Section 3.1.1; Bock et al., 2021; Joge et al., 2025). A model sensitivity study focusing on the Arctic region shows that DMS emission could increase approximately 30% between 2000 and 2050 under the high greenhouse gas emission scenario (RCP8.5) with fixed seawater DMS concentration and reduced ice cover, resulting in a regional RF of -0.14 W m^{-2} (Mahmood et al., 2019). However, this projection bears a large uncertainty of future changes in seawater DMS concentration in the Arctic owing to a lack of modeled sea-ice biogeochemistry (Mahmood et al., 2019). To our knowledge, there has been no similar sensitivity study focusing on coastal Antarctica (>60°S), likely due to the poor reproducibility in sea ice dynamics (Section 3.1.2) as well as a lack of model representation of sea ice slush-layer communities which is particularly important in this region (Section 3.1.3). To set the starting point of our quantitative understanding of polar VMS climate feedback effects, more dedicated modeling studies are needed that include polar-specific VMS production, emissions, and oxidation pathways.

Modeled climate sensitivity to changes in DMS emission also potentially holds severe uncertainties owing to a large negative bias in particle number concentrations over the remote marine atmosphere (Williamson et al., 2019; Regayre et al., 2020; Mallet et al., 2023). Particularly over the summertime Southern Ocean, the modeled CCN number concentrations are generally biased negative by more than 50%, with larger biases at smaller particle sizes, when compared across station-based, shipborne, and airborne observations (Schmale et al., 2019; McCoy et al., 2021; Fiddes et al., 2025). This bias tends to be larger around coastal Antarctica where sea ice is present (Schmale et al., 2019; Fiddes et al., 2025), suggesting a larger uncertainty in the climate impact near Antarctica.

The insufficient representation of VMS oxidation processes, and complete lack of MeSH, in models is one of the potential causes of the negative particle bias (Revell et al., 2019; McCoy et al., 2021; Fung et al., 2022; Berndt et al., 2023). As introduced in Section 2.3, the balance between gas phase and multiphase reactions during VMS oxidation exerts an important control on the contribution of VMS to the CCN population (e.g., Woodhouse et al., 2010). Implementing a series of reactions discovered in the last decade, including those for both DMS and MeSH (Section 2.3), can either increase or decrease the CCN formation efficiency, leaving an unquantified error in the VMS climate impact estimates (see Section 3.4.2 for details). On the other hand, multiple potential processes may contribute to the negative bias in particle numbers, such as the lack of nano-size sea spray aerosol emissions (Xu et al., 2022; Sellegri et al., 2023), primary and secondary organic particles (McCoy et al., 2015; Willis et al., 2016; Willis et al., 2017; Williamson et al., 2019), and/or other nucleation mechanisms (Dunne et al., 2016; Sipilä et al., 2016). Improvement in dry and wet deposition schemes can also have a large effect on particle number budgets (e.g., Browse et al., 2014; Emerson et al., 2020; Luo et al., 2020). Correcting the bias introduced through processes other than VMS oxidation can also increase or decrease the contribution of VMS to CCN formation, for example, by providing more seeds to grow to CCN sizes or scavenging gaseous H_2SO_4 to suppress NPF (Browse et al., 2014; Mahmood et al., 2019). Model sensitivity studies to realistically correct the particle number bias with different processes are highly encouraged to assess the uncertainty in the response of CCN number concentrations to VMS emission changes.

The large negative bias of particle numbers in remote marine atmosphere, including polar regions, in current models also limits our ability to accurately estimate anthropogenic aerosol RF, and especially the very uncertain indirect effect due to aerosol–cloud interactions (Carslaw et al., 2013; Regayre et al., 2020). Carslaw et al.

(2013) found that the anthropogenic aerosol RF through aerosol–cloud interactions is very sensitive to natural, background particle concentrations due to 3 steps contributing to a nonlinear response of cloud albedo to emissions: (1) CCN concentrations are more sensitive to anthropogenic aerosol increases when the natural aerosol background concentration is low, (2) cloud droplet number concentrations are more sensitive to CCN concentrations when droplet numbers are low, and (3) cloud albedo is more sensitive to cloud droplet number increases when cloud droplet numbers are low. Based on this concept, correcting this negative bias in aerosol concentrations will further weaken the RF from anthropogenic aerosols (Regayre et al., 2020). Indeed, using the CAM6-Chem climate model, Fung et al. (2022) showed that the anthropogenic aerosol RF is reduced from -2.3 to -1.7 W m^{-2} by changing the representation of DMS oxidation chemistry from a model with multiphase oxidation pathways to one with gas phase DMS oxidation only. Considering only gas phase DMS chemistry increases background CCN number concentrations, thus producing a lower anthropogenic aerosol RF. Overall, a more accurate representation of VMS-driven particle formation processes will better constrain both the climate impact of VMS itself and the anthropogenic aerosol RF.

3.4.2. Model representation of VMS oxidation processes

Publicly available global atmospheric chemistry models generally represent DMS oxidation to SO_2 by only 3 reactions, H-abstraction with OH and NO_3, and O-addition with OH, which are all gas phase pathways (Section 2.3; e.g., Chin et al., 1996; Bian et al., 2024). Models generally do not consider important intermediates including DMSO, MSIA, MSA, HPMTF, and CH_3SO_2 radical, multiphase oxidation pathways, or emission and oxidation of MeSH (Sections 2.1 and 2.4). The 3-reaction gas phase DMS oxidation is highly simplified compared to the current understanding of complex chemistry summarized in Section 2.3 and **Figure 1**. On the other hand, SO_2 oxidation is usually represented with both gas phase and in-cloud (aqueous phase) pathways to form H_2SO_4 and SO_4^{2-} separately (Chin et al., 1996). Therefore, the production efficiency of gas phase H_2SO_4, which is necessary for the occurrence of NPF (Section 2.3), is largely regulated by the branching of SO_2 oxidation pathways between $H_2SO_{4(g)}$ and SO_4^{2-} (Woodhouse et al., 2010; Woodhouse et al., 2013). With the simplified gas phase chemistry, Woodhouse et al. (2010) showed a low sensitivity of CCN formation to the DMS emission changes in TOMCAT-GLOMAP model, such that CCN concentrations increase by 0.01%–0.1% in response to a DMS increase of 1%. This low sensitivity of CCN numbers to DMS underlies the weak estimates of global climate sensitivity to DMS emission changes discussed in Section 3.4.1.

Updating DMS oxidation chemistry and incorporating MeSH (Section 2.3) has the potential to significantly change the production efficiency of H_2SO_4 from VMS, and thus will affect NPF and the CCN budget (**Figure 1**; Berndt et al., 2023). Despite the robust understanding that gaseous H_2SO_4 is a minor product from SO_2 oxidation (10%–40%; Barth et al., 2000; Faloona et al., 2009), the overall yield of H_2SO_4 from VMS varies over a large range depending on the representation of VMS speciation and oxidation (30%–100%; Faloona et al., 2009; Novak et al., 2022; Wohl et al., 2024). Increasing numbers of modeling studies incorporate a fuller complexity of VMS chemistry into their atmospheric chemistry modules (e.g., Chen et al., 2018; Fung et al., 2022; Tashmim et al., 2024; Tashmim et al., 2025).

Adding multiphase oxidation pathways (e.g., considering MSA and HPMTF) into models significantly decreases the SO_2 yield from DMS, from 80%–90% to 40%–50%, thus suppressing H_2SO_4 production (Hoffmann et al., 2016; Fung et al., 2022; Cala et al., 2023; Tashmim et al., 2024). Still, existing studies struggle to reproduce the balance among different stable DMS oxidation products, highlighting the need for more laboratory studies on reaction kinetics, for example, for the production and loss processes of HPMTF (Ye et al., 2021; Jernigan et al., 2022; Assaf et al., 2023; Jernigan et al., 2024). Critically, the potential enhancement of H_2SO_4 production through $CH_3SO_2\cdot$ remains highly uncertain due to the limited knowledge of its steeply temperature-dependent fate (Shen et al., 2022; Berndt et al., 2023; Chen et al., 2023). Chen et al. (2023) implemented the temperature dependency of $CH_3SO_2\cdot$ fate into a global model and found a large increase of gaseous MSA ($\sim$170%), which was particularly pronounced in high-latitude regions in both hemispheres. However, their model did not consider multiphase oxidation pathways and did not evaluate H_2SO_4 (Chen et al., 2023), so our understanding of the overall impacts of temperature-dependent $CH_3SO_2\cdot$ fate remains incomplete. Furthermore, MeSH oxidation can supply $CH_3SO_2\cdot$ and thus SO_2 and/or H_2SO_4 depending on temperature (Section 2.3.2.2). The first work testing MeSH emission in a global model (Wohl et al., 2024) highlights the large potential RE of MeSH in the summertime Southern Ocean of -0.3 to -1.5 W m^{-2}. But again, multiphase oxidation and $CH_3SO_2\cdot$ pathways were missing in this atmospheric model, leaving the evaluation incomplete. Rapid H_2SO_4 formation through $CH_3SO_2\cdot$ at low temperatures (Chen et al., 2023) combined with strong MeSH emissions at high latitudes (Wohl et al., 2024) likely produces an important impact on biogenic sulfur-driven NPF in polar regions (Section 2.4); however, a complete model evaluation of these processes is lacking. Thus, there remains a long way to go in order to provide a comprehensive and predictive understanding of the impacts of VMS chemistry on the CCN budget and climate.

Challenges also remain for model evaluations. Model evaluations mostly rely on relatively stable compounds, such as gaseous DMS, SO_2, HPMTF, and particle phase MS^- and SO_4^{2-}. However, all these biogenic sulfur compounds can be affected by both an incorrect representation in emissions of VMS (Section 3.3) and inaccurate representations in oxidation chemistry, which complicates the interpretation of gaps between observations and models (Hoffmann et al., 2021; Cala et al., 2023; Bian et al., 2024). For example, Bian et al. (2024) evaluated 5 global

aerosol models with simplified DMS chemistry against NASA ATom flight observations and clarified that SO_2 tends to be biased low while DMS and SO_4^{2-} tend to be biased high across most regions and seasons. Although DMS concentrations during the ATom campaign were unusually low compared to other aircraft measurements (e.g., Yang et al. 2009; Andrews et al., 2016), Kang et al. (2025) reported a similar imbalance between modeled DMS, SO_2, and SO_4^{2-} over the Southern Ocean using independent aircraft data. This imbalance may result from overestimated DMS emission combined with other chemistry and dynamics uncertainties including overestimated SO_2 to SO_4^{2-} conversion rates, underestimated DMS to SO_2 conversion rates, and underestimated transport of SO_2 from the boundary layer to the free troposphere (Bian et al., 2024). In addition, SO_2 and SO_4^{2-} include anthropogenic and volcanic sources (Jongebloed et al., 2023a; Bian et al., 2024), which poses a concern for evaluating against 2 compounds only. Evaluation of modeled DMS seasonality against station observations further illustrates this challenge. Studies using the GEOS-Chem model (Tashmim et al., 2024; Jongebloed et al., 2025) show that an unexpected wintertime increase in DMS concentrations across Southern Hemispheric stations can be apparently fixed by adding DMS oxidation reactions (e.g., DMS + BrO, DMS + $O_{3(aq)}$). However, the ability of the model to reproduce seasonality in oxidation products at the same stations has not been confirmed, so potential issues in the representation of DMS emissions cannot be ruled out based on existing studies.

Thus, the best possible approach for the evaluation of chemistry separately from VMS emission issues in models would be to use ratios of multiple compounds including those specific to biogenic sulfur sources, such as HPMTF/DMS, DMSO/DMS, and MS^-/DMS (Cala et al., 2023). Sulfur isotopic measurements ($\delta^{34}S$) of SO_2 and SO_4^{2-} will assist in discriminating between the relative contribution of biogenic sulfur from other natural and anthropogenic sulfur sources (Ghahreman et al., 2016; Ishino et al., 2019; Jongebloed et al., 2023b; Section 2.4.1), enabling us to utilize MS^-/biogenic-SO_4^{2-} ratios for the model evaluation (Norman et al., 1999; Jongebloed et al., 2025). Oxygen isotope analysis ($\Delta^{17}O$) of MS^- (Hong et al., 2025), in addition to that of SO_4^{2-} (Alexander et al., 2009; Ishino et al., 2021), is also emerging as a novel tool for evaluating VMS oxidation processes.

Running a comprehensive set of observations covering the sulfur cycle across the OIA interface represents a large cost and significant logistical difficulties, and thus requires strong scientific rationale. To assess this rationale, model studies exploring the VMS-to-CCN sensitivity with comprehensive chemistry are essential. Similar to the case of seawater VMS data products (Section 3.2), ML-based, data-driven models have strong potential for addressing issues in VMS oxidation chemistry in process-based models. For example, Pernov et al. (2024, 2025) have made an initial attempt to develop data-driven models of particulate MSA (MS^-) in Arctic regions; this work suggests that atmospheric oxidation process may be the main driver of MSA (MS^-) variation. Such approaches may help reconcile complex interpretations that combine changes in DMS emission, oxidation, and deposition processes across sites (e.g., Sharma et al., 2019; Moffett et al., 2020; Schmale et al., 2022), while helping to elucidate the underlying chemistry. In addition, given the potential importance of reactive halogens in controlling VMS oxidation, particularly in spring when both species are enhanced in polar regions (Section 2.3, **Figure 4**), associated efforts on improving our understanding of halogen cycles, including their emission from sea ice and snow sources (Toyota et al., 2011; Marelle et al., 2021; Swanson et al., 2022), will synergistically enhance our understanding of VMS oxidation.

4. Summary and recommendations

We synthesized current knowledge on the polar biogenic sulfur cycle and its representation in numerical models to explore its potential future change and climate impacts under ongoing changes in sea-ice environments. We identified key features in the polar biogenic sulfur cycle (**Figures 1**, **3**, and **Table 1**), most of which remain poorly represented in numerical models (Section 3). This synthesis highlights that reasonable future prediction of the polar biogenic sulfur cycle requires more than just the coupling of existing ocean biogeochemistry and atmospheric chemistry models. To foster comprehensive model development for polar regions, we summarize 4 major open questions and associated recommendations for future work.

1. *How do production and emissions of VMS in polar regions respond to changes in sea ice and warming?* Current ESMs predict inconsistent future changes (increase and decrease) in seawater DMS concentrations at both poles, whereas all models consistently predict a future increase in DMS emissions due to increases in open water area and higher wind speeds (Section 3.1). However, VMS production and emission processes specific to sea-ice regions are completely absent from these ESMs, leaving unquantified uncertainties in model predictions. A priority area should be implementation of biogeochemical processes at the bottom and surface slush layer of sea ice. To adequately represent Antarctic sea-ice VMS, we advocate extending regional-scale modeling of bottom-ice communities to the entire ice column. Representation of detailed features, such as VMS production in melt ponds, autumn blooms, platelet ice, modulation of sea-to-air VMS emission by turbulence and/or meltwater layers around sea ice, and direct ice-to-air emission (Sections 2.1 and 2.2), requires more observational data to evaluate their importance and heterogeneity. To supply required observations for models and develop our process-level understanding, our community requires advances in analytical capabilities to measure concentrations, production and loss rates, and fluxes of DMSP, DMS, and MeSH in sea-ice environments. New targeted observations of the polar biogenic sulfur cycle, covering ecoregions and seasons, will also enable development of ML-based

empirical models of seawater VMS concentrations considering polar-specific predictors (e.g., sea ice concentrations, low seawater temperatures, nutrient and light limitations; Section 3.2). Finally, enhanced coverage of sea-ice VMS observations and their compilation (as done recently for Antarctica; Burke et al., 2024) is critical for developing our understanding of polar VMS response to warming and changes in sea ice.

2. *What is the sensitivity of CCN number concentrations to polar VMS emissions with updated gas and multiphase oxidation chemistry?* Most current global-scale aerosol models simulate a small increase of CCN (0.01%–0.1%) in response to a DMS emission increase of 1% globally, which inherently has only a weak climate impact (Section 3.4). However, these models underpredict CCN concentrations (i.e., by >50%) in remote marine atmospheres, including polar regions during biologically active seasons, with significant implications for representation of aerosol-cloud interactions. Multiple model deficiencies may cause this gap, including inaccurate VMS oxidation chemistry, submicron sea spray emissions, iodine or organic-driven NPF mechanisms, and/or aerosol removal processes. Model improvement in these areas may have large, but highly uncertain, impacts on VMS-to-CCN sensitivity. An essential step toward quantification of polar VMS-to-CCN sensitivity with aerosol models is incorporation of more complete multiphase oxidation pathways and steeply temperature-dependent gas phase $CH_3SO_2\cdot$ radical chemistry (Section 2.3). Critically, laboratory kinetic studies applicable to polar atmospheres are required, particularly for the role of ice and supercooled, mixed-phase clouds for multiphase VMS oxidation. We recommended use of concentration ratios between DMS, MeSH, and multiple VMS oxidation products for model evaluation to isolate from potential errors in VMS emission (Section 3.4). Compilation of ship, ground, and aircraft VMS measurements will enhance our ability to evaluate models against a set of atmospheric measurements that are as representative as possible. While a global seawater DMS database exists, no such consolidation of atmospheric DMS has been undertaken, and existing measurements are not yet extensive enough to support such efforts for atmospheric MeSH and VMS oxidation products. Some initial work toward developing ML-based, data-driven models is emerging, with focus on particulate MSA in the Arctic (Section 3.4). Simultaneous observations of VMS and reactive halogens are necessary to understand the role of reactive halogen chemistry in VMS oxidation. Simultaneous model development for non-sulfur aerosol processes and reactive halogen chemistry will synergistically enhance our understanding on VMS-to-CCN sensitivity globally and in polar regions.
3. *How important is MeSH in the polar biogenic sulfur cycle?* Implementation of MeSH into aerosol models will enhance VMS-to-CCN sensitivity, globally and in polar regions, through its rapid gas phase oxidation to SO_2, MSA, and H_2SO_4 (Section 2.3). Available seawater MeSH observations reveal broadly higher MeSH/VMS ratios in biologically productive areas of the Southern Ocean and Arctic regions (Wohl et al., 2024), while available atmospheric observations highlight both the prevalence of MeSH and the dependence of atmospheric MeSH/VMS on both the flux ratio and likely variable atmospheric lifetimes (**Figure 2**). Improved seasonal and regional coverage of simultaneous dissolved and atmospheric MeSH and DMS observations (Figure S2) in sea-ice environments is required not only to evaluate the importance of MeSH in polar oceans and sea-ice regions but also to understand the biogeochemical drivers of apparent latitudinal and SST-dependency in MeSH/VMS ratios (**Figure 2**; Wohl et al., 2024). Implementation of MeSH production and loss in prognostic sea-ice biogeochemistry models and development of empirical models to estimate seawater MeSH concentration are also critically important. However, efforts toward standardized atmospheric and seawater measurement and calibration practices are critically needed to address potential biases in existing MeSH measurements (Sections 2.1 and 2.3).
4. *How important are episodic extreme VMS emissions from sea-ice environments for the polar CCN budget?* Even though episodic and strong DMS emissions at the onset of sea ice breakup was first hypothesized more than 3 decades ago (Levasseur et al., 1994), capturing such events has been technically challenging, and we still lack knowledge on their scale, frequency, and consequent impact on the polar CCN budget (Section 2.4.3). Evaluation of this phenomena in models requires direct coupling of regional-scale ocean models with atmospheric models that both have sufficiently high resolution to represent the heterogeneity of sea-ice algal blooms (i.e., subdaily timescales, horizontal spatial scales of $\sim$10's of kilometers, vertical extents of meters or less) and NPF and growth events (i.e., hourly timescales, horizontal spatial scales of less than 100 km, and vertical extents on the scale of 100's of meters). A key step may be parameterization of sea-to-air flux processes in sea-ice leads, with potentially different drivers than in open ocean (Section 3.3). Atmospheric models must have detailed gas and multiphase chemistry including MeSH oxidation to represent efficient NPF and growth, and therefore ocean models should have sea ice sulfur biogeochemistry that includes MeSH production and ventilation to the atmosphere. Development of ML-based, high-resolution seawater VMS estimation products may compensate for challenges faced by prognostic models in reproducing even the seasonality in sea-ice biogeochemistry (Section 3.1). Comparison of CCN number concentrations between cases with episodically strong VMS emissions and with

averaged homogeneous emissions will provide insights for upscaling this phenomenon to large-scale ESMs, which is ultimately required for future projections.

Data accessibility statement

Seawater MeSH and DMS

TRANSSIZ data during spring in the Norwegian Sea and Svalbard archipelago are available at (https://doi.org/10.1594/PANGAEA.953917). Summer Baltic Sea, Skagerrak Sea, and North Sea data from Leck and Rodhe (1991; https://doi.org/10.1007/BF00053934) are available upon request. OC1607A and OC1708A data during summer in the sub-Arctic Northeast Pacific are available at https://doi.org/10.26008/1912/bco-dmo.705636.2. Blanes Bay observatory data covering nearly a full year of measurements in the Mediterranean Catalan Coast are available at https://doi.org/10.5281/zenodo.12758702. AMT-7 data spanning from England to the Falkland Islands during September and October are available at https://doi.org/10.5281/zenodo.12759177. Great Barrier Reef data during summer in the central Great Barrier Reef are available at https://doi.org/10.25918/data.410. POLAR-CHANGE data in the summer/autumn Antarctic Peninsula and Weddell sea are available at https://doi.org/10.5281/zenodo.12758981.

Atmospheric MeSH and DMS

WAO data during spring/summer in UK East Coast are available at https://doi.org/10.5281/zenodo.14697890. AGENA data during summer in the Azores are available at https://minds.wisconsin.edu/handle/1793/85493. Scripps Pier data during autumn in South West California, USA, are available at https://minds.wisconsin.edu/handle/1793/82383. Kennaook/Cape Grim data during autumn, winter, spring, and summer, in North West Tasmania, are available at https://doi.org/10.25919/njv7-a719 and https://doi.org/10.25919/we93-1306. SOAP data during the summer/autumn in the Chatham Rise are available at https://doi.org/10.25919/5d914b00c5759. CAPRICORN data during the summer/autumn in the Southern Ocean south of Tasmania are available at https://doi.org/10.25919/574m-7e47. MISO data during the summer/autumn Southern Ocean/Antarctic ice edge are available at https://doi.org/10.25919/p8bz-p724. ARTofMELT data during the spring/summer Fram Strait are available upon request.

Aerosol size distributions and atmospheric chemical compositions

Aerosol size distributions and atmospheric chemical compositions data used to produce **Figure 5** are publicly available or extracted from graphs in published papers using an image extraction technique, WebPlotDizitizer (https://automeris.io/). Monthly occurrence probability of aerosol size distribution types at Zeppelin, Villum, and Halley was extracted from figures in Dall´Osto et al. (2017), Pernov et al. (2022), and Lachlan-Cope et al. (2020), respectively. DMS concentrations at Villum and Halley are available at Pernov et al. (2020) and Read and Lewis (2007), while those at Gruvebadet and Dumont d'Urville were extracted from Jang et al. (2021) and Legrand et al. (2017), respectively. Chemical compositions for total particulate matter (TPM) and ozone concentrations at Alert (2000–2002) and Zeppelin (2000–2015) were downloaded from EBAS data repository (https://ebas.nilu.no/). Chemical compositions for PM1 and ozone concentrations at Utqiaġvik for 2000–2010 are available at NOAA PMEL data repository (https://www.pmel.noaa.gov/acg/data/) for aerosols and NOAA ESRL data repository for ozone (McClure-Begley et al. 2014; http://dx.doi.org/10.7289/V57P8WBF). Non-sea-salt sulfate and MSA for PM10 at Gruvebadet (2010–2017) were extracted from Jang et al. (2021) and Becagli et al. (2019), respectively. Non-sea-salt sulfate and MSA for TPM (1991–1996), sodium for TPM (2004–2013), and ozone concentrations (2004–2014) at Dumont d'Urville were extracted from Legrand et al. (2017), Legrand et al. (2016a), and Legrand et al. (2016b), respectively. Chemical compositions for PM10 (2000–2007) and ozone (2000–2004) at Neumayer are available at PANGAEA (Weller et al., 2011b; https://doi.org/10.1594/PANGAEA.756382) and EBAS data repository, respectively. Tropospheric column BrO levels were extracted from Theys et al. (2011).

Supplemental material

The supplemental files for this article can be found as follows:

Figure S1. Absolute DMS and MeSH concentrations from existing simultaneous measurements in seawater and air, corresponding to the data underlying MeSH/VMS ratios shown in **Figure 2**.

Figure S2. Latitudinal and seasonal coverage of seawater and atmospheric DMS and MeSH measurements, corresponding to datasets shown in **Figure 2**.

Figure S3. Temperature-dependent reaction rates of MeSH with ·OH, Cl·, Br·, and BrO·.

Table S1. Classifications of particle number size distribution (PNSD) types in **Figure 5**.

Table S2. Summary of models mentioned in the main text.

Acknowledgments

This work is an outcome of the Scientific Committee on Oceanic Research (SCOR) Working Group #163 Coupling of ocean–ice–atmosphere processes: from sea-ice biogeochemistry to aerosols and Clouds (CIce2Clouds). The authors thank SCOR, and the U.S. National Science Foundation for financial support for CIce2Clouds workshops that led to this synthesis paper. The authors thank the International Global Atmospheric Chemistry (IGAC) project for support that led to the graphics in this work. Graphics were designed by Mrinmayi Dalvi (aranyagaatha.wordpress.com, mrinmayi@aranyagaatha.in). The authors gratefully acknowledge Jakob Boyd Pernov and Lisa Miller for the valuable discussions.

Funding

The authors thank SCOR and the U.S. National Science Foundation through a grant to SCOR (grant no. OCE-2140395).

The authors thank IGAC (NASA grant no. 80NSSC22K0786 for the IGAC International Project Office). SI was funded by JSPS KAKENHI grant no. JP23K28212 and Public Promoting Association Kura Foundation. MDW, CLZ, and KAP were funded by the U.S. National Science Foundation (grant no. AGS-2211153, CHE-2441875, and OPP-2000493). AH was funded by NSERC-NFRF funding for the Horizon2020 project CRiceS (grant no. 101003826). JLT, LM, RL and RP are funded by the Horizon Europe program under Grant 101137680 via the project CERTAINTY and the European Union's Horizon 2020 program under Grant 101003826 via the project CRiceS. NS was funded by Fisheries and Oceans Canada. RS was funded by the European Research Council (ERC-2018-AdG 834162), the Spanish Ministry of Science and Innovation through the GOOSE grant (PID2022-140872NB-I00), and the "Severo Ochoa Centre of Excellence" accreditation CEX2019-000928-S. IP was funded by Helmholtz Association through the POF-IV program "Changing Earth—Sustaining our Future." MDM was funded by the Australian Government as part of the Antarctic Science Collaboration Initiative program, under the Australian Antarctic Program Partnership, ASCI000002. HGL was funded by the Korea Institute of Ocean Science and Technology through a project titled "Ocean Circulation and ecosystem variability and predictability research in the earth system model (PEA0175)." SDJ and ASM thank the IITM funding by the Ministry of Earth Sciences, Government of India. GM was funded by the National Oceanic and Atmospheric Administration (NOAA), U.S. Department of Commerce (award no. NA23OAR4320198). BD is a research associate at the F.R.S-FNRS.

Competing interests

Hélène Angot is an associate editor at Elementa. They were not involved in the review process of this article. The authors declare no other competing interests.

Author contributions

Contributed to conception and design: All authors.
Acquisition of data: SI, MDW, EF, ED, CLZ, AH, HH, SDJ, ASM.
Analysis and interpretation of data: All authors.
Drafted and/or revised the article: All authors.
Approved the submitted version for publication: All authors.

References

Abbatt, JPD, **Leaitch, WR**, **Aliabadi, AA**, **Bertram, AK**, **Blanchet, J-P**, **Boivin-Rioux, A**, **Bozem, H**, **Burkart, J**, **Chang, RYW**, **Charette, J**, **Chaubey, JP**, **Christensen, RJ**, **Cirisan, A**, **Collins, DB**, **Croft, B**, **Dionne, J**, **Evans, GJ**, **Fletcher, CG**, **Galí, M**, **Ghahreman, R**, **Girard, E**, **Gong, W**, **Gosselin, M**, **Gourdal, M**, **Hanna, SJ**, **Hayashida, H**, **Herber, AB**, **Hesaraki, S**, **Hoor, P**, **Huang, L**, **Hussherr, R**, **Irish, VE**, **Keita, SA**, **Kodros, JK**, **Köllner, F**, **Kolonjari, F**, **Kunkel, D**, **Ladino, LA**, **Law, K**, **Levasseur, M**, **Libois, Q**, **Liggio, J**, **Lizotte, M**, **Macdonald, KM**, **Mahmood, R**, **Martin, RV**, **Mason, RH**, **Miller, LA**, **Moravek, A**, **Mortenson, E**, **Mungall, EL**, **Murphy, JG**, **Namazi, M**, **Norman, A-L**, **O'Neill, NT**, **Pierce, JR**, **Russell, LM**, **Schneider, J**, **Schulz, H**, **Sharma, S**, **Si, M**, **Staebler, RM**, **Steiner, NS**, **Thomas, JL**, **von Salzen, K**, **Wentzell, JJB**, **Willis, MD**, **Wentworth, GR**, **Xu, J-W**, **Yakobi-Hancock, JD.** 2019. Overview paper: New insights into aerosol and climate in the Arctic. *Atmospheric Chemistry and Physics* **19**: 2527–2560. DOI: https://doi.org/10.5194/acp-19-2527-2019.

Abbatt, JPD, **Ravishankara, AR.** 2023. Opinion: Atmospheric multiphase chemistry—Past, present, and future. *Atmospheric Chemistry and Physics* **23**: 9765–9785. DOI: https://doi.org/10.5194/acp-23-9765-2023.

Adcroft, A, **Anderson, W**, **Balaji, V**, **Blanton, C**, **Bushuk, M**, **Dufour, CO**, **Dunne, JP**, **Griffies, SM**, **Hallberg, R**, **Harrison, MJ**, **Held, IM**, **Jansen, MF**, **John, JG**, **Krasting, JP**, **Langenhorst, AR**, **Legg, S**, **Liang, Z**, **McHugh, C**, **Radhakrishnan, A**, **Reichl, BG**, **Rosati, T**, **Samuels, BL**, **Shao, A**, **Stouffer, R**, **Winton, M**, **Wittenberg, AT**, **Xiang, B**, **Zadeh, N**, **Zhang, R.** 2019. The GFDL global ocean and sea ice model OM4.0: Model description and simulation features. *Journal of Advances in Modeling Earth Systems* **11**: 3167–3211. DOI: https://doi.org/10.1029/2019MS001726.

Ahmed, S, **Thomas, JL**, **Tuite, K**, **Stutz, J**, **Flocke, F**, **Orlando, JJ**, **Hornbrook, RS**, **Apel, EC**, **Emmons, LK**, **Helmig, D**, **Boylan, P**, **Huey, LG**, **Hall, SR**, **Ullmann, K**, **Cantrell, CA**, **Fried, A.** 2022. The role of snow in controlling halogen chemistry and boundary layer oxidation during Arctic spring: A 1D modeling case study. *Journal of Geophysical Research: Atmospheres* **127**: e2021JD036140. DOI: https://doi.org/10.1029/2021JD036140.

Albu, M, **Barnes, I**, **Becker, KH**, **Patroescu-Klotz, I**, **Mocanu, R**, **Benter, T.** 2006. Rate coefficients for the gas-phase reaction of OH radicals with dimethyl sulfide: Temperature and O_2 partial pressure dependence. *Physical Chemistry Chemical Physics* **8**: 728–736. DOI: https://doi.org/10.1039/B512536G.

Alexander, B, **Park, RJ**, **Jacob, DJ**, **Gong, S.** 2009. Transition metal-catalyzed oxidation of atmospheric sulfur: Global implications for the sulfur budget. *Journal of Geophysical Research: Atmospheres* **114**. DOI: https://doi.org/10.1029/2008JD010486.

Ammann, M, **Artiglia, L.** 2022. Solvation, surface propensity, and chemical reactions of solutes at atmospheric liquid–vapor interfaces. *Accounts of Chemical Research* **55**: 3641–3651. DOI: https://doi.org/10.1021/acs.accounts.2c00604.

Anastasio, C, **Jordan, AL.** 2004. Photoformation of hydroxyl radical and hydrogen peroxide in aerosol particles from Alert, Nunavut: Implications for aerosol and snowpack chemistry in the Arctic. *Atmospheric Environment* **38**: 1153–1166. DOI: https://doi.org/10.1016/j.atmosenv.2003.11.016.

Anderson, TR, **Spall, SA**, **Yool, A**, **Cipollini, P**, **Challenor, PG**, **Fasham, MJR.** 2001. Global fields of sea surface

dimethylsulfide predicted from chlorophyll, nutrients and light. *Journal of Marine Systems* **30**: 1–20. DOI: https://doi.org/10.1016/S0924-7963(01)00028-8.

Andreae, MO, **Rosenfeld, D.** 2008. Aerosol–cloud–precipitation interactions. Part 1. The nature and sources of cloud-active aerosols. *Earth-Science Reviews* **89**: 13–41. DOI: https://doi.org/10.1016/j.earscirev.2008.03.001.

Andrews, SJ, **Carpenter, LJ**, **Apel, EC**, **Atlas, E**, **Donets, V**, **Hopkins, JR**, **Hornbrook, RS**, **Lewis, AC**, **Lidster, RT**, **Lueb, R**, **Minaeian, J**, **Navarro, M**, **Punjabi, S**, **Riemer, D**, **Schauffler, S.** 2016. A comparison of Very Short Lived Halocarbon (VSLS) and DMS aircraft measurements in the tropical west Pacific from CAST, ATTREX and CONTRAST. *Atmospheric Measurement Techniques* **9**: 5213–5225. DOI:https://doi.org/10.5194/amt-9-5213-2016.

Arakaki, T, **Anastasio, C**, **Kuroki, Y**, **Nakajima, H**, **Okada, K**, **Kotani, Y**, **Handa, D**, **Azechi, S**, **Kimura, T**, **Tsuhako, A**, **Miyagi, Y.** 2013. A general scavenging rate constant for reaction of hydroxyl radical with organic carbon in atmospheric waters. *Environmental Science & Technology* **47**: 8196–8203. DOI: https://doi.org/10.1021/es401927b.

Aranami, K, **Tsunogai, S.** 2004. Seasonal and regional comparison of oceanic and atmospheric dimethylsulfide in the northern North Pacific: Dilution effects on its concentration during winter. *Journal of Geophysical Research: Atmospheres* **109**. DOI: https://doi.org/10.1029/2003JD004288.

Aranda, A, **Díaz de Mera, Y**, **Rodríguez, D**, **Salgado, S**, **Martínez, E.** 2002. Kinetic and products of the BrO+CH_3SH reaction: Temperature and pressure dependence. *Chemical Physics Letters* **357**: 471–476. DOI: https://doi.org/10.1016/S0009-2614(02)00561-4.

Arrigo, KR. 2014. Sea ice ecosystems. *Annual Review of Marine Science* **6**: 439–467. DOI: https://doi.org/10.1146/annurev-marine-010213-135103.

Arrigo, KR, **Dieckmann, GS**, **Gosselin, M**, **Robinson, DH**, **Fritsen, CH**, **Sullivan, CW.** 1995. High resolution study of the platelet ice ecosystem in McMurdo Sound, Antarctica: Biomass, nutrient, and production profiles within a dense microalgal bloom. *Marine Ecology Progress Series* **127**: 255–268. DOI: https://doi.org/10.3354/meps127255.

Asher, EC, **Dacey, JWH**, **Mills, MM**, **Arrigo, KR**, **Tortell, PD.** 2011. High concentrations and turnover rates of DMS, DMSP and DMSO in Antarctic sea ice. *Geophysical Research Letters* **38**. DOI: https://doi.org/10.1029/2011GL049712.

Assaf, E, **Finewax, Z**, **Marshall, P**, **Veres, PR**, **Neuman, JA**, **Burkholder, JB.** 2023. Measurement of the intramolecular hydrogen-shift rate coefficient for the CH_3SCH_2OO radical between 314 and 433 K. *The Journal of Physical Chemistry A* **127**: 2336–2350. DOI:https://doi.org/10.1021/acs.jpca.2c09095.

Atkinson, R, **Baulch, DL**, **Cox, RA**, **Crowley, JN**, **Hampson, RF**, **Hynes, RG**, **Jenkin, ME**, **Rossi, MJ**, **Troe, J.** 2007. Evaluated kinetic and photochemical data for atmospheric chemistry: Volume III—Gas phase reactions of inorganic halogens. *Atmospheric Chemistry and Physics* **7**: 981–1191. DOI: https://doi.org/10.5194/acp-7-981-2007.

Atkinson, R, **Baulch, DL**, **Cox, RA**, **Crowley, JN**, **Hampson, RF**, **Hynes, RG**, **Jenkin, ME**, **Rossi, MJ**, **Troe, J.** 2004. Evaluated kinetic and photochemical data for atmospheric chemistry: Volume I—Gas phase reactions of O_x, HO_x, NO_x and SO_x species. *Atmospheric Chemistry and Physics* **4**: 1461–1738. DOI: https://doi.org/10.5194/acp-4-1461-2004.

Baccarini, A, **Dommen, J**, **Lehtipalo, K**, **Henning, S**, **Modini, RL**, **Gysel-Beer, M**, **Baltensperger, U**, **Schmale, J.** 2021. Low-volatility vapors and new particle formation over the Southern Ocean during the Antarctic Circumnavigation Expedition. *Journal of Geophysical Research: Atmospheres* **126**: e2021JD035126. DOI: https://doi.org/10.1029/2021JD035126.

Baccarini, A, **Karlsson, L**, **Dommen, J**, **Duplessis, P**, **Vüllers, J**, **Brooks, IM**, **Saiz-Lopez, A**, **Salter, M**, **Tjernström, M**, **Baltensperger, U**, **Zieger, P**, **Schmale, J.** 2020. Frequent new particle formation over the high Arctic pack ice by enhanced iodine emissions. *Nature Communications* **11**: 4924. DOI: https://doi.org/10.1038/s41467-020-18551-0.

Bach, MG, **Gademann, T**, **van Leeuwe, MA**, **Elzenga, JTM**, **Stefels, J.** 2025. Coupling of dimethylsulfoniopropionate production and carbon fixation in four temperate phytoplankton species excludes active short-term regulation of dimethylsulfoniopropionate synthesis under increased light-stress. *Limnology and Oceanography* **70**: 217–231. DOI: https://doi.org/10.1002/lno.12745.

Bange, HW, **Mongwe, P**, **Shutler, JD**, **Arévalo-Martínez, DL**, **Bianchi, D**, **Lauvset, SK**, **Liu, C**, **Löscher, CR**, **Martins, H**, **Rosentreter, JA**, **Schmale, O**, **Steinhoff, T**, **Upstill-Goddard, RC**, **Wanninkhof, R**, **Wilson, ST**, **Xie, H.** 2024. Advances in understanding of air–sea exchange and cycling of greenhouse gases in the upper ocean. *Elementa: Science of the Anthropocene* **12**: 00044. DOI: https://doi.org/10.1525/elementa.2023.00044.

Barnes, I, **Hjorth, J**, **Mihalopoulos, N.** 2006. Dimethyl sulfide and dimethyl sulfoxide and their oxidation in the atmosphere. *Chemical Reviews* **106**: 940–975. DOI: https://doi.org/10.1021/cr020529+.

Bartels-Rausch, T, **Creamean, J**, **Thomas, JL**, **Willis, M**, **Zieger, P.** 2025. Spiers Memorial Lecture: Ten crucial unknowns in atmospheric chemistry in the cold. *Faraday Discussions* DOI: https://doi.org/10.1039/D5FD00056D.

Bartels-Rausch, T, **Jacobi, H-W**, **Kahan, TF**, **Thomas, JL**, **Thomson, ES**, **Abbatt, JPD**, **Ammann, M**, **Blackford, JR**, **Bluhm, H**, **Boxe, C**, **Domine, F**, **Frey, MM**, **Gladich, I**, **Guzmán, MI**, **Heger, D**, **Huthwelker, T**, **Klán, P**, **Kuhs, WF**, **Kuo, MH**, **Maus, S**, **Moussa, SG**, **McNeill, VF**, **Newberg, JT**, **Pettersson, JBC**, **Roeselová, M**, **Sodeau, JR.** 2014. A review of air–ice

chemical and physical interactions (AICI): Liquids, quasi-liquids, and solids in snow. *Atmospheric Chemistry and Physics* **14**: 1587–1633. DOI: https://doi.org/10.5194/acp-14-1587-2014.

Bartels-Rausch, T, **Kong, X**, **Orlando, F**, **Artiglia, L**, **Waldner, A**, **Huthwelker, T**, **Ammann, M.** 2021. Interfacial supercooling and the precipitation of hydrohalite in frozen NaCl solutions as seen by X-ray absorption spectroscopy. *The Cryosphere* **15**: 2001–2020. DOI: https://doi.org/10.5194/tc-15-2001-2021.

Barth, MC, **Rasch, PJ**, **Kiehl, JT**, **Benkovitz, CM**, **Schwartz, SE.** 2000. Sulfur chemistry in the National Center for Atmospheric Research Community Climate Model: Description, evaluation, features, and sensitivity to aqueous chemistry. *Journal of Geophysical Research: Atmospheres* **105**: 1387–1415. DOI: https://doi.org/10.1029/1999JD900773.

Becagli, S, **Amore, A**, **Caiazzo, L**, **Iorio, TD**, **di Sarra, A**, **Lazzara, L**, **Marchese, C**, **Meloni, D**, **Mori, G**, **Muscari, G**, **Nuccio, C**, **Pace, G**, **Severi, M**, **Traversi, R.** 2019. Biogenic aerosol in the Arctic from eight years of MSA data from Ny Ålesund (Svalbard Islands) and Thule (Greenland). *Atmosphere* **10**: 349. DOI: https://doi.org/10.3390/atmos10070349.

Becagli, S, **Barbaro, E**, **Bonamano, S**, **Caiazzo, L**, **di Sarra, A**, **Feltracco, M**, **Grigioni, P**, **Heintzenberg, J**, **Lazzara, L**, **Legrand, M**, **Madonia, A**, **Marcelli, M**, **Melillo, C**, **Meloni, D**, **Nuccio, C**, **Pace, G**, **Park, K-T**, **Preunkert, S**, **Severi, M**, **Vecchiato, M**, **Zangrando, R**, **Traversi, R.** 2022. Factors controlling atmospheric DMS and its oxidation products (MSA and $_{nss}SO_4^{2-}$) in the aerosol at Terra Nova Bay, Antarctica. *Atmospheric Chemistry and Physics* **22**: 9245–9263. DOI: https://doi.org/10.5194/acp-22-9245-2022.

Beck, LJ, **Sarnela, N**, **Junninen, H**, **Hoppe, CJM**, **Garmash, O**, **Bianchi, F**, **Riva, M**, **Rose, C**, **Peräkylä, O**, **Wimmer, D**, **Kausiala, O**, **Jokinen, T**, **Ahonen, L**, **Mikkilä, J**, **Hakala, J**, **He, X-C**, **Kontkanen, J**, **Wolf, KKE**, **Cappelletti, D**, **Mazzola, M**, **Traversi, R**, **Petroselli, C**, **Viola, AP**, **Vitale, V**, **Lange, R**, **Massling, A**, **Nøjgaard, JK**, **Krejci, R**, **Karlsson, L**, **Zieger, P**, **Jang, S**, **Lee, K**, **Vakkari, V**, **Lampilahti, J**, **Thakur, RC**, **Leino, K**, **Kangasluoma, J**, **Duplissy, E-M**, **Siivola, E**, **Marbouti, M**, **Tham, YJ**, **Saiz-Lopez, A**, **Petäjä, T**, **Ehn, M**, **Worsnop, DR**, **Skov, H**, **Kulmala, M**, **Kerminen, V-M**, **Sipilä, M.** 2021. Differing mechanisms of new particle formation at two Arctic sites. *Geophysical Research Letters* **48**: e2020GL091334. DOI: https://doi.org/10.1029/2020GL091334.

Beine, HJ, **Honrath, RE**, **Dominé, F**, **Simpson, WR**, **Fuentes, JD.** 2002. NO_x during background and ozone depletion periods at Alert: Fluxes above the snow surface. *Journal of Geophysical Research: Atmospheres* **107**: ACH 7-1–ACH 7-12. DOI: https://doi.org/10.1029/2002JD002082.

Bell, TG, **Landwehr, S**, **Miller, SD**, **de Bruyn, WJ**, **Callaghan, AH**, **Scanlon, B**, **Ward, B**, **Yang, M**, **Saltzman, ES.** 2017. Estimation of bubble-mediated air–sea gas exchange from concurrent DMS and CO_2 transfer velocities at intermediate–-high wind speeds. *Atmospheric Chemistry and Physics* **17**: 9019–9033. DOI: https://doi.org/10.5194/acp-17-9019-2017.

Belviso, S, **Masotti, I**, **Tagliabue, A**, **Bopp, L**, **Brockmann, P**, **Fichot, C**, **Caniaux, G**, **Prieur, L**, **Ras, J**, **Uitz, J**, **Loisel, H**, **Dessailly, D**, **Alvain, S**, **Kasamatsu, N**, **Fukuchi, M.** 2012. DMS dynamics in the most oligotrophic subtropical zones of the global ocean. *Biogeochemistry* **110**: 215–241. DOI: https://doi.org/10.1007/s10533-011-9648-1.

Belviso, S, **Moulin, C**, **Bopp, L**, **Stefels, J.** 2004. Assessment of a global climatology of oceanic dimethylsulfide (DMS) concentrations based on SeaWiFS imagery (1998-2001). *Canadian Journal of Fisheries and Aquatic Sciences* **61**: 804–816. DOI:https://doi.org/10.1139/f04-001.

Benavent, N, **Mahajan, AS**, **Li, Q**, **Cuevas, CA**, **Schmale, J**, **Angot, H**, **Jokinen, T**, **Quéléver, LLJ**, **Blechschmidt, A-M**, **Zilker, B**, **Richter, A**, **Serna, JA**, **Garcia-Nieto, D**, **Fernandez, RP**, **Skov, H**, **Dumitrascu, A**, **Simões Pereira, P**, **Abrahamsson, K**, **Bucci, S**, **Duetsch, M**, **Stohl, A**, **Beck, I**, **Laurila, T**, **Blomquist, B**, **Howard, D**, **Archer, SD**, **Bariteau, L**, **Helmig, D**, **Hueber, J**, **Jacobi, H-W**, **Posman, K**, **Dada, L**, **Daellenbach, KR**, **Saiz-Lopez, A.** 2022. Substantial contribution of iodine to Arctic ozone destruction. *Nature Geoscience* **15**: 770–773. DOI: https://doi.org/10.1038/s41561-022-01018-w.

Berndt, T, **Chen, J**, **Møller, KH**, **Hyttinen, N**, **Prisle, NL**, **Tilgner, A**, **Hoffmann, EH**, **Herrmann, H**, **Kjaergaard, HG.** 2020. SO_2 formation and peroxy radical isomerization in the atmospheric reaction of OH radicals with dimethyl disulfide. *Chemical Communications* **56**: 13634–13637. DOI: https://doi.org/10.1039/D0CC05783E.

Berndt, T, **Hoffmann, EH**, **Tilgner, A**, **Stratmann, F**, **Herrmann, H.** 2023. Direct sulfuric acid formation from the gas-phase oxidation of reduced-sulfur compounds. *Nature Communications* **14**: 4849. DOI: https://doi.org/10.1038/s41467-023-40586-2.

Berndt, T, **Scholz, W**, **Mentler, B**, **Fischer, L**, **Hoffmann, EH**, **Tilgner, A**, **Hyttinen, N**, **Prisle, NL**, **Hansel, A**, **Herrmann, H.** 2019. Fast peroxy radical isomerization and OH recycling in the reaction of OH radicals with dimethyl sulfide. *The Journal of Physical Chemistry Letters* **10**: 6478–6483. DOI: https://doi.org/10.1021/acs.jpclett.9b02567.

Berresheim, H, **Elste, T**, **Tremmel, HG**, **Allen, AG**, **Hansson, H-C**, **Rosman, K**, **Dal Maso, M**, **Mäkelä, JM**, **Kulmala, M**, **O'Dowd, CD.** 2002. Gas-aerosol relationships of H_2SO_4, MSA, and OH: Observations in the coastal marine boundary layer at Mace Head, Ireland. *Journal of Geophysical Research: Atmospheres* **107**: PAR 5-1–PAR 5-12. DOI:https://doi.org/10.1029/2000JD000229.

Bhatti, YA, **Revell, LE**, **Schuddeboom, AJ**, **McDonald, AJ**, **Archibald, AT**, **Williams, J**, **Venugopal, AU**, **Hardacre, C**, **Behrens, E.** 2023. The sensitivity of Southern Ocean atmospheric dimethyl sulfide (DMS) to modeled oceanic DMS concentrations and emissions. *Atmospheric Chemistry and Physics* **23**: 15181–15196. DOI: https://doi.org/10.5194/acp-23-15181-2023.

Bian, H, **Chin, M**, **Colarco, PR**, **Apel, EC**, **Blake, DR**, **Froyd, K**, **Hornbrook, RS**, **Jimenez, J**, **Jost, PC**, **Lawler, M**, **Liu, M**, **Lund, MT**, **Matsui, H**, **Nault, BA**, **Penner, JE**, **Rollins, AW**, **Schill, G**, **Skeie, RB**, **Wang, H**, **Xu, L**, **Zhang, K**, **Zhu, J.** 2024. Observationally constrained analysis of sulfur cycle in the marine atmosphere with NASA ATom measurements and AeroCom model simulations. *Atmospheric Chemistry and Physics* **24**: 1717–1741. DOI: https://doi.org/10.5194/acp-24-1717-2024.

Blomquist, BW, **Brumer, SE**, **Fairall, CW**, **Huebert, BJ**, **Zappa, CJ**, **Brooks, IM**, **Yang, M**, **Bariteau, L**, **Prytherch, J**, **Hare, JE**, **Czerski, H**, **Matei, A**, **Pascal, RW.** 2017. Wind speed and sea state dependencies of air-sea gas transfer: Results from the High Wind speed Gas exchange Study (HiWinGS). *Journal of Geophysical Research: Oceans* **122**: 8034–8062. DOI: https://doi.org/10.1002/2017JC013181.

Bock, J, **Michou, M**, **Nabat, P**, **Abe, M**, **Mulcahy, JP**, **Olivié, DJL**, **Schwinger, J**, **Suntharalingam, P**, **Tjiputra, J**, **van Hulten, M**, **Watanabe, M**, **Yool, A**, **Séférian, R.** 2021. Evaluation of ocean dimethylsulfide concentration and emission in CMIP6 models. *Biogeosciences* **18**: 3823–3860. DOI: https://doi.org/10.5194/bg-18-3823-2021.

Boetius, A, **Anesio, AM**, **Deming, JW**, **Mikucki, JA**, **Rapp, JZ.** 2015. Microbial ecology of the cryosphere: Sea ice and glacial habitats. *Nature Reviews Microbiology* **13**: 677–690. DOI: https://doi.org/10.1038/nrmicro3522.

Borissenko, D, **Kukui, A**, **Laverdet, G**, **Le Bras, G.** 2003. Experimental study of SO_2 formation in the reactions of CH_3SO radical with NO_2 and O_3 in relation with the atmospheric oxidation mechanism of dimethyl sulfide. *The Journal of Physical Chemistry A* **107**: 1155–1161. DOI: https://doi.org/10.1021/jp021701g.

Bork, N, **Elm, J**, **Olenius, T**, **Vehkamäki, H.** 2014. Methane sulfonic acid-enhanced formation of molecular clusters of sulfuric acid and dimethyl amine. *Atmospheric Chemistry and Physics* **14**: 12023–12030. DOI: https://doi.org/10.5194/acp-14-12023-2014.

Boutin, G, **Ólason, E**, **Rampal, P**, **Regan, H**, **Lique, C**, **Talandier, C**, **Brodeau, L**, **Ricker, R.** 2023. Arctic sea ice mass balance in a new coupled ice–ocean model using a brittle rheology framework. *The Cryosphere* **17**: 617–638. DOI: https://doi.org/10.5194/tc-17-617-2023.

Bowman, JS, **Berthiaume, CT**, **Armbrust, EV**, **Deming, JW.** 2014. The genetic potential for key biogeochemical processes in Arctic frost flowers and young sea ice revealed by metagenomic analysis. *FEMS Microbiology Ecology* **89**: 376–387. DOI: https://doi.org/10.1111/1574-6941.12331.

Boyer, M, **Quéléver, L**, **Brasseur, Z**, **McManus, B**, **Herndon, S**, **Agnese, M**, **Nelson, D**, **Roscioli, J**, **Weis, F**, **Sel, S**, **Marincovich, GL**, **Quarin, FJ**, **Buchholz, A**, **Xavier, C**, **Perchivale, PJ**, **Kerminen, V-M**, **Kulmala, M**, **Petäjä, T**, **He, X-C**, **Sofieva-Rios, S**, **Timonen, H**, **Aurela, M**, **Barreira, L**, **Virkkula, A**, **Asmi, E**, **Worsnop, D**, **Sipilä, M.** 2025. Penguin guano is an important source of climate-relevant aerosol particles in Antarctica. *Communications Earth & Environment* **6**: 368. DOI: https://doi.org/10.1038/s43247-025-02312-2.

Brean, J, **Dall'Osto, M**, **Simó, R**, **Shi, Z**, **Beddows, DCS**, **Harrison, RM.** 2021. Open ocean and coastal new particle formation from sulfuric acid and amines around the Antarctic Peninsula. *Nature Geoscience* **14**: 383–388. DOI: https://doi.org/10.1038/s41561-021-00751-y.

Bronselaer, B, **Russell, JL**, **Winton, M**, **Williams, NL**, **Key, RM**, **Dunne, JP**, **Feely, RA**, **Johnson, KS**, **Sarmiento, JL.** 2020. Importance of wind and meltwater for observed chemical and physical changes in the Southern Ocean. *Nature Geoscience* **13**: 35–42. DOI: https://doi.org/10.1038/s41561-019-0502-8.

Bronselaer, B, **Winton, M**, **Griffies, SM**, **Hurlin, WJ**, **Rodgers, KB**, **Sergienko, OV**, **Stouffer, RJ**, **Russell, JL.** 2018. Change in future climate due to Antarctic meltwater. *Nature* **564**: 53–58. DOI: https://doi.org/10.1038/s41586-018-0712-z.

Brough, N, **Jones, AE**, **Griffiths, PT.** 2019. Influence of sea ice-derived halogens on atmospheric HO_x as observed in springtime coastal Antarctica. *Geophysical Research Letters* **46**: 10168–10176. DOI: https://doi.org/10.1029/2019GL083825.

Browse, J, **Carslaw, KS**, **Mann, GW**, **Birch, CE**, **Arnold, SR**, **Leck, C.** 2014. The complex response of Arctic aerosol to sea-ice retreat. *Atmospheric Chemistry and Physics* **14**: 7543–7557. DOI: https://doi.org/10.5194/acp-14-7543-2014.

Burd, JA, **Peterson, PK**, **Nghiem, SV**, **Perovich, DK**, **Simpson, WR.** 2017. Snowmelt onset hinders bromine monoxide heterogeneous recycling in the Arctic. *Journal of Geophysical Research: Atmospheres* **122**: 8297–8309. DOI: https://doi.org/10.1002/2017JD026906.

Burke, G, **Wongpan, P**, **Lannuzel, D**, **Hayashida, H.** 2024. Data collation for climate-cooling gas dimethylsulfide in Antarctic snow, sea ice and underlying seawater. *Scientific Data* **11**: 1185. DOI: https://doi.org/10.1038/s41597-024-04038-w.

Burkholder, JB, **Sander, SP**, **Abbatt, JPD**, **Barker, JR**, **Cappa, C**, **Crounse, JD**, **Dibble, TS**, **Huie, RE**, **Kolb, CE**, **Kurylo, MJ**, **Orkin, VL**, **Percival, CJ**, **Wilmouth, DM**, **Wine, PH.** 2019. Chemical kinetics and photochemical data for use in atmospheric studies, Evaluation No. 19. JPL Publication. Available at https://jpldataeval.jpl.nasa.gov/. Accessed January 14, 2026.

Bushuk, M, **Winton, M**, **Haumann, FA**, **Delworth, T**, **Lu, F**, **Zhang, Y**, **Jia, L**, **Zhang, L**, **Cooke, W**, **Harrison, M**, **Hurlin, B**, **Johnson, NC**, **Kapnick, SB**, **McHugh, C**, **Murakami, H**, **Rosati, A**, **Tseng, K-C**, **Wittenberg, AT**, **Yang, X**, **Zeng, F.** 2021. Seasonal prediction and predictability of regional Antarctic sea ice. *Journal of Climate* **34**: 6207–6233. DOI: https://doi.org/10.1175/JCLI-D-20-0965.1.

Butkovskaya, NI, **Barnes, I.** 2002. Model study of the photooxidation of $CH_3SO_2SCH_3$ at atmospheric pressure: Thermal decomposition of the CH_3SO_2 radical, in Barnes, I ed., *Global atmospheric change and its impact on regional air quality*. Dordrecht, the Netherlands: Springer: 147–152. DOI: https://doi.org/10.1007/978-94-010-0082-6_22.

Buys, Z, **Brough, N**, **Huey, LG**, **Tanner, DJ**, **von Glasow, R**, **Jones, AE.** 2013. High temporal resolution Br_2, BrCl and BrO observations in coastal Antarctica. *Atmospheric Chemistry and Physics* **13**: 1329–1343. DOI: https://doi.org/10.5194/acp-13-1329-2013.

Cala, BA, **Archer-Nicholls, S**, **Weber, J**, **Abraham, NL**, **Griffiths, PT**, **Jacob, L**, **Shin, YM**, **Revell, LE**, **Woodhouse, M**, **Archibald, AT.** 2023. Development, intercomparison, and evaluation of an improved mechanism for the oxidation of dimethyl sulfide in the UKCA model. *Atmospheric Chemistry and Physics* **23**: 14735–14760. DOI: https://doi.org/10.5194/acp-23-14735-2023.

Campbell, JR, **Battaglia, MJr**, **Dingilian, KK**, **Cesler-Maloney, M**, **Simpson, WR**, **Robinson, ES**, **DeCarlo, PF**, **Temime-Roussel, B**, **D'Anna, B**, **Holen, AL**, **Wu, J**, **Pratt, KA**, **Dibb, JE**, **Nenes, A**, **Weber, RJ**, **Mao, J.** 2024. Enhanced aqueous formation and neutralization of fine atmospheric particles driven by extreme cold. *Science Advances* **10**: eado4373. DOI: https://doi.org/10.1126/sciadv.ado4373.

Campbell, JR, **Battaglia, MJr**, **Dingilian, K**, **Cesler-Maloney, M**, **St Clair, JM**, **Hanisco, TF**, **Robinson, E**, **DeCarlo, P**, **Simpson, W**, **Nenes, A**, **Weber, RJ**, **Mao, J.** 2022. Source and chemistry of Hydroxymethanesulfonate (HMS) in Fairbanks, Alaska. *Environmental Science & Technology* **56**: 7657–7667. DOI: https://doi.org/10.1021/acs.est.2c00410.

Carnat, G, **Zhou, J**, **Papakyriakou, T**, **Delille, B**, **Goossens, T**, **Haskell, T**, **Schoemann, V**, **Fripiat, F**, **Rintala, J-M**, **Tison, J-L.** 2014. Physical and biological controls on DMS,P dynamics in ice shelf-influenced fast ice during a winter-spring and a spring-summer transitions. *Journal of Geophysical Research: Oceans* **119**: 2882–2905. DOI: https://doi.org/10.1002/2013JC009381.

Carslaw, KS, **Lee, LA**, **Reddington, CL**, **Pringle, KJ**, **Rap, A**, **Forster, PM**, **Mann, GW**, **Spracklen, DV**, **Woodhouse, MT**, **Regayre, LA**, **Pierce, JR.** 2013. Large contribution of natural aerosols to uncertainty in indirect forcing. *Nature* **503**: 67–71. DOI: https://doi.org/10.1038/nature12674.

Castebrunet, H, **Martinerie, P**, **Genthon, C**, **Cosme, E.** 2009. A three-dimensional model study of methanesulphonic acid to non sea salt sulphate ratio at mid and high-southern latitudes. *Atmospheric Chemistry and Physics* **9**: 9449–9469. DOI: https://doi.org/10.5194/acp-9-9449-2009.

Cesana, G, **Kay, JE**, **Chepfer, H**, **English, JM**, **de Boer, G.** 2012. Ubiquitous low-level liquid-containing Arctic clouds: New observations and climate model constraints from CALIPSO-GOCCP. *Geophysical Research Letters* **39**. DOI: https://doi.org/10.1029/2012GL053385.

Chakraborty, S, **Kahan, TF.** 2020. Physical characterization of frozen aqueous solutions containing sodium chloride and humic acid at environmentally relevant temperatures. *ACS Earth and Space Chemistry* **4**: 305–310. DOI: https://doi.org/10.1021/acsearthspacechem.9b00319.

Chalif, JI, **Jongebloed, UA**, **Osterberg, EC**, **Koffman, BG**, **Alexander, B**, **Winski, DA**, **Polashenski, DJ**, **Stamieszkin, K**, **Ferris, DG**, **Kreutz, KJ**, **Wake, CP**, **Cole-Dai, J.** 2024. Pollution drives multidecadal decline in subarctic methanesulfonic acid. *Nature Geoscience* **17**: 1016–1021. DOI: https://doi.org/10.1038/s41561-024-01543-w.

Chang, RY-W, **Sjostedt, SJ**, **Pierce, JR**, **Papakyriakou, TN**, **Scarratt, MG**, **Michaud, S**, **Levasseur, M**, **Leaitch, WR**, **Abbatt, JPD.** 2011. Relating atmospheric and oceanic DMS levels to particle nucleation events in the Canadian Arctic. *Journal of Geophysical Research: Atmospheres* **116**. DOI: https://doi.org/10.1029/2011JD015926.

Chapman, CC, **Lea, M-A**, **Meyer, A**, **Sallée, J-B**, **Hindell, M.** 2020. Defining Southern Ocean fronts and their influence on biological and physical processes in a changing climate. *Nature Climate Change* **10**: 209–219. DOI: https://doi.org/10.1038/s41558-020-0705-4.

Chen, H, **Finlayson-Pitts, BJ.** 2017. New particle formation from methanesulfonic acid and amines/ammonia as a function of temperature. *Environmental Science & Technology* **51**: 243–252. DOI: https://doi.org/10.1021/acs.est.6b04173.

Chen, J, **Berndt, T**, **Møller, KH**, **Lane, JR**, **Kjaergaard, HG.** 2021. Atmospheric fate of the CH_3SOO radical from the $CH_3S + O_2$ equilibrium. *The Journal of Physical Chemistry A* **125**: 8933–8941. DOI: https://doi.org/10.1021/acs.jpca.1c06900.

Chen, J, **Lane, JR**, **Bates, KH**, **Kjaergaard, HG.** 2023. Atmospheric gas-phase formation of methanesulfonic acid. *Environmental Science & Technology* **57**: 21168–21177. DOI: https://doi.org/10.1021/acs.est.3c07120.

Chen, L, **Wang, J**, **Gao, Y**, **Xu, G**, **Yang, X**, **Lin, Q**, **Zhang, Y.** 2012. Latitudinal distributions of atmospheric MSA and MSA/nss-SO_4^{2-} ratios in summer over the high latitude regions of the Southern and Northern Hemispheres. *Journal of Geophysical Research: Atmospheres* **117**. DOI: https://doi.org/10.1029/2011JD016559.

Chen, Q, **Sherwen, T**, **Evans, M**, **Alexander, B.** 2018. DMS oxidation and sulfur aerosol formation in the marine troposphere: A focus on reactive halogen

and multiphase chemistry. *Atmospheric Chemistry and Physics* **18**: 13617–13637. DOI: https://doi.org/10.5194/acp-18-13617-2018.

Chin, M, **Jacob, DJ**, **Gardner, GM**, **Foreman-Fowler, MS**, **Spiro, PA**, **Savoie, DL.** 1996. A global three-dimensional model of tropospheric sulfate. *Journal of Geophysical Research: Atmospheres* **101**: 18667–18690. DOI: https://doi.org/10.1029/96JD01221.

Clegg, M, **Abbatt, D.** 2001a. Uptake of gas-phase SO_2 and H_2O_2 by ice surfaces: Dependence on partial pressure, temperature, and surface acidity. *The Journal of Physical Chemistry A* **105**: 6630–6636. DOI: https://doi.org/10.1021/jp010062r.

Clegg, SM, **Abbatt, JPD.** 2001b. Oxidation of SO_2 by H_2O_2 on ice surfaces at 228 K: A sink for SO_2 in ice clouds. *Atmospheric Chemistry and Physics* **1**: 73–78. DOI: https://doi.org/10.5194/acp-1-73-2001.

Collow, TW, **Wang, W**, **Kumar, A**, **Zhang, J.** 2015. Improving Arctic sea ice prediction using PIOMAS initial sea ice thickness in a coupled ocean–atmosphere model. *Monthly Weather Review* **143**: 4618–4630. DOI: https://doi.org/10.1175/MWR-D-15-0097.1.

Creamean, J, **Miller, LA**, **van Pinxteren, M**, **Crabeck, O**, **Steiner, NS**, **Marelle, L**, **Deschepper, I**, **Lapere, R**, **Leon-Marcos, A**, **Pratt, KA**, **Thomas, JL**, **Da Silva, A**, **Frey, MM**, **Peeken, I**, **Horowitz, HM**, **Willis, MD**, **Price, R.** n.d. Polar primary aerosols across the ocean-sea ice-snow-atmosphere interface: From sources to impacts. *Elementa: Science of the Anthropocene*, in press.

Croft, B, **Martin, RV**, **Leaitch, WR**, **Burkart, J**, **Chang, RY-W**, **Collins, DB**, **Hayes, PL**, **Hodshire, AL**, **Huang, L**, **Kodros, JK**, **Moravek, A**, **Mungall, EL**, **Murphy, JG**, **Sharma, S**, **Tremblay, S**, **Wentworth, GR**, **Willis, MD**, **Abbatt, JPD**, **Pierce, JR.** 2019. Arctic marine secondary organic aerosol contributes significantly to summertime particle size distributions in the Canadian Arctic Archipelago. *Atmospheric Chemistry and Physics* **19**: 2787–2812. DOI: https://doi.org/10.5194/acp-19-2787-2019.

Croft, B, **Martin, RV**, **Leaitch, WR**, **Tunved, P**, **Breider, TJ**, **D'Andrea, SD**, **Pierce, JR.** 2016a. Processes controlling the annual cycle of Arctic aerosol number and size distributions. *Atmospheric Chemistry and Physics* **16**: 3665–3682. DOI: https://doi.org/10.5194/acp-16-3665-2016.

Croft, B, **Wentworth, GR**, **Martin, RV**, **Leaitch, WR**, **Murphy, JG**, **Murphy, BN**, **Kodros, JK**, **Abbatt, JPD**, **Pierce, JR.** 2016b. Contribution of Arctic seabird-colony ammonia to atmospheric particles and cloud-albedo radiative effect. *Nature Communications* **7**: 13444. DOI: https://doi.org/10.1038/ncomms13444.

Custard, KD, **Pratt, KA**, **Wang, S**, **Shepson, PB.** 2016. Constraints on Arctic atmospheric chlorine production through measurements and simulations of Cl_2 and ClO. *Environmental Science & Technology* **50**: 12394–12400. DOI: https://doi.org/10.1021/acs.est.6b03909.

Dall´Osto, M, **Beddows, DCS**, **Tunved, P**, **Krejci, R**, **Ström, J**, **Hansson, HC**, **Yoon, YJ**, **Park, KT**, **Becagli, S**, **Udisti, R**, **Onasch, T**, **O´Dowd, CD**, **Simó, R**, **Harrison, RM.** 2017. Arctic sea ice melt leads to atmospheric new particle formation. *Scientific Reports* **7**: 3318. DOI: https://doi.org/10.1038/s41598-017-03328-1.

Dall´Osto, M, **Simo, R**, **Harrison, RM**, **Beddows, DCS**, **Saiz-Lopez, A**, **Lange, R**, **Skov, H**, **Nøjgaard, JK**, **Nielsen, IE**, **Massling, A.** 2018. Abiotic and biotic sources influencing spring new particle formation in North East Greenland. *Atmospheric Environment* **190**: 126–134. DOI: https://doi.org/10.1016/j.atmosenv.2018.07.019.

Davis, D, **Chen, G**, **Bandy, A**, **Thornton, D**, **Eisele, F**, **Mauldin, L**, **Tanner, D**, **Lenschow, D**, **Fuelberg, H**, **Huebert, B**, **Heath, J**, **Clarke, A**, **Blake, D.** 1999. Dimethyl sulfide oxidation in the equatorial Pacific: Comparison of model simulations with field observations for DMS, SO_2, H_2SO_4(g), MSA(g), MS and NSS. *Journal of Geophysical Research: Atmospheres* **104**: 5765–5784. DOI: https://doi.org/10.1029/1998JD100002.

De Bruyn, WJ, **Swartz, E**, **Hu, JH**, **Shorter, JA**, **Davidovits, P**, **Worsnop, DR**, **Zahniser, MS**, **Kolb, CE.** 1995. Henry's law solubilities and Śetchenow coefficients for biogenic reduced sulfur species obtained from gas-liquid uptake measurements. *Journal of Geophysical Research: Atmospheres* **100**: 7245–7251. DOI: https://doi.org/10.1029/95JD00217.

DeJong, HB, **Dunbar, RB**, **Koweek, DA**, **Mucciarone, DA**, **Bercovici, SK**, **Hansell, DA.** 2017. Net community production and carbon export during the late summer in the Ross Sea, Antarctica. *Global Biogeochemical Cycles* **31**: 473–491. DOI: https://doi.org/10.1002/2016GB005417.

DeJong, HB, **Dunbar, RB**, **Lyons, EA.** 2018. Late summer frazil ice-associated algal blooms around Antarctica. *Geophysical Research Letters* **45**: 826–833. DOI: https://doi.org/10.1002/2017GL075472.

Delille, B, **Vancoppenolle, M**, **Geilfus, N-X**, **Tilbrook, B**, **Lannuzel, D**, **Schoemann, V**, **Becquevort, S**, **Carnat, G**, **Delille, D**, **Lancelot, C**, **Chou, L**, **Dieckmann, GS**, **Tison, J-L.** 2014. Southern Ocean CO_2 sink: The contribution of the sea ice. *Journal of Geophysical Research: Oceans* **119**: 6340–6355. DOI: https://doi.org/10.1002/2014JC009941.

Dingilian, K, **Hebert, E**, **Battaglia, MJr**, **Campbell, JR**, **Cesler-Maloney, M**, **Simpson, W**, **St. Clair, JM**, **Dibb, J**, **Temime-Roussel, B**, **D'Anna, B**, **Moon, A**, **Alexander, B**, **Yang, Y**, **Nenes, A**, **Mao, J**, **Weber, RJ**. 2024. Hydroxymethanesulfonate and Sulfur(IV) in Fairbanks winter during the ALPACA study. *ACS ES&T Air* **1**: 646–659. DOI: https://doi.org/10.1021/acsestair.4c00012.

Dirkson, A, **Merryfield, WJ**, **Monahan, A.** 2017. Impacts of sea ice thickness initialization on seasonal Arctic sea ice predictions. *Journal of Climate* **30**:

1001–1017. DOI: https://doi.org/10.1175/JCLI-D-16-0437.1.

Dixon, JL, **Hopkins, FE**, **Stephens, JA**, **Schäfer, H.** 2020. Seasonal changes in microbial dissolved organic sulfur transformations in coastal waters. *Microorganisms* **8**: 337. DOI:https://doi.org/10.3390/microorganisms8030337.

Dunne, EM, **Gordon, H**, **Kürten, A**, **Almeida, J**, **Duplissy, J**, **Williamson, C**, **Ortega, IK**, **Pringle, KJ**, **Adamov, A**, **Baltensperger, U**, **Barmet, P**, **Benduhn, F**, **Bianchi, F**, **Breitenlechner, M**, **Clarke, A**, **Curtius, J**, **Dommen, J**, **Donahue, NM**, **Ehrhart, S**, **Flagan, RC**, **Franchin, A**, **Guida, R**, **Hakala, J**, **Hansel, A**, **Heinritzi, M**, **Jokinen, T**, **Kangasluoma, J**, **Kirkby, J**, **Kulmala, M**, **Kupc, A**, **Lawler, MJ**, **Lehtipalo, K**, **Makhmutov, V**, **Mann, G**, **Mathot, S**, **Merikanto, J**, **Miettinen, P**, **Nenes, A**, **Onnela, A**, **Rap, A**, **Reddington, CLS**, **Riccobono, F**, **Richards, NAD**, **Rissanen, MP**, **Rondo, L**, **Sarnela, N**, **Schobesberger, S**, **Sengupta, K**, **Simon, M**, **Sipilä, M**, **Smith, JN**, **Stozkhov, Y**, **Tomé, A**, **Tröstl, J**, **Wagner, PE**, **Wimmer, D**, **Winkler, PM**, **Worsnop, DR**, **Carslaw, KS.** 2016. Global atmospheric particle formation from CERN CLOUD measurements. *Science* **354**: 1119–1124. DOI: https://doi.org/10.1126/science.aaf2649.

Edebeli, J, **Ammann, M**, **Bartels-Rausch, T.** 2019. Microphysics of the aqueous bulk counters the water activity driven rate acceleration of bromide oxidation by ozone from 289–245 K. *Environmental Science: Processes & Impacts* **21**: 63–73. DOI: https://doi.org/10.1039/C8EM00417J.

Elliott, S, **Deal, C**, **Humphries, G**, **Hunke, E**, **Jeffery, N**, **Jin, M**, **Levasseur, M**, **Stefels, J.** 2012. Pan-Arctic simulation of coupled nutrient-sulfur cycling due to sea ice biology: Preliminary results. *Journal of Geophysical Research: Biogeosciences* **117**. DOI: https://doi.org/10.1029/2011JG001649.

Emerson, EW, **Hodshire, AL**, **DeBolt, HM**, **Bilsback, KR**, **Pierce, JR**, **McMeeking, GR**, **Farmer, DK.** 2020. Revisiting particle dry deposition and its role in radiative effect estimates. *Proceedings of the National Academy of Sciences* **117**: 26076–26082. DOI: https://doi.org/10.1073/pnas.2014761117.

Ervens, B. 2015. Modeling the processing of aerosol and trace gases in clouds and fogs. *Chemical Reviews* **115**: 4157–4198. DOI: https://doi.org/10.1021/cr5005887.

Faloona, I, **Conley, SA**, **Blomquist, B**, **Clarke, AD**, **Kapustin, V**, **Howell, S**, **Lenschow, DH**, **Bandy, AR.** 2009. Sulfur dioxide in the tropical marine boundary layer: Dry deposition and heterogeneous oxidation observed during the Pacific Atmospheric Sulfur Experiment. *Journal of Atmospheric Chemistry* **63**: 13–32. DOI: https://doi.org/10.1007/s10874-010-9155-0.

Fiddes, SL, **Woodhouse, MT**, **Mallet, MD**, **Lamprey, LJ**, **Humphries, RS**, **Protat, A**, **Alexander, SP**, **Hayashida, H**, **Putland, S**, **Miljevic, B**, **Schofield, R.** 2025. The ACCESS-AM2 climate model underestimates aerosol concentration in the Southern Ocean; improving aerosol representation could be problematic for the global energy balance. *Atmospheric Chemistry and Physics* **25**: 16451–16477. DOI: https://doi.org/10.5194/acp-25-16451-2025.

Fiddes, SL, **Woodhouse, MT**, **Nicholls, Z**, **Lane, TP**, **Schofield, R.** 2018. Cloud, precipitation and radiation responses to large perturbations in global dimethyl sulfide. *Atmospheric Chemistry and Physics* **18**: 10177–10198. DOI: https://doi.org/10.5194/acp-18-10177-2018.

Flöck, OR, **Andreae, MO.** 1996. Photochemical and non-photochemical formation and destruction of carbonyl sulfide and methyl mercaptan in ocean waters. *Marine Chemistry* **54**: 11–26. DOI: https://doi.org/10.1016/0304-4203(96)00027-8.

Forster, P, **Strelvmo, T**, **Armour, K**, **Collins, W**, **Dufresne, JL**, **Frame, D**, **lunt, DJ**, **Mauritsen, T**, **Palmer, MD**, **Watanabe, M**, **Wild, M**, **Zhang, H.** 2021. The Earth's energy budget, climate feedbacks and climate sensitivity, in Intergovernmental Panel on Climate Change (IPCC) eds., *Climate change 2021—The physical science basis: Working group I contribution to the sixth assessment report of the Intergovernmental Panel on Climate Change*. Cambridge, UK: Cambridge University Press: 923–1054. DOI: https://doi.org/10.1017/9781009157896.009.

Fossum, KN, **Ovadnevaite, J**, **Ceburnis, D**, **Dall'Osto, M**, **Marullo, S**, **Bellacicco, M**, **Simó, R**, **Liu, D**, **Flynn, M**, **Zuend, A**, **O'Dowd, C.** 2018. Summertime primary and secondary contributions to Southern Ocean cloud condensation nuclei. *Scientific Reports* **8**: 13844. DOI: https://doi.org/10.1038/s41598-018-32047-4.

Fritsen, CH, **Coale, SL**, **Neenan, DR**, **Gibson, AH**, **Garrison, DL.** 2001. Biomass, production and microhabitat characteristics near the freeboard of ice floes in the Ross Sea, Antarctica, during the austral summer. *Annals of Glaciology* **33**: 280–286. DOI: https://doi.org/10.3189/172756401781818653.

Fritsen, CH, **Lytle, VI**, **Ackley, SF**, **Sullivan, CW.** 1994. Autumn bloom of Antarctic pack-ice algae. *Science* **266**: 782–784. DOI: https://doi.org/10.1126/science.266.5186.782.

Fung, KM, **Heald, CL**, **Kroll, JH**, **Wang, S**, **Jo, DS**, **Gettelman, A**, **Lu, Z**, **Liu, X**, **Zaveri, RA**, **Apel, EC**, **Blake, DR**, **Jimenez, JL**, **Campuzano-Jost, P**, **Veres, PR**, **Bates, TS**, **Shilling, JE**, **Zawadowicz, M.** 2022. Exploring dimethyl sulfide (DMS) oxidation and implications for global aerosol radiative forcing. *Atmospheric Chemistry and Physics* **22**: 1549–1573. DOI: https://doi.org/10.5194/acp-22-1549-2022.

Galí, M, **Devred, E**, **Babin, M**, **Levasseur, M.** 2019. Decadal increase in Arctic dimethylsulfide emission. *Proceedings of the National Academy of Sciences* **116**: 19311–19317. DOI: https://doi.org/10.1073/pnas.1904378116.

Galí, M, **Devred, E**, **Levasseur, M**, **Royer, S-J**, **Babin, M.** 2015. A remote sensing algorithm for planktonic dimethylsulfoniopropionate (DMSP) and an analysis of global patterns. *Remote Sensing of Environment* **171**: 171–184. DOI: https://doi.org/10.1016/j.rse.2015.10.012.

Galí, M, **Levasseur, M**, **Devred, E**, **Simó, R**, **Babin, M.** 2018. Sea-surface dimethylsulfide (DMS) concentration from satellite data at global and regional scales. *Biogeosciences* **15**: 3497–3519. DOI: https://doi.org/10.5194/bg-15-3497-2018.

Galí, M, **Lizotte, M**, **Kieber, DJ**, **Randelhoff, A**, **Hussherr, R**, **Xue, L**, **Dinasquet, J**, **Babin, M**, **Rehm, E**, **Levasseur, M.** 2021. DMS emissions from the Arctic marginal ice zone. *Elementa: Science of the Anthropocene* **9**(1). DOI:https://doi.org/10.1525/elementa.2020.00113.

Galí, M, **Simó, R.** 2010. Occurrence and cycling of dimethylated sulfur compounds in the Arctic during summer receding of the ice edge. *Marine Chemistry* **122**: 105–117. DOI: https://doi.org/10.1016/j.marchem.2010.07.003.

Galindo, V, **Levasseur, M**, **Mundy, CJ**, **Gosselin, M**, **Scarratt, M**, **Papakyriakou, T**, **Stefels, J**, **Gale, MA**, **Tremblay, J-É**, **Lizotte, M.** 2016. Contrasted sensitivity of DMSP production to high light exposure in two Arctic under-ice blooms. *Journal of Experimental Marine Biology and Ecology* **475**: 38–48. DOI: https://doi.org/10.1016/j.jembe.2015.11.009.

Galindo, V, **Levasseur, M**, **Mundy, CJ**, **Gosselin, M**, **Tremblay, J-É**, **Scarratt, M**, **Gratton, Y**, **Papakiriakou, T**, **Poulin, M**, **Lizotte, M.** 2014. Biological and physical processes influencing sea ice, under-ice algae, and dimethylsulfoniopropionate during spring in the Canadian Arctic Archipelago. *Journal of Geophysical Research: Oceans* **119**: 3746–3766. DOI: https://doi.org/10.1002/2013JC009497.

Ghahreman, R, **Gong, W**, **Beagley, SR**, **Akingunola, A**, **Makar, PA**, **Leaitch, WR.** 2021. Modeling aerosol effects on liquid clouds in the summertime Arctic. *Journal of Geophysical Research: Atmospheres* **126**: e2021JD034962. DOI: https://doi.org/10.1029/2021JD034962.

Ghahreman, R, **Gong, W**, **Galí, M**, **Norman, A-L**, **Beagley, SR**, **Akingunola, A**, **Zheng, Q**, **Lupu, A**, **Lizotte, M**, **Levasseur, M**, **Leaitch, WR.** 2019. Dimethyl sulfide and its role in aerosol formation and growth in the Arctic summer—A modelling study. *Atmospheric Chemistry and Physics* **19**: 14455–14476. DOI: https://doi.org/10.5194/acp-19-14455-2019.

Ghahreman, R, **Norman, A-L**, **Abbatt, JPD**, **Levasseur, M**, **Thomas, JL.** 2016. Biogenic, anthropogenic and sea salt sulfate size-segregated aerosols in the Arctic summer. *Atmospheric Chemistry and Physics* **16**: 5191–5202. DOI: https://doi.org/10.5194/acp-16-5191-2016.

Gharagheizi, F. 2012. Determination of diffusion coefficient of organic compounds in water using a simple molecular-based method. *Industrial & Engineering Chemistry Research* **51**: 2797–2803. DOI: https://doi.org/10.1021/ie201944h.

Giamarelou, M, **Eleftheriadis, K**, **Nyeki, S**, **Tunved, P**, **Torseth, K**, **Biskos, G.** 2016. Indirect evidence of the composition of nucleation mode atmospheric particles in the high Arctic. *Journal of Geophysical Research: Atmospheres* **121**: 965–975. DOI: https://doi.org/10.1002/2015JD023646.

Gilgen, A, **Huang, WTK**, **Ickes, L**, **Neubauer, D**, **Lohmann, U.** 2018. How important are future marine and shipping aerosol emissions in a warming Arctic summer and autumn? *Atmospheric Chemistry and Physics* **18**: 10521–10555. DOI: https://doi.org/10.5194/acp-18-10521-2018.

Goddijn-Murphy, L, **Woolf, DK**, **Marandino, C.** 2012. Space-based retrievals of air-sea gas transfer velocities using altimeters: Calibration for dimethyl sulfide. *Journal of Geophysical Research: Oceans* **117**. DOI: https://doi.org/10.1029/2011JC007535.

Goldman, JC, **Dennett, MR**, **Frew, NM.** 1988. Surfactant effects on air-sea gas exchange under turbulent conditions. *Deep Sea Research Part A. Oceanographic Research Papers* **35**: 1953–1970. DOI: https://doi.org/10.1016/0198-0149(88)90119-7.

Gondwe, M, **Krol, M**, **Klaassen, W**, **Gieskes, W**, **de Baar, H.** 2004. Comparison of modeled versus measured MSA:nss $SO_4^=$ ratios: A global analysis. *Global Biogeochemical Cycles* **18**. DOI: https://doi.org/10.1029/2003GB002144.

Gong, X, **Zhang, J**, **Croft, B**, **Yang, X**, **Frey, MM**, **Bergner, N**, **Chang, RY-W**, **Creamean, JM**, **Kuang, C**, **Martin, RV**, **Ranjithkumar, A**, **Sedlacek, AJ**, **Uin, J**, **Willmes, S**, **Zawadowicz, MA**, **Pierce, JR**, **Shupe, MD**, **Schmale, J**, **Wang, J.** 2023. Arctic warming by abundant fine sea salt aerosols from blowing snow. *Nature Geoscience* **16**: 768–774. DOI: https://doi.org/10.1038/s41561-023-01254-8.

Gordon, H, **Kirkby, J**, **Baltensperger, U**, **Bianchi, F**, **Breitenlechner, M**, **Curtius, J**, **Dias, A**, **Dommen, J**, **Donahue, NM**, **Dunne, EM**, **Duplissy, J**, **Ehrhart, S**, **Flagan, RC**, **Frege, C**, **Fuchs, C**, **Hansel, A**, **Hoyle, CR**, **Kulmala, M**, **Kürten, A**, **Lehtipalo, K**, **Makhmutov, V**, **Molteni, U**, **Rissanen, MP**, **Stozkhov, Y**, **Tröstl, J**, **Tsagkogeorgas, G**, **Wagner, R**, **Williamson, C**, **Wimmer, D**, **Winkler, PM**, **Yan, C**, **Carslaw, KS.** 2017. Causes and importance of new particle formation in the present-day and preindustrial atmospheres. *Journal of Geophysical Research: Atmospheres* **122**: 8739–8760. DOI: https://doi.org/10.1002/2017JD026844.

Goss, MB, **Kroll, JH**, 2024. Chamber studies of OH + dimethyl sulfoxide and dimethyl disulfide: Insights into the dimethyl sulfide oxidation mechanism. *Atmospheric Chemistry and Physics* **24**: 1299–1314. DOI: https://doi.org/10.5194/acp-24-1299-2024.

Gourdal, M, **Crabeck, O**, **Lizotte, M**, **Galindo, V**, **Gosselin, M**, **Babin, M**, **Scarratt, M**, **Levasseur, M.** 2019. Upward transport of bottom-ice dimethyl sulfide during advanced melting of arctic first-year sea ice.

Elementa: Science of the Anthropocene **7**: 33. DOI: https://doi.org/10.1525/elementa.370.

Gourdal, M, **Lizotte, M**, **Massé, G**, **Gosselin, M**, **Poulin, M**, **Scarratt, M**, **Charette, J**, **Levasseur, M**, 2018. Dimethyl sulfide dynamics in first-year sea ice melt ponds in the Canadian Arctic Archipelago. *Biogeosciences* **15**: 3169–3188. DOI: https://doi.org/10.5194/bg-15-3169-2018.

Grannas, AM, **Jones, AE**, **Dibb, J**, **Ammann, M**, **Anastasio, C**, **Beine, HJ**, **Bergin, M**, **Bottenheim, J**, **Boxe, CS**, **Carver, G**, **Chen, G**, **Crawford, JH**, **Dominé, F**, **Frey, MM**, **Guzmán, MI**, **Heard, DE**, **Helmig, D**, **Hoffmann, MR**, **Honrath, RE**, **Huey, LG**, **Hutterli, M**, **Jacobi, HW**, **Klán, P**, **Lefer, B**, **McConnell, J**, **Plane, J**, **Sander, R**, **Savarino, J**, **Shepson, PB**, **Simpson, WR**, **Sodeau, JR**, **von Glasow, R**, **Weller, R**, **Wolff, EW**, **Zhu, T**, 2007. An overview of snow photochemistry: Evidence, mechanisms and impacts. *Atmospheric Chemistry and Physics* **7**: 4329–4373. DOI: https://doi.org/10.5194/acp-7-4329-2007.

Grant, WS, **Horner, RA.** 1976. Growth responses to salinity variation in four Arctic ice diatoms. *Journal of Phycology* **12**: 180–185. DOI: https://doi.org/10.1111/j.1529-8817.1976.tb00498.x.

Griesche, HJ, **Ohneiser, K**, **Seifert, P**, **Radenz, M**, **Engelmann, R**, **Ansmann, A.** 2021. Contrasting ice formation in Arctic clouds: Surface-coupled vs. surface-decoupled clouds. *Atmospheric Chemistry and Physics* **21**: 10357–10374. DOI: https://doi.org/10.5194/acp-21-10357-2021.

Gros, V, **Bonsang, B**, **Sarda-Estève, R**, **Nikolopoulos, A**, **Metfies, K**, **Wietz, M**, **Peeken, I.** 2023. Concentrations of dissolved dimethyl sulfide (DMS), methanethiol and other trace gases in context of microbial communities from the temperate Atlantic to the Arctic Ocean. *Biogeosciences* **20**: 851–867. DOI: https://doi.org/10.5194/bg-20-851-2023.

Gunsch, MJ, **Liu, J**, **Moffett, CE**, **Sheesley, RJ**, **Wang, N**, **Zhang, Q**, **Watson, TB**, **Pratt, KA**, 2020. Diesel soot and amine-containing organic sulfate aerosols in an Arctic oil field. *Environmental Science & Technology* **54**: 92–101. DOI: https://doi.org/10.1021/acs.est.9b04825.

Haddon, A, **Monahan, AH**, **Sou, T**, **Steiner, N.** 2025. Simulated increases of future Arctic dimethylsulfide ocean concentrations, emissions and high-flux events. *Elementa: Science of the Anthropocene* **13**(1): 00090. DOI: https://doi.org/10.1525/elementa.2024.00090.

Hara, K, **Nishita-Hara, C**, **Osada, K**, **Yabuki, M**, **Yamanouchi, T.** 2021. Characterization of aerosol number size distributions and their effect on cloud properties at Syowa Station, Antarctica. *Atmospheric Chemistry and Physics* **21**: 12155–12172. DOI: https://doi.org/10.5194/acp-21-12155-2021.

Hara, K, **Osada, K**, **Nishita-Hara, C**, **Yamanouchi, T.** 2011. Seasonal variations and vertical features of aerosol particles in the Antarctic troposphere. *Atmospheric Chemistry and Physics* **11**: 5471–5484. DOI: https://doi.org/10.5194/acp-11-5471-2011.

Hayashida, H, **Carnat, G**, **Galí, M**, **Monahan, AH**, **Mortenson, E**, **Sou, T**, **Steiner, NS.** 2020. Spatio-temporal variability in modeled bottom ice and sea surface dimethylsulfide concentrations and fluxes in the Arctic during 1979–2015. *Global Biogeochemical Cycles* **34**: e2019GB006456. DOI: https://doi.org/10.1029/2019GB006456.

Hayashida, H, **Christian, JR**, **Holdsworth, AM**, **Hu, X**, **Monahan, AH**, **Mortenson, E**, **Myers, PG**, **Riche, OGJ**, **Sou, T**, **Steiner, NS.** 2019. CSIB v1 (Canadian Sea-ice Biogeochemistry): A sea-ice biogeochemical model for the NEMO community ocean modelling framework. *Geoscientific Model Development* **12**: 1965–1990. DOI: https://doi.org/10.5194/gmd-12-1965-2019.

Hayashida, H, **Steiner, N**, **Monahan, A**, **Galindo, V**, **Lizotte, M**, **Levasseur, M.** 2017. Implications of sea-ice biogeochemistry for oceanic production and emissions of dimethyl sulfide in the Arctic. *Biogeosciences* **14**: 3129–3155. DOI: https://doi.org/10.5194/bg-14-3129-2017.

Hayward, A, **Wright, SW**, **Carroll, D**, **Law, CS**, **Wongpan, P**, **Gutiérrez-Rodriguez, A**, **Pinkerton, MH.** 2025. Antarctic phytoplankton communities restructure under shifting sea-ice regimes. *Nature Climate Change* **15**: 889–896. DOI: https://doi.org/10.1038/s41558-025-02379-x.

Heald, CL, **Ridley, DA**, **Kroll, JH**, **Barrett, SRH**, **Cady-Pereira, KE**, **Alvarado, MJ**, **Holmes, CD.** 2014. Contrasting the direct radiative effect and direct radiative forcing of aerosols. *Atmospheric Chemistry and Physics* **14**: 5513–5527. DOI: https://doi.org/10.5194/acp-14-5513-2014.

Hellmer, HH, **Holtappels, M.** 2021. The Expedition PS124 of the research vessel POLARSTERN to the southern Weddell Sea in 2021 [WWW Document]. Berichte zur Polar- und Meeresforschung = Reports on polar and marine research. DOI: https://doi.org/10.48433/BzPM_0755_2021.

Herenz, P, **Wex, H**, **Mangold, A**, **Laffineur, Q**, **Gorodetskaya, IV**, **Fleming, ZL**, **Panagi, M**, **Stratmann, F.** 2019. CCN measurements at the Princess Elisabeth Antarctica research station during three austral summers. *Atmospheric Chemistry and Physics* **19**: 275–294. DOI: https://doi.org/10.5194/acp-19-275-2019.

Herrmann, H, **Ervens, B**, **Jacobi, H-W**, **Wolke, R**, **Nowacki, P**, **Zellner, R.** 2000. CAPRAM2.3: A Chemical Aqueous Phase Radical Mechanism for tropospheric chemistry. *Journal of Atmospheric Chemistry* **36**: 231–284. DOI: https://doi.org/10.1023/A:1006318622743.

Hodshire, AL, **Campuzano-Jost, P**, **Kodros, JK**, **Croft, B**, **Nault, BA**, **Schroder, JC**, **Jimenez, JL**, **Pierce, JR.** 2019. The potential role of methanesulfonic acid (MSA) in aerosol formation and growth and the associated radiative forcings. *Atmospheric Chemistry and*

Physics **19**: 3137–3160. DOI: https://doi.org/10.5194/acp-19-3137-2019.

Hoffmann, EH, **Heinold, B**, **Kubin, A**, **Tegen, I**, **Herrmann, H.** 2021. The importance of the representation of DMS oxidation in global chemistry-climate simulations. *Geophysical Research Letters* **48**: e2021GL094068. DOI: https://doi.org/10.1029/2021GL094068.

Hoffmann, EH, **Tilgner, A**, **Schrödner, R**, **Bräuer, P**, **Wolke, R**, **Herrmann, H.** 2016. An advanced modeling study on the impacts and atmospheric implications of multiphase dimethyl sulfide chemistry. *Proceedings of the National Academy of Sciences* **113**: 11776–11781. DOI: https://doi.org/10.1073/pnas.1606320113.

Holmes, CD. 2022. Technical note: Entrainment-limited kinetics of bimolecular reactions in clouds. *Atmospheric Chemistry and Physics* **22**: 9011–9015. DOI: https://doi.org/10.5194/acp-22-9011-2022.

Holmes, CD, **Bertram, TH**, **Confer, KL**, **Graham, KA**, **Ronan, AC**, **Wirks, CK, Shah, V.** 2019. The role of clouds in the tropospheric NO_x cycle: A new modeling approach for cloud chemistry and its global implications. *Geophysical Research Letters* **46**: 4980–4990. DOI: https://doi.org/10.1029/2019GL081990.

Hong, Y, **Zhu, L**, **Crocker, DR**, **Liu, T**, **Wang, Z**, **Wei, Z**, **Yu, C**, **Wei, Y**, **Yan, H**, **Johnston, DT**, **Kohl, IE**, **Peng, Y**, **Hilkert, A**, **Neubauer, C**, **Hattori, S.** 2025. Triple oxygen isotope analysis of methanesulfonate using the SO_3^- fragment in ESI-Orbitrap-MS. *Analytical Chemistry* **97**: 14339–14348. DOI: https://doi.org/10.1021/acs.analchem.5c01382.

Honrath, RE, **Peterson, MC**, **Guo, S**, **Dibb, JE**, **Shepson, PB**, **Campbell, B.** 1999. Evidence of NO_x production within or upon ice particles in the Greenland snowpack. *Geophysical Research Letters* **26**: 695–698. DOI: https://doi.org/10.1029/1999GL900077.

Hopkins, FE, **Archer, SD**, **Bell, TG**, **Suntharalingam, P**, **Todd, JD.** 2023. The biogeochemistry of marine dimethylsulfide. *Nature Reviews Earth & Environment* **4**: 361–376. DOI: https://doi.org/10.1038/s43017-023-00428-7.

Hoppmann, M, **Richter, ME**, **Smith, IJ**, **Jendersie, S**, **Langhorne, PJ**, **Thomas, DN**, **Dieckmann, GS.** 2020. Platelet ice, the Southern Ocean's hidden ice: A review. *Annals of Glaciology* **61**: 341–368. DOI: https://doi.org/10.1017/aog.2020.54.

Hulswar, S, **Simó, R**, **Galí, M**, **Bell, TG**, **Lana, A**, **Inamdar, S**, **Halloran, PR**, **Manville, G**, **Mahajan, AS.** 2022. Third revision of the global surface seawater dimethyl sulfide climatology (DMS-Rev3). *Earth System Science Data* **14**: 2963–2987. DOI: https://doi.org/10.5194/essd-14-2963-2022.

Humphries, RS, **Klekociuk, AR**, **Schofield, R**, **Keywood, M**, **Ward, J**, **Wilson, SR.** 2016. Unexpectedly high ultrafine aerosol concentrations above East Antarctic sea ice. *Atmospheric Chemistry and Physics* **16**: 2185–2206. DOI: https://doi.org/10.5194/acp-16-2185-2016.

Hynes, AJ, **Wine, PH**, **Semmes, DH.** 1986. Kinetics and mechanism of hydroxyl reactions with organic sulfides. *The Journal of Physical Chemistry* **90**: 4148–4156. DOI: https://doi.org/10.1021/j100408a062.

Ingham, T, **Bauer, D**, **Sander, R**, **Crutzen, PJ**, **Crowley, JN.** 1999. Kinetics and products of the reactions BrO + DMS and Br + DMS at 298 K. *The Journal of Physical Chemistry A* **103**: 7199–7209. DOI: https://doi.org/10.1021/jp9905979.

Ishino, S, **Hattori, S**, **Legrand, M**, **Chen, Q**, **Alexander, B**, **Shao, J**, **Huang, J**, **Jaeglé, L**, **Jourdain, B**, **Preunkert, S**, **Yamada, A**, **Yoshida, N**, **Savarino, J.** 2021. Regional characteristics of atmospheric sulfate formation in East Antarctica imprinted on ^{17}O-excess signature. *Journal of Geophysical Research: Atmospheres* **126**: e2020JD033583. DOI: https://doi.org/10.1029/2020JD033583.

Ishino, S, **Hattori, S**, **Savarino, J**, **Legrand, M**, **Albalat, E**, **Albarede, F**, **Preunkert, S**, **Jourdain, B**, **Yoshida, N.** 2019. Homogeneous sulfur isotope signature in East Antarctica and implication for sulfur source shifts through the last glacial-interglacial cycle. *Scientific Reports* **9**: 12378. DOI: https://doi.org/10.1038/s41598-019-48801-1.

Jang, E, **Park, K-T**, **Yoon, YJ**, **Kim, K**, **Gim, Y**, **Chung, HY**, **Lee, K**, **Choi, J**, **Park, J**, **Park, S-J**, **Koo, J-H**, **Fernandez, RP**, **Saiz-Lopez, A.** 2022. First-year sea ice leads to an increase in dimethyl sulfide-induced particle formation in the Antarctic Peninsula. *Science of The Total Environment* **803**: 150002. DOI: https://doi.org/10.1016/j.scitotenv.2021.150002.

Jang, E, **Park, K-T**, **Yoon, YJ**, **Kim, T-W**, **Hong, S-B**, **Becagli, S**, **Traversi, R**, **Kim, J**, **Gim, Y.** 2019. New particle formation events observed at the King Sejong Station, Antarctic Peninsula—Part 2: Link with the oceanic biological activities. *Atmospheric Chemistry and Physics* **19**: 7595–7608. DOI: https://doi.org/10.5194/acp-19-7595-2019.

Jang, S, **Park, K-T**, **Lee, K**, **Yoon, YJ**, **Kim, K**, **Chung, HY**, **Jang, E**, **Becagli, S**, **Lee, BY**, **Traversi, R**, **Eleftheriadis, K**, **Krejci, R**, **Hermansen, O.** 2021. Large seasonal and interannual variations of biogenic sulfur compounds in the Arctic atmosphere (Svalbard; 78.9° N, 11.9° E). *Atmospheric Chemistry and Physics* **21**: 9761–9777. DOI: https://doi.org/10.5194/acp-21-9761-2021.

Jarníková, T, **Tortell, PD.** 2016. Towards a revised climatology of summertime dimethylsulfide concentrations and sea–air fluxes in the Southern Ocean. *Environmental Chemistry* **13**: 364–378. DOI: https://doi.org/10.1071/EN14272.

Jeffery, N, **Maltrud, ME**, **Hunke, EC**, **Wang, S**, **Wolfe, J**, **Turner, AK**, **Burrows, SM**, **Shi, X**, **Lipscomb, WH**, **Maslowski, W**, **Calvin, KV.** 2020. Investigating controls on sea ice algal production using E3SMv1.1-BGC. *Annals of Glaciology* **61**: 51–72. DOI: https://doi.org/10.1017/aog.2020.7.

Jeong, D, **McNamara, SM**, **Barget, AJ**, **Raso, ARW**, **Upchurch, LM**, **Thanekar, S**, **Quinn, PK**, **Simpson,**

WR, **Fuentes, JD**, **Shepson, PB**, **Pratt, KA.** 2022. Multiphase reactive bromine chemistry during late spring in the Arctic: Measurements of gases, particles, and snow. *ACS Earth and Space Chemistry* **6**: 2877–2887. DOI:https://doi.org/10.1021/acsearthspacechem.2c00189.

Jernigan, CM, **Cappa, CD**, **Bertram, TH.** 2022. Reactive uptake of hydroperoxymethyl thioformate to sodium chloride and sodium iodide aerosol particles. *The Journal of Physical Chemistry A* **126**: 4476–4481. DOI: https://doi.org/10.1021/acs.jpca.2c03222.

Jernigan, CM, **Rivard, MJ**, **Berkelhammer, MB**, **Bertram, TH.** 2024. Sulfate and carbonyl sulfide production in aqueous reactions of hydroperoxymethyl thioformate. *ACS ES&T Air* **1**: 397–404. DOI: https://doi.org/10.1021/acsestair.3c00098.

Joge, SD, **Mahajan, AS**, **Hulswar, S**, **Marandino, CA**, **Galí, M**, **Bell, TG**, **Simó, R.** 2024a. Dimethyl sulfide (DMS) climatologies, fluxes, and trends—Part 1: Differences between seawater DMS estimations. *Biogeosciences* **21**: 4439–4452. DOI:https://doi.org/10.5194/bg-21-4439-2024.

Joge, SD, **Mahajan, AS**, **Hulswar, S**, **Marandino, CA**, **Galí, M**, **Bell, TG**, **Yang, M**, **Simó, R.** 2024b. Dimethyl sulfide (DMS) climatologies, fluxes, and trends—Part 2: Sea–air fluxes. *Biogeosciences* **21**: 4453–4467. DOI: https://doi.org/10.5194/bg-21-4453-2024.

Joge, SD, **Mansour, K**, **Simó, R**, **Galí, M**, **Steiner, N**, **Saiz-Lopez, A**, **Mahajan, AS.** 2025. Climate warming increases global oceanic dimethyl sulfide emissions. *Proceedings of the National Academy of Sciences* **122**: e2502077122. DOI: https://doi.org/10.1073/pnas.2502077122.

Johnson, JS, **Jen, CN.** 2023. Role of methanesulfonic acid in sulfuric acid–amine and ammonia new particle formation. *ACS Earth and Space Chemistry* **7**: 653–660. DOI: https://doi.org/10.1021/acsearthspacechem.3c00017.

Johnson, MT. 2010. A numerical scheme to calculate temperature and salinity dependent air-water transfer velocities for any gas. *Ocean Science* **6**: 913–932. DOI:https://doi.org/10.5194/os-6-913-2010.

Jokinen, T, **Sipilä, M**, **Kontkanen, J**, **Vakkari, V**, **Tisler, P**, **Duplissy, E-M**, **Junninen, H**, **Kangasluoma, J**, **Manninen, HE**, **Petäjä, T**, **Kulmala, M**, **Worsnop, DR**, **Kirkby, J**, **Virkkula, A**, **Kerminen, V-M.** 2018. Ion-induced sulfuric acid–ammonia nucleation drives particle formation in coastal Antarctica. *Science Advances* **4**: eaat9744. DOI: https://doi.org/10.1126/sciadv.aat9744.

Jongebloed, UA, **Chalif, JI**, **Tashmim, L**, **Porter, WC**, **Bates, KH**, **Chen, Q**, **Osterberg, EC**, **Koffman, BG**, **Cole-Dai, J**, **Winski, DA**, **Ferris, DG**, **Kreutz, KJ**, **Wake, CP**, **Alexander, B.** 2025. Dimethyl sulfide chemistry over the industrial era: Comparison of key oxidation mechanisms and long-term observations. *Atmospheric Chemistry and Physics* **25**: 4083–4106. DOI: https://doi.org/10.5194/acp-25-4083-2025.

Jongebloed, UA, **Schauer, AJ**, **Cole-Dai, J**, **Larrick, CG**, **Wood, R**, **Fischer, TP**, **Carn, SA**, **Salimi, S**, **Edouard, SR**, **Zhai, S**, **Geng, L**, **Alexander, B.** 2023a. Underestimated passive volcanic sulfur degassing implies overestimated anthropogenic aerosol forcing. *Geophysical Research Letters* **50**: e2022GL102061. DOI: https://doi.org/10.1029/2022GL102061.

Jongebloed, UA, **Schauer, AJ**, **Hattori, S**, **Cole-Dai, J**, **Larrick, CG**, **Salimi, S**, **Edouard, SR**, **Geng, L**, **Alexander, B.** 2023b. Sulfur isotopes quantify the impact of anthropogenic activities on industrial-era Arctic sulfate in a Greenland ice core. *Environmental Research Letters* **18**: 074020. DOI: https://doi.org/10.1088/1748-9326/acdc3d.

Judd, KD, **Parsons, SW**, **Majumder, T**, **Dawlaty, JM.** 2025. Electrostatics, hydration, and chemical equilibria at charged monolayers on water. *Chemical Reviews* **125**: 2440–2473. DOI: https://doi.org/10.1021/acs.chemrev.4c00676.

Kang, L, **Marchand, R**, **Ma, P-L**, **Huang, M**, **Wood, R**, **Jongebloed, U**, **Alexander, B.** 2025. Impacts of DMS emissions and chemistry on E3SMv2 simulated cloud droplet numbers and aerosol concentrations over the Southern Ocean. *Journal of Advances in Modeling Earth Systems* **17**: e2024MS004683. DOI: https://doi.org/10.1029/2024MS004683.

Kasamatsu, N, **Kawaguchi, S**, **Watanabe, S**, **Odate, T**, **Fukuchi, M.** 2004. Possible impacts of zooplankton grazing on dimethylsulfide production in the Antarctic Ocean. *Canadian Journal of Fisheries and Aquatic Science* **61**: 736–743. DOI: https://doi.org/10.1139/f04-072.

Kaur, R, **Anastasio, C.** 2017. Light absorption and the photoformation of hydroxyl radical and singlet oxygen in fog waters. *Atmospheric Environment* **164**: 387–397. DOI:https://doi.org/10.1016/j.atmosenv.2017.06.006.

Kazil, J, **Wang, H**, **Feingold, G**, **Clarke, AD**, **Snider, JR**, **Bandy, AR.** 2011. Modeling chemical and aerosol processes in the transition from closed to open cells during VOCALS-REx. *Atmospheric Chemistry and Physics* **11**: 7491–7514. DOI:https://doi.org/10.5194/acp-11-7491-2011.

Kecorius, S, **Hoffmann, EH**, **Tilgner, A**, **Barrientos-Velasco, C**, **van Pinxteren, M**, **Zeppenfeld, S**, **Vogl, T**, **Madueño, L**, **Lovrić, M**, **Wiedensohler, A**, **Kulmala, M**, **Paasonen, P**, **Herrmann, H.** 2023. Rapid growth of Aitken-mode particles during Arctic summer by fog chemical processing and its implication. *PNAS Nexus* **2**: pgad124. DOI: https://doi.org/10.1093/pnasnexus/pgad124.

Kerminen, V-M, **Chen, X**, **Vakkari, V**, **Petäjä, T**, **Kulmala, M**, **Bianchi, F.** 2018. Atmospheric new particle formation and growth: Review of field observations. *Environmental Research Letters* **13**: 103003. DOI: https://doi.org/10.1088/1748-9326/aadf3c.

Kettle, AJ, **Andreae, MO**, **Amouroux, D**, **Andreae, TW**, **Bates, TS**, **Berresheim, H**, **Bingemer, H**, **Boniforti, R**, **Curran, MAJ**, **DiTullio, GR**, **Helas, G**, **Jones, GB**,

Keller, MD, **Kiene, RP**, **Leck, C**, **Levasseur, M**, **Malin, G**, **Maspero, M**, **Matrai, P**, **McTaggart, AR**, **Mihalopoulos, N**, **Nguyen, BC**, **Novo, A**, **Putaud, JP**, **Rapsomanikis, S**, **Roberts, G**, **Schebeske, G**, **Sharma, S**, **Simó, R**, **Staubes, R**, **Turner, S**, **Uher, G.** 1999. A global database of sea surface dimethylsulfide (DMS) measurements and a procedure to predict sea surface DMS as a function of latitude, longitude, and month. *Global Biogeochemical Cycles* **13**: 399–444. DOI: https://doi.org/10.1029/1999GB900004.

Kettle, AJ, **Rhee, TS**, **von Hobe, M**, **Poulton, A**, **Aiken, J**, **Andreae, MO.** 2001. Assessing the flux of different volatile sulfur gases from the ocean to the atmosphere. *Journal of Geophysical Research: Atmospheres* **106**: 12193–12209. DOI:https://doi.org/10.1029/2000JD900630.

Kiene, RP. 1996. Production of methanethiol from dimethylsulfoniopropionate in marine surface waters. *Marine Chemistry* **54**: 69–83. DOI: https://doi.org/10.1016/0304-4203(96)00006-0.

Kiene, RP, **Linn, LJ.** 2000. The fate of dissolved dimethylsulfoniopropionate (DMSP) in seawater: Tracer studies using ^{35}S-DMSP. *Geochimica et Cosmochimica Acta* **64**: 2797–2810. DOI: https://doi.org/10.1016/S0016-7037(00)00399-9.

Kiene, RP, **Linn, LJ**, **Bruton, JA.** 2000. New and important roles for DMSP in marine microbial communities. *Journal of Sea Research* **43**: 209–224. DOI: https://doi.org/10.1016/S1385-1101(00)00023-X.

Kiene, RP, **Linn, LJ**, **González, J**, **Moran, MA**, **Bruton, JA.** 1999. Dimethylsulfoniopropionate and methanethiol are important precursors of methionine and protein-sulfur in marine bacterioplankton. *Applied and Environmental Microbiology* **65**: 4549–4558. DOI:https://doi.org/10.1128/AEM.65.10.4549-4558.1999.

Kilgour, DB, **Jernigan, CM**, **Garmash, O**, **Aggarwal, S**, **Zhou, S**, **Mohr, C**, **Salter, ME**, **Thornton, JA**, **Wang, J**, **Zieger, P**, **Bertram, TH.** 2025. Cloud processing of dimethyl sulfide (DMS) oxidation products limits sulfur dioxide (SO_2) and carbonyl sulfide (OCS) production in the eastern North Atlantic marine boundary layer. *Atmospheric Chemistry and Physics* **25**: 1931–1947. DOI: https://doi.org/10.5194/acp-25-1931-2025.

Kilgour, DB, **Novak, GA**, **Sauer, JS**, **Moore, AN**, **Dinasquet, J**, **Amiri, S**, **Franklin, EB**, **Mayer, K**, **Winter, M**, **Morris, CK**, **Price, T**, **Malfatti, F**, **Crocker, DR**, **Lee, C**, **Cappa, CD**, **Goldstein, AH**, **Prather, KA**, **Bertram, TH.** 2022. Marine gas-phase sulfur emissions during an induced phytoplankton bloom. *Atmospheric Chemistry and Physics* **22**: 1601–1613. DOI: https://doi.org/10.5194/acp-22-1601-2022.

Kirpes, RM, **Lei, Z**, **Fraund, M**, **Gunsch, MJ**, **May, NW**, **Barrett, TE**, **Moffett, CE**, **Schauer, AJ**, **Alexander, B**, **Upchurch, LM**, **China, S**, **Quinn, PK**, **Moffet, RC**, **Laskin, A**, **Sheesley, RJ**, **Pratt, KA**, **Ault, AP.** 2022. Solid organic-coated ammonium sulfate particles at high relative humidity in the summertime Arctic atmosphere. *Proceedings of the National Academy of Sciences* **119**: e2104496119. DOI: https://doi.org/10.1073/pnas.2104496119.

Kirst, GO, **Thiel, C**, **Wolff, H**, **Nothnagel, J**, **Wanzek, M**, **Ulmke, R.** 1991. Dimethylsulfoniopropionate (DMSP) in icealgae and its possible biological role. *Marine Chemistry* **35**: 381–388. DOI: https://doi.org/10.1016/S0304-4203(09)90030-5.

Kloster, S, **Feichter, J**, **Maier-Reimer, E**, **Six, KD**, **Stier, P**, **Wetzel, P.** 2006. DMS cycle in the marine ocean-atmosphere system—a global model study. *Biogeosciences* **3**: 29–51. DOI:https://doi.org/10.5194/bg-3-29-2006.

Knopf, DA, **Alpert, PA.** 2023. Atmospheric ice nucleation. *Nature Reviews Physics* **5**: 203–217. DOI: https://doi.org/10.1038/s42254-023-00570-7.

Koga, S, **Nomura, D**, **Wada, M.** 2014. Variation of dimethylsulfide mixing ratio over the Southern Ocean from 36°S to 70°S. *Polar Science* **8**: 306–313. DOI: https://doi.org/10.1016/j.polar.2014.04.002.

Kojoj, J, **Freitas, GP**, **Muilwijk, M**, **Granskog, MA**, **Naakka, T**, **Ekman, AML**, **Heutte, B**, **Schmale, J**, **Da Silva, AD**, **Lapere, R**, **Marelle, L**, **Thomas, JL**, **Melsheimer, C**, **Murray, BJ**, **Zieger, P.** 2024. An Arctic marine source of fluorescent primary biological aerosol particles during the transition from summer to autumn at the North Pole. *Tellus B: Chemical and Physical Meteorology* **76**. DOI: https://doi.org/10.16993/tellusb.1880.

Kolesar, KR, **Cellini, J**, **Peterson, PK**, **Jefferson, A**, **Tuch, T**, **Birmili, W**, **Wiedensohler, A**, **Pratt, KA.** 2017. Effect of Prudhoe Bay emissions on atmospheric aerosol growth events observed in Utqiaġvik (Barrow), Alaska. *Atmospheric Environment* **152**: 146–155. DOI:https://doi.org/10.1016/j.atmosenv.2016.12.019.

Koop, T, **Luo, B**, **Tsias, A**, **Peter, T.** 2000. Water activity as the determinant for homogeneous ice nucleation in aqueous solutions. *Nature* **406**: 611–614. DOI: https://doi.org/10.1038/35020537.

Kukui, A, **Legrand, M**, **Ancellet, G**, **Gros, V**, **Bekki, S**, **Sarda-Estève, R**, **Loisil, R**, **Preunkert, S.** 2012. Measurements of OH and RO_2 radicals at the coastal Antarctic site of Dumont d'Urville (East Antarctica) in summer 2010–2011. *Journal of Geophysical Research: Atmospheres* **117**. DOI: https://doi.org/10.1029/2012JD017614.

Kulmala, M, **Pirjola, L**, **Mäkelä, JM.** 2000. Stable sulphate clusters as a source of new atmospheric particles. *Nature* **404**: 66–69. DOI: https://doi.org/10.1038/35003550.

Kwong, KC, **Chim, MM**, **Hoffmann, EH**, **Tilgner, A**, **Herrmann, H**, **Davies, JF**, **Wilson, KR**, **Chan, MN.** 2018. Chemical transformation of methanesulfonic acid and sodium methanesulfonate through heterogeneous OH oxidation. *ACS Earth and Space Chemistry* **2**: 895–903. DOI: https://doi.org/10.1021/acsearthspacechem.8b00072.

Lachlan-Cope, T, **Beddows, DCS**, **Brough, N**, **Jones, AE**, **Harrison, RM**, **Lupi, A**, **Yoon, YJ**, **Virkkula, A**, **Dall'Osto, M.** 2020. On the annual variability of Antarctic aerosol size distributions at Halley Research Station. *Atmospheric Chemistry and Physics* **20**: 4461–4476. DOI: https://doi.org/10.5194/acp-20-4461-2020.

Lana, A, **Bell, TG**, **Simó, R**, **Vallina, SM**, **Ballabrera-Poy, J**, **Kettle, AJ**, **Dachs, J**, **Bopp, L**, **Saltzman, ES**, **Stefels, J**, **Johnson, JE**, **Liss, PS.** 2011. An updated climatology of surface dimethlysulfide concentrations and emission fluxes in the global ocean. *Global Biogeochemical Cycles* **25**: GB1004. DOI: https://doi.org/10.1029/2010GB003850.

Lapere, R, **Haddon, A**, **Price, R**, **Marelle, L**, **Monahan, AH**, **Steiner, NS**, **Raut, JC**, **Bastien, L, Thomas, JL.** n.d. Oceanic DMS strongly affects aerosols and clouds in the Arctic. *Geophysical Research Letters*, submitted, in review.

Lawler, MJ, **Saltzman, ES**, **Karlsson, L**, **Zieger, P**, **Salter, M**, **Baccarini, A**, **Schmale, J**, **Leck, C.** 2021. New insights into the composition and origins of ultrafine aerosol in the summertime high Arctic. *Geophysical Research Letters* **48**: e2021GL094395. DOI: https://doi.org/10.1029/2021GL094395.

Lawson, SJ, **Law, CS**, **Harvey, MJ**, **Bell, TG**, **Walker, CF**, **de Bruyn, WJ**, **Saltzman, ES.** 2020. Methanethiol, dimethyl sulfide and acetone over biologically productive waters in the southwest Pacific Ocean. *Atmospheric Chemistry and Physics* **20**: 3061–3078. DOI: https://doi.org/10.5194/acp-20-3061-2020.

Leaitch, WR, **Korolev, A**, **Aliabadi, AA**, **Burkart, J**, **Willis, MD**, **Abbatt, JPD**, **Bozem, H**, **Hoor, P**, **Köllner, F**, **Schneider, J**, **Herber, A**, **Konrad, C**, **Brauner, R.** 2016. Effects of 20–100 nm particles on liquid clouds in the clean summertime Arctic. *Atmospheric Chemistry and Physics* **16**: 11107–11124. DOI: https://doi.org/10.5194/acp-16-11107-2016.

Leaitch, WR, **Sharma, S**, **Huang, L**, **Toom-Sauntry, D**, **Chivulescu, A**, **Macdonald, AM**, **von Salzen, K**, **Pierce, JR**, **Bertram, AK**, **Schroder, JC**, **Shantz, NC**, **Chang, RY-W**, **Norman, A-L.** 2013. Dimethyl sulfide control of the clean summertime Arctic aerosol and cloud. *Elementa: Science of the Anthropocene* **1**: 000017. DOI:https://doi.org/10.12952/journal.elementa.000017.

Leck, C, **Persson, C.** 1996. The central Arctic Ocean as a source of dimethyl sulfide: Seasonal variability in relation to biological activity. *Tellus B: Chemical and Physical Meteorology* **48**: 156–177. DOI: https://doi.org/10.3402/tellusb.v48i2.15834.

Leck, C, **Rodhe, H.** 1991. Emissions of marine biogenic sulfur to the atmosphere of northern Europe. *Journal of Atmospheric Chemistry* **12**: 63–86. DOI: https://doi.org/10.1007/BF00053934.

Legrand, M, **Preunkert, S**, **Savarino, J**, **Frey, MM**, **Kukui, A**, **Helmig, D**, **Jourdain, B**, **Jones, AE**, **Weller, R**, **Brough, N**, **Gallée, H.** 2016a. Inter-annual variability of surface ozone at coastal (Dumont d'Urville, 2004–2014) and inland (Concordia, 2007–2014) sites in East Antarctica. *Atmospheric Chemistry and Physics* **16**: 8053–8069. DOI: https://doi.org/10.5194/acp-16-8053-2016.

Legrand, M, **Preunkert, S**, **Weller, R**, **Zipf, L**, **Elsässer, C**, **Merchel, S**, **Rugel, G**, **Wagenbach, D.** 2017. Year-round record of bulk and size-segregated aerosol composition in central Antarctica (Concordia site)—Part 2: Biogenic sulfur (sulfate and methanesulfonate) aerosol. *Atmospheric Chemistry and Physics* **17**: 14055–14073. DOI:https://doi.org/10.5194/acp-17-14055-2017.

Legrand, M, **Sciare, J**, **Jourdain, B**, **Genthon, C.** 2001. Subdaily variations of atmospheric dimethylsulfide, dimethylsulfoxide, methanesulfonate, and non-sea-salt sulfate aerosols in the atmospheric boundary layer at Dumont d'Urville (coastal Antarctica) during summer. *Journal of Geophysical Research: Atmospheres* **106**: 14409–14422. DOI:https://doi.org/10.1029/2000JD900840.

Legrand, M, **Yang, X**, **Preunkert, S**, **Theys, N.** 2016b. Year-round records of sea salt, gaseous, and particulate inorganic bromine in the atmospheric boundary layer at coastal (Dumont d'Urville) and central (Concordia) East Antarctic sites. *Journal of Geophysical Research: Atmospheres* **121**: 997–1023. DOI: https://doi.org/10.1002/2015JD024066.

Lelieveld, J, **Peters, W**, **Dentener, FJ**, **Krol, MC.** 2002. Stability of tropospheric hydroxyl chemistry. *Journal of Geophysical Research: Atmospheres* **107**: ACH 17-1–ACH 17-11. DOI: https://doi.org/10.1029/2002JD002272.

Levasseur, M. 2013. Impact of Arctic meltdown on the microbial cycling of sulphur. *Nature Geoscience* **6**: 691–700. DOI: https://doi.org/10.1038/ngeo1910.

Levasseur, M, **Gosselin, M**, **Michaud, S.** 1994. A new source of dimethylsulfide (DMS) for the arctic atmosphere: Ice diatoms. *Marine Biology* **121**: 381–387. DOI: https://doi.org/10.1007/BF00346748.

Li, C-X, **Chen, K**, **Sun, X**, **Liu, L**, **Xin, M**, **Liu, X-L**, **Wang, B-D.** 2024a. Summer sea ice melting enhances phytoplankton and dimethyl sulfide production. *Limnology and Oceanography* **69**: 2453–2472. DOI: https://doi.org/10.1002/lno.12681.

Li, C-X, **Wang, B-D**, **Yang, G-P**, **Wang, Z-C**, **Chen, J-F**, **Lyu, Y.** 2017. Occurrence and turnover of biogenic sulfur in the Bering Sea during summer. *Journal of Geophysical Research: Oceans* **122**: 8567–8592. DOI: https://doi.org/10.1002/2017JC013299.

Li, T, **Li, J**, **Xie, L**, **Lin, B**, **Jiang, H**, **Sun, R**, **Wang, X**, **Liu, B**, **Tian, C**, **Li, Q**, **Jia, W**, **Zhang, G**, **Peng, P.** 2024b. In situ biomass burning enhanced the contribution of biogenic sources to sulfate aerosol in subtropical cities. *Science of The Total Environment* **908**: 168384. DOI: https://doi.org/10.1016/j.scitotenv.2023.168384.

Liao, J, **Huey, LG**, **Liu, Z**, **Tanner, DJ**, **Cantrell, CA**, **Orlando, JJ**, **Flocke, FM**, **Shepson, PB**, **Weinheimer, AJ**, **Hall, SR**, **Ullmann, K**, **Beine, HJ**, **Wang,**

Y, **Ingall, ED**, **Stephens, CR**, **Hornbrook, RS**, **Apel, EC**, **Riemer, D**, **Fried, A**, **Mauldin, RL** III, **Smith, JN**, **Staebler, RM**, **Neuman, JA**, **Nowak, JB.** 2014. High levels of molecular chlorine in the Arctic atmosphere. *Nature Geoscience* **7**: 91–94. DOI: https://doi.org/10.1038/ngeo2046.

Lieser, JL, **Curran, MAJ**, **Bowie, AR**, **Davidson, AT**, **Doust, SJ**, **Fraser, AD**, **Galton-Fenzi, BK**, **Massom, RA**, **Meiners, KM**, **Melbourne-Thomas, J**, **Reid, PA**, **Strutton, PG**, **Vance, TR**, **Vancoppenolle, M**, **Westwood, KJ**, **Wright, SW.** 2015. Antarctic slush-ice algal accumulation not quantified through conventional satellite imagery: Beware the ice of March. *The Cryosphere Discussions* **9**: 6187–6222. DOI: https://doi.org/10.5194/tcd-9-6187-2015.

Limmer, DT, **Götz, AW**, **Bertram, TH**, **Nathanson, GM.** 2024. Molecular insights into chemical reactions at aqueous aerosol interfaces. *Annual Review of Physical Chemistry* **75**: 111–135. DOI: https://doi.org/10.1146/annurev-physchem-083122-121620.

Lin, X, **Chameides, WL.** 1993. CCN formation from DMS oxidation without SO_2 acting as an intermediate. *Geophysical Research Letters* **20**: 579–582. DOI: https://doi.org/10.1029/93GL00805.

Liss, PS, **Merlivat, L.** 1986. Air-sea gas exchange rates: Introduction and synthesis, in Buat-Ménard, P ed., *The role of air-sea exchange in geochemical cycling, NATO ASI series*. Dordrecht, the Netherlands: Springer: 113–127. DOI: https://doi.org/10.1007/978-94-009-4738-2_5.

Liu, J, **Gunsch, MJ**, **Moffett, CE**, **Xu, L**, **El Asmar, R**, **Zhang, Q**, **Watson, TB**, **Allen, HM**, **Crounse, JD**, **St. Clair, J**, **Kim, M**, **Wennberg, PO**, **Weber, RJ**, **Sheesley, RJ**, **Pratt, KA.** 2021a. Hydroxymethanesulfonate (HMS) formation during summertime fog in an Arctic oil field. *Environmental Science & Technology Letters* **8**: 511–518. DOI: https://doi.org/10.1021/acs.estlett.1c00357.

Liu, T, **Abbatt, JPD.** 2021. Oxidation of sulfur dioxide by nitrogen dioxide accelerated at the interface of deliquesced aerosol particles. *Nature Chemistry* **13**: 1173–1177. DOI: https://doi.org/10.1038/s41557-021-00777-0.

Liu, T, **Chan, AWH**, **Abbatt, JPD.** 2021b. Multiphase oxidation of sulfur dioxide in aerosol particles: Implications for sulfate formation in polluted environments. *Environmental Science & Technology* **55**: 4227–4242. DOI: https://doi.org/10.1021/acs.est.0c06496.

Liu, T, **Clegg, SL**, **Abbatt, JPD.** 2020. Fast oxidation of sulfur dioxide by hydrogen peroxide in deliquesced aerosol particles. *Proceedings of the National Academy of Sciences* **117**: 1354–1359. DOI: https://doi.org/10.1073/pnas.1916401117.

Liu, T, **Ma, L**, **Yang, Y**, **Ding, A.** 2023. Kinetics of the reaction $MSI^- + O_3$ in deliquesced aerosol particles: Implications for sulfur chemistry in the marine boundary layer. *Geophysical Research Letters* **50**: e2023GL105945. DOI: https://doi.org/10.1029/2023GL105945.

Lizotte, M, **Levasseur, M**, **Galindo, V**, **Gourdal, M**, **Gosselin, M**, **Tremblay, J-É**, **Blais, M**, **Charette, J**, **Hussherr, R.** 2020. Phytoplankton and dimethylsulfide dynamics at two contrasting Arctic ice edges. *Biogeosciences* **17**: 1557–1581. DOI:https://doi.org/10.5194/bg-17-1557-2020.

Loose, B, **Fer, I**, **Ulfsbo, A**, **Chierici, M**, **Droste, ES**, **Nomura, D**, **Fransson, A**, **Hoppema, M**, **Torres-Valdés, S.** 2024. An analysis of air-sea gas exchange for the entire MOSAiC Arctic drift. *Elementa: Science of the Anthropocene* **12**: 00128. DOI:https://doi.org/10.1525/elementa.2023.00128.

Loose, B, **Kelly, RP**, **Bigdeli, A**, **Williams, W**, **Krishfield, R**, **van der Loeff, MR**, **Moran, SB.** 2017. How well does wind speed predict air-sea gas transfer in the sea ice zone? A synthesis of radon deficit profiles in the upper water column of the Arctic Ocean. *Journal of Geophysical Research: Oceans* **122**: 3696–3714. DOI:https://doi.org/10.1002/2016JC012460.

Luo, G, **Yu, F**, **Moch, JM.** 2020. Further improvement of wet process treatments in GEOS-Chem v12.6.0: Impact on global distributions of aerosols and aerosol precursors. *Geoscientific Model Development* **13**: 2879–2903. DOI: https://doi.org/10.5194/gmd-13-2879-2020.

Lyon, BR, **Lee, PA**, **Bennett, JM**, **DiTullio, GR**, **Janech, MG.** 2011. Proteomic analysis of a sea-ice diatom: Salinity acclimation provides new insight into the dimethylsulfoniopropionate production pathway. *Plant Physiology* **157**: 1926–1941. DOI: https://doi.org/10.1104/pp.111.185025.

Mace, GG, **Protat, A**, **Benson, S.** 2021. Mixed-phase clouds over the Southern Ocean as observed from satellite and surface based lidar and radar. *Journal of Geophysical Research: Atmospheres* **126**: e2021JD034569. DOI: https://doi.org/10.1029/2021JD034569.

Mahajan, AS, **Fadnavis, S**, **Thomas, MA**, **Pozzoli, L**, **Gupta, S**, **Royer, S-J**, **Saiz-Lopez, A**, **Simó, R.** 2015. Quantifying the impacts of an updated global dimethyl sulfide climatology on cloud microphysics and aerosol radiative forcing. *Journal of Geophysical Research: Atmospheres* **120**: 2524–2536. DOI: https://doi.org/10.1002/2014JD022687.

Mahmood, R, **von Salzen, K**, **Norman, A-L**, **Galí, M**, **Levasseur, M.** 2019. Sensitivity of Arctic sulfate aerosol and clouds to changes in future surface seawater dimethylsulfide concentrations. *Atmospheric Chemistry and Physics* **19**: 6419–6435. DOI: https://doi.org/10.5194/acp-19-6419-2019.

Mai, TV-T, **Nguyen, HT**, **Huynh, LK.** 2020. Kinetics of hydrogen abstraction from CH_3SH by OH radicals: An *ab initio* RRKM-based master equation study. *Atmospheric Environment* **242**: 117833. DOI: https://doi.org/10.1016/j.atmosenv.2020.117833.

Mallet, MD, **Humphries, RS**, **Fiddes, SL**, **Alexander, SP**, **Altieri, K**, **Angot, H**, **Anilkumar, N**, **Bartels-Rausch, T**, **Creamean, J**, **Dall'Osto, M**, **Dommergue, A**, **Frey, M**, **Henning, S**, **Lannuzel, D**, **Lapere, R**, **Mace, GG**, **Mahajan, AS**, **McFarquhar, GM**,

Meiners, KM, **Miljevic, B**, **Peeken, I**, **Protat, A**, **Schmale, J**, **Steiner, N**, **Sellegri, K**, **Simó, R**, **Thomas, JL**, **Willis, MD**, **Winton, VHL**, **Woodhouse, MT.** 2023. Untangling the influence of Antarctic and Southern Ocean life on clouds. *Elementa: Science of the Anthropocene* **11**: 00130. DOI: https://doi.org/10.1525/elementa.2022.00130.

Mallet, MD, **Miljevic, B**, **Humphries, RS**, **Mace, GG**, **Alexander, SP**, **Protat, A**, **Chambers, S**, **Cravigan, L**, **DeMott, PJ**, **Fiddes, S**, **Harnwell, J**, **Keywood, MD**, **McFarquhar, GM**, **McRobert, I**, **Moore, KA**, **Mynard, C**, **Osuagwu, CG**, **Ristovski, Z**, **Selleck, P**, **Taylor, S**, **Ward, J**, **Williams, A.** 2025. Biological enhancement of cloud droplet concentrations observed off East Antarctica. *npj Climate and Atmospheric Science* **8**: 1–7. DOI:https://doi.org/10.1038/s41612-025-00990-5.

Malley, PPA, **Chakraborty, S**, **Kahan, TF.** 2018. Physical characterization of frozen saltwater solutions using Raman microscopy. *ACS Earth and Space Chemistry* **2**: 702–710. DOI:https://doi.org/10.1021/acsearthspacechem.8b00045.

Mansour, K, **Decesari, S**, **Ceburnis, D**, **Ovadnevaite, J**, **Rinaldi, M.** 2023. Machine learning for prediction of daily sea surface dimethylsulfide concentration and emission flux over the North Atlantic Ocean (1998–2021). *Science of The Total Environment* **871**: 162123. DOI: https://doi.org/10.1016/j.scitotenv.2023.162123.

Mansour, K, **Decesari, S**, **Ceburnis, D**, **Ovadnevaite, J**, **Russell, LM**, **Paglione, M**, **Poulain, L**, **Huang, S**, **O'Dowd, C**, **Rinaldi, M.** 2024. IPB-MSA&SO_4: A daily 0.25° resolution dataset of in situ-produced biogenic methanesulfonic acid and sulfate over the North Atlantic during 1998–2022 based on machine learning. *Earth System Science Data* **16**: 2717–2740. DOI: https://doi.org/10.5194/essd-16-2717-2024.

Manville, G, **Bell, TG**, **Mulcahy, JP**, **Simó, R**, **Galí, M**, **Mahajan, AS**, **Hulswar, S**, **Halloran, PR.** 2023. Global analysis of the controls on seawater dimethylsulfide spatial variability. *Biogeosciences* **20**: 1813–1828. DOI: https://doi.org/10.5194/bg-20-1813-2023.

Marelle, L, **Thomas, JL**, **Ahmed, S**, **Tuite, K**, **Stutz, J**, **Dommergue, A**, **Simpson, WR**, **Frey, MM**, **Baladima, F.** 2021. Implementation and impacts of surface and blowing snow sources of Arctic bromine activation within WRF-Chem 4.1.1. *Journal of Advances in Modeling Earth Systems* **13**: e2020MS002391. DOI: https://doi.org/10.1029/2020MS002391.

Matrai, P, **Vernet, M**, **Wassmann, P.** 2007. Relating temporal and spatial patterns of DMSP in the Barents Sea to phytoplankton biomass and productivity. *Journal of Marine Systems* **67**: 83–101. DOI: https://doi.org/10.1016/j.jmarsys.2006.10.001.

Matrai, PA, **Tranvik, L**, **Leck, C**, **Knulst, JC.** 2008. Are high Arctic surface microlayers a potential source of aerosol organic precursors? *Marine Chemistry* **108**: 109–122. DOI:https://doi.org/10.1016/j.marchem.2007.11.001.

Mauritsen, T, **Sedlar, J**, **Tjernström, M**, **Leck, C**, **Martin, M**, **Shupe, M**, **Sjogren, S**, **Sierau, B**, **Persson, POG**, **Brooks, IM**, **Swietlicki, E.** 2011. An Arctic CCN-limited cloud-aerosol regime. *Atmospheric Chemistry and Physics* **11**: 165–173. DOI:https://doi.org/10.5194/acp-11-165-2011.

McCluskey, CS, **Gettelman, A**, **Bardeen, CG**, **DeMott, PJ**, **Moore, KA**, **Kreidenweis, SM**, **Hill, TCJ**, **Barry, KR**, **Twohy, CH**, **Toohey, DW**, **Rainwater, B**, **Jensen, JB**, **Reeves, JM**, **Alexander, SP**, **McFarquhar, GM.** 2023. Simulating Southern Ocean aerosol and ice nucleating particles in the Community Earth System Model Version 2. *Journal of Geophysical Research: Atmospheres* **128**: e2022JD036955. DOI: https://doi.org/10.1029/2022JD036955.

McCluskey, CS, **Hill, TCJ**, **Humphries, RS**, **Rauker, AM**, **Moreau, S**, **Strutton, PG**, **Chambers, SD**, **Williams, AG**, **McRobert, I**, **Ward, J**, **Keywood, MD**, **Harnwell, J**, **Ponsonby, W**, **Loh, ZM**, **Krummel, PB**, **Protat, A**, **Kreidenweis, SM**, **DeMott, PJ.** 2018. Observations of ice nucleating particles over Southern Ocean waters. *Geophysical Research Letters* **45**: 11,989–11,997. DOI: https://doi.org/10.1029/2018GL079981.

McCoy, DT, **Burrows, SM**, **Wood, R**, **Grosvenor, DP**, **Elliott, SM**, **Ma, P-L**, **Rasch, PJ**, **Hartmann, DL.** 2015. Natural aerosols explain seasonal and spatial patterns of Southern Ocean cloud albedo. *Science Advances* **1**: e1500157. DOI: https://doi.org/10.1126/sciadv.1500157.

McCoy, IL, **Bretherton, CS**, **Wood, R**, **Twohy, CH**, **Gettelman, A**, **Bardeen, CG**, **Toohey, DW.** 2021. Influences of recent particle formation on Southern Ocean aerosol variability and low cloud properties. *Journal of Geophysical Research: Atmospheres* **126**: e2020JD033529. DOI: https://doi.org/10.1029/2020JD033529.

McCrindle, SL, **Kappler, U**, **McEwan, AG.** 2005. Microbial dimethylsulfoxide and trimethylamine-N-oxide respiration, in Poole, RK ed., *Advances in microbial physiology*. Academic Press: 147–201e. DOI: https://doi.org/10.1016/S0065-2911(05)50004-3.

McNabb, BJ, **Tortell, PD.** 2022. Improved prediction of dimethyl sulfide (DMS) distributions in the northeast subarctic Pacific using machine-learning algorithms. *Biogeosciences* **19**: 1705–1721. DOI: https://doi.org/10.5194/bg-19-1705-2022.

McNabb, BJ, **Tortell, PD.** 2023. Oceanographic controls on Southern Ocean dimethyl sulfide distributions revealed by machine learning algorithms. *Limnology and Oceanography* **68**: 616–630. DOI: https://doi.org/10.1002/lno.12298.

McNamara, SM, **Raso, ARW**, **Wang, S**, **Thanekar, S**, **Boone, EJ**, **Kolesar, KR**, **Peterson, PK**, **Simpson, WR**, **Fuentes, JD**, **Shepson, PB**, **Pratt, KA.** 2019. Springtime nitrogen oxide-influenced chlorine chemistry in the coastal Arctic. *Environmental*

Science & Technology **53**: 8057–8067. DOI: https://doi.org/10.1021/acs.est.9b01797.

McPhee, MG, **Martinson, DG.** 1994. Turbulent mixing under drifting pack ice in the Weddell Sea. *Science* **263**: 218–221. DOI: https://doi.org/10.1126/science.263.5144.218.

Meiners, KM, **Vancoppenolle, M**, **Carnat, G**, **Castellani, G**, **Delille, B**, **Delille, D**, **Dieckmann, GS**, **Flores, H**, **Fripiat, F**, **Grotti, M**, **Lange, BA**, **Lannuzel, D**, **Martin, A**, **McMinn, A**, **Nomura, D**, **Peeken, I**, **Rivaro, P**, **Ryan, KG**, **Stefels, J**, **Swadling, KM**, **Thomas, DN**, **Tison, J-L**, **van der Merwe, P**, **van Leeuwe, MA**, **Weldrick, C**, **Yang, EJ.** 2018. Chlorophyll-*a* in Antarctic landfast sea ice: A first synthesis of historical ice core data. *Journal of Geophysical Research: Oceans* **123**: 8444–8459. DOI:https://doi.org/10.1029/2018JC014245.

Meiners, KM, **Vancoppenolle, M**, **Thanassekos, S**, **Dieckmann, GS**, **Thomas, DN**, **Tison, J-L**, **Arrigo, KR**, **Garrison, DL**, **McMinn, A**, **Lannuzel, D**, **van der Merwe, P**, **Swadling, KM**, **Smith, WO Jr**, **Melnikov, I**, **Raymond, B.** 2012. Chlorophyll *a* in Antarctic sea ice from historical ice core data. *Geophysical Research Letters* **39**. DOI:https://doi.org/10.1029/2012GL053478.

Moffett, CE, **Barrett, TE**, **Liu, J**, **Gunsch, MJ**, **Upchurch, LM**, **Quinn, PK**, **Pratt, KA**, **Sheesley, RJ.** 2020. Long-term trends for marine sulfur aerosol in the Alaskan Arctic and relationships with temperature. *Journal of Geophysical Research: Atmospheres* **125**: e2020JD033225. DOI: https://doi.org/10.1029/2020JD033225.

Moran, MA, **Durham, BP.** 2019. Sulfur metabolites in the pelagic ocean. *Nature Reviews Microbiology* **17**: 665–678. DOI: https://doi.org/10.1038/s41579-019-0250-1.

Morrison, H, **de Boer, G**, **Feingold, G**, **Harrington, J**, **Shupe, MD**, **Sulia, K.** 2012. Resilience of persistent Arctic mixed-phase clouds. *Nature Geoscience* **5**: 11–17. DOI:https://doi.org/10.1038/ngeo1332.

Mungall, EL, **Abbatt, JPD**, **Wentzell, JJB**, **Lee, AKY**, **Thomas, JL**, **Blais, M**, **Gosselin, M**, **Miller, LA**, **Papakyriakou, T**, **Willis, MD**, **Liggio, J.** 2017. Microlayer source of oxygenated volatile organic compounds in the summertime marine Arctic boundary layer. *Proceedings of the National Academy of Sciences* **114**: 6203–6208. DOI:https://doi.org/10.1073/pnas.1620571114.

Mungall, EL, **Croft, B**, **Lizotte, M**, **Thomas, JL**, **Murphy, JG**, **Levasseur, M**, **Martin, RV**, **Wentzell, JJB**, **Liggio, J**, **Abbatt, JPD.** 2016. Dimethyl sulfide in the summertime Arctic atmosphere: Measurements and source sensitivity simulations. *Atmospheric Chemistry and Physics* **16**: 6665–6680. DOI:https://doi.org/10.5194/acp-16-6665-2016.

Mungall, EL, **Wong, JPS**, **Abbatt, JPD.** 2018. Heterogeneous oxidation of particulate methanesulfonic acid by the hydroxyl radical: Kinetics and atmospheric implications. *ACS Earth and Space Chemistry* **2**: 48–55. DOI:https://doi.org/10.1021/acsearthspacechem.7b00114.

Murphy, JG, **Wentworth, GR**, **Moravek, A**, **Collins, DB**, **Sharma, S.** 2024. Processes regulating the sources and sinks of ammonia in the Canadian Arctic. *Faraday Discussions* DOI: https://doi.org/10.1039/D4FD00173G.

Myers, DC, **Lawler, MJ**, **Mauldin, RL**, **Sjostedt, S**, **Dubey, M**, **Abbatt, J**, **Smith, JN.** 2021. Indirect measurements of the composition of ultrafine particles in the Arctic late-winter. *Journal of Geophysical Research: Atmospheres* **126**: e2021JD035428. DOI: https://doi.org/10.1029/2021JD035428.

Mynard, C, **Franklin, EB**, **Alroe, J**, **Somerville, N**, **Patti, A**, **Siems, ST**, **Williams, A**, **Mallet, MD**, **Humphries, R**, **Dunne, E.** 2025. Constraining atmospheric methanethiol estimates over the Southern Ocean. *Geophysical Research Letters* **52**: e2025GL116470. DOI: https://doi.org/10.1029/2025GL116470.

Nesbitt, DJ, **Leone, SR.** 1981. Laser initiated chain reactions: A generalized extension to complex chemical chain systems. *The Journal of Chemical Physics* **75**: 4949–4959. DOI:https://doi.org/10.1063/1.441883.

Nicovich, JM, **Kreutter, KD**, **Van Dijk, CA**, **Wine, PH.** 1992. Temperature-dependent kinetics studies of the reactions bromine atom(2P3/2) + hydrogen sulfide ↔ mercapto + hydrogen bromide and bromine atom(2P3/2) + methanethiol ↔ methylthiol + hydrogen bromide. Heats of formation of mercapto and methylthio radicals. *The Journal of Physical Chemistry* **96**: 2518–2528. DOI: https://doi.org/10.1021/j100185a025.

Nicovich, JM, **Wang, S**, **Wine, PH.** 1995. Kinetics of the reactions of atomic chlorine with H_2S, D_2S, CH_3SH, and CD_3SD. *International Journal of Chemical Kinetics* **27**: 359–368. DOI: https://doi.org/10.1002/kin.550270407.

Nightingale, PD, **Malin, G**, **Law, CS**, **Watson, AJ**, **Liss, PS**, **Liddicoat, MI**, **Boutin, J**, **Upstill-Goddard, RC.** 2000. In situ evaluation of air-sea gas exchange parameterizations using novel conservative and volatile tracers. *Global Biogeochemical Cycles* **14**: 373–387. DOI: https://doi.org/10.1029/1999GB900091.

Nomura, D, **Granskog, MA**, **Fransson, A**, **Chierici, M**, **Silyakova, A**, **Ohshima, KI**, **Cohen, L**, **Delille, B**, **Hudson, SR**, **Dieckmann, GS.** 2018. CO_2 flux over young and snow-covered Arctic pack ice in winter and spring. *Biogeosciences* **15**: 3331–3343. DOI: https://doi.org/10.5194/bg-15-3331-2018.

Nomura, D, **Koga, S**, **Kasamatsu, N**, **Shinagawa, H**, **Simizu, D**, **Wada, M**, **Fukuchi, M.** 2012. Direct measurements of DMS flux from Antarctic fast sea ice to the atmosphere by a chamber technique. *Journal of Geophysical Research: Oceans* **117**. DOI: https://doi.org/10.1029/2010JC006755.

Norman, AL, **Barrie, LA**, **Toom-Sauntry, D**, **Sirois, A**, **Krouse, HR**, **Li, SM**, **Sharma, S.** 1999. Sources of aerosol sulphate at Alert: Apportionment using

stable isotopes. *Journal of Geophysical Research: Atmospheres* **104**: 11619–11631. DOI:https://doi.org/10.1029/1999JD900078.

Notz, D, **SIMIP Community.** 2020. Arctic sea ice in CMIP6. *Geophysical Research Letters* **47**: e2019GL086749. DOI: https://doi.org/10.1029/2019GL086749.

Novak, GA, **Fite, CH**, **Holmes, CD**, **Veres, PR**, **Neuman, JA**, **Faloona, I**, **Thornton, JA**, **Wolfe, GM**, **Vermeuel, MP**, **Jernigan, CM**, **Peischl, J**, **Ryerson, TB**, **Thompson, CR**, **Bourgeois, I**, **Warneke, C**, **Gkatzelis, GI**, **Coggon, MM**, **Sekimoto, K**, **Bui, TP**, **Dean-Day, J**, **Diskin, GS**, **DiGangi, JP**, **Nowak, JB**, **Moore, RH**, **Wiggins, EB**, **Winstead, EL**, **Robinson, C**, **Thornhill, KL**, **Sanchez, KJ**, **Hall, SR**, **Ullmann, K**, **Dollner, M**, **Weinzierl, B**, **Blake, DR**, **Bertram, TH.** 2021. Rapid cloud removal of dimethyl sulfide oxidation products limits SO_2 and cloud condensation nuclei production in the marine atmosphere. *Proceedings of the National Academy of Sciences* **118**: e2110472118. DOI: https://doi.org/10.1073/pnas.2110472118.

Novak, GA, **Kilgour, DB**, **Jernigan, CM**, **Vermeuel, MP**, **Bertram, TH.** 2022. Oceanic emissions of dimethyl sulfide and methanethiol and their contribution to sulfur dioxide production in the marine atmosphere. *Atmospheric Chemistry and Physics* **22**: 6309–6325. DOI: https://doi.org/10.5194/acp-22-6309-2022.

Oh, J-H, **Noh, KM**, **Lim, H-G**, **Jin, EK**, **Jun, S-Y**, **Kug, J-S.** 2022. Antarctic meltwater-induced dynamical changes in phytoplankton in the Southern Ocean. *Environmental Research Letters* **17**: 024022. DOI: https://doi.org/10.1088/1748-9326/ac444e.

Oh, J-H, **Park, W**, **Lim, H-G**, **Noh, KM**, **Jin, EK**, **Kug, J-S.** 2020. Impact of Antarctic meltwater forcing on East Asian climate under greenhouse warming. *Geophysical Research Letters* **47**: e2020GL089951. DOI: https://doi.org/10.1029/2020GL089951.

Park, J, **Kang, H**, **Gim, Y**, **Jang, E**, **Park, K-T**, **Park, S**, **Jung, CH**, **Ceburnis, D**, **O'Dowd, C**, **Yoon, YJ.** 2023. New particle formation leads to enhanced cloud condensation nuclei concentrations on the Antarctic Peninsula. *Atmospheric Chemistry and Physics* **23**: 13625–13646. DOI: https://doi.org/10.5194/acp-23-13625-2023.

Park, K, **Kim, I**, **Choi, J-O**, **Lee, Y**, **Jung, J**, **Ha, S-Y**, **Kim, J-H**, **Zhang, M.** 2019. Unexpectedly high dimethyl sulfide concentration in high-latitude Arctic sea ice melt ponds. *Environmental Science: Processes & Impacts* **21**: 1642–1649. DOI:https://doi.org/10.1039/C9EM00195F.

Park, K-T, **Jang, S**, **Lee, K**, **Yoon, YJ**, **Kim, M-S**, **Park, K**, **Cho, H-J**, **Kang, J-H**, **Udisti, R**, **Lee, B-Y**, **Shin, K-H.** 2017. Observational evidence for the formation of DMS-derived aerosols during Arctic phytoplankton blooms. *Atmospheric Chemistry and Physics* **17**: 9665–9675. DOI: https://doi.org/10.5194/acp-17-9665-2017.

Park, K-T, **Yoon, YJ**, **Lee, K**, **Tunved, P**, **Krejci, R**, **Ström, J**, **Jang, E**, **Kang, HJ**, **Jang, S**, **Park, J**, **Lee, BY**, **Traversi, R**, **Becagli, S**, **Hermansen, O.** 2021. Dimethyl sulfide-induced increase in cloud condensation nuclei in the Arctic atmosphere. *Global Biogeochemical Cycles* **35**: e2021GB006969. DOI: https://doi.org/10.1029/2021GB006969.

Park, W, **Latif, M.** 2019. Ensemble global warming simulations with idealized Antarctic meltwater input. *Climate Dynamics* **52**: 3223–3239. DOI: https://doi.org/10.1007/s00382-018-4319-8.

Pereira Freitas, G, **Kopec, B**, **Adachi, K**, **Krejci, R**, **Heslin-Rees, D**, **Yttri, KE**, **Hubbard, A**, **Welker, JM**, **Zieger, P.** 2024. Contribution of fluorescent primary biological aerosol particles to low-level Arctic cloud residuals. *Atmospheric Chemistry and Physics* **24**: 5479–5494. DOI: https://doi.org/10.5194/acp-24-5479-2024.

Pernov, JB, **Aeberhard, WH**, **Volpi, M**, **Harris, E**, **Hohermuth, B**, **Ishino, S**, **Skeie, RB**, **Henne, S**, **Im, U**, **Quinn, PK**, **Upchurch, LM**, **Schmale, J.** 2025. Data-driven modeling of environmental factors influencing Arctic methanesulfonic acid aerosol concentrations. *Atmospheric Chemistry and Physics* **25**: 6497–6537. DOI: https://doi.org/10.5194/acp-25-6497-2025.

Pernov, JB, **Beddows, D**, **Thomas, DC**, **Dall´Osto, M**, **Harrison, RM**, **Schmale, J**, **Skov, H**, **Massling, A.** 2022. Increased aerosol concentrations in the High Arctic attributable to changing atmospheric transport patterns. *npj Climate and Atmospheric Science* **5**: 1–13. DOI: https://doi.org/10.1038/s41612-022-00286-y.

Pernov, JB, **Bossi, R**, **Lebourgeois, T**, **Nøjgaard, JK**, **Holzinger, R**, **Hjorth, J**, **Skov, H.** 2020. Dataset for "Atmospheric VOC measurements at a High Arctic site: Characteristics and source apportionment." DOI: https://doi.org/10.5281/zenodo.4299817.

Pernov, JB, **Harris, E**, **Volpi, M**, **Baumgartner, T**, **Hohermuth, B**, **Henne, S**, **Aeberhard, WH**, **Becagli, S**, **Quinn, PK**, **Traversi, R**, **Upchurch, LM**, **Schmale, J.** 2024. Pan-Arctic methanesulfonic acid aerosol: Source regions, atmospheric drivers, and future projections. *npj Climate and Atmospheric Science* **7**: 1–18. DOI: https://doi.org/10.1038/s41612-024-00712-3.

Perraud, V, **Meinardi, S**, **Blake, DR**, **Finlayson-Pitts, BJ.** 2016. Challenges associated with the sampling and analysis of organosulfur compounds in air using real-time PTR-ToF-MS and offline GC-FID. *Atmospheric Measurement Techniques* **9**: 1325–1340. DOI:https://doi.org/10.5194/amt-9-1325-2016.

Petrou, K, **Nielsen, DA.** 2018. Uptake of dimethylsulphoniopropionate (DMSP) by the diatom *Thalassiosira weissflogii*: A model to investigate the cellular function of DMSP. *Biogeochemistry* **141**: 265–271. DOI: https://doi.org/10.1007/s10533-018-0507-1.

Pratt, KA. 2019. Tropospheric halogen photochemistry in the rapidly changing Arctic. *Trends in Chemistry* **1**:

545–548. DOI: https://doi.org/10.1016/j.trechm.2019.06.001.

Pratt, KA, **Custard, KD**, **Shepson, PB**, **Douglas, TA**, **Pöhler, D**, **General, S**, **Zielcke, J**, **Simpson, WR**, **Platt, U**, **Tanner, DJ**, **Huey, LG**, **Carlsen, M**, **Stirm, BH.** 2013. Photochemical production of molecular bromine in Arctic surface snowpacks. *Nature Geoscience* **6**: 351–356. DOI: https://doi.org/10.1038/ngeo1779.

Preunkert, S, **Legrand, M**, **Jourdain, B**, **Moulin, C**, **Belviso, S**, **Kasamatsu, N**, **Fukuchi, M**, **Hirawake, T.** 2007. Interannual variability of dimethylsulfide in air and seawater and its atmospheric oxidation by-products (methanesulfonate and sulfate) at Dumont d'Urville, coastal Antarctica (1999–2003). *Journal of Geophysical Research: Atmospheres* **112**. DOI: https://doi.org/10.1029/2006JD007585.

Price, R, **Baccarini, A**, **Schmale, J**, **Zieger, P**, **Brooks, IM**, **Field, P**, **Carslaw, KS.** 2023. Late summer transition from a free-tropospheric to boundary layer source of Aitken mode aerosol in the high Arctic. *Atmospheric Chemistry and Physics* **23**: 2927–2961. DOI:https://doi.org/10.5194/acp-23-2927-2023.

Prytherch, J, **Murto, S**, **Brown, I**, **Ulfsbo, A**, **Thornton, BF**, **Brüchert, V**, **Tjernström, M**, **Hermansson, AL**, **Nylund, AT**, **Holthusen, LA.** 2024. Central Arctic Ocean surface–atmosphere exchange of CO_2 and CH_4 constrained by direct measurements. *Biogeosciences* **21**: 671–688. DOI: https://doi.org/10.5194/bg-21-671-2024.

Prytherch, J, **Yelland, MJ.** 2021. Wind, convection and fetch dependence of gas transfer velocity in an Arctic sea-ice lead determined from eddy covariance CO_2 flux measurements. *Global Biogeochemical Cycles* **35**: e2020GB006633. DOI: https://doi.org/10.1029/2020GB006633.

Przyjazny, A, **Janicki, W**, **Chrzanowski, W**, **Staszewski, R.** 1983. Headspace gas chromatographic determination of distribution coefficients of selected organosulphur compounds and their dependence on some parameters. *Journal of Chromatography A* **280**: 249–260. DOI: https://doi.org/10.1016/S0021-9673(00)91567-X.

Quinn, PK, **Coffman, DJ**, **Johnson, JE**, **Upchurch, LM**, **Bates, TS.** 2017. Small fraction of marine cloud condensation nuclei made up of sea spray aerosol. *Nature Geoscience* **10**: 674–679. DOI: https://doi.org/10.1038/ngeo3003.

Quinn, PK, **Miller, TL**, **Bates, TS**, **Ogren, JA**, **Andrews, E**, **Shaw, GE.** 2002. A 3-year record of simultaneously measured aerosol chemical and optical properties at Barrow, Alaska. *Journal of Geophysical Research: Atmospheres* **107**: AAC 8-1–AAC 8-15. DOI:https://doi.org/10.1029/2001JD001248.

Ravishankara, AR, **Rudick, Y**, **Talukdar, R**, **Barone, SB.** 1997. Oxidation of atmospheric reduced sulphur compounds: Perspective from laboratory studies. *Philosophical Transactions of the Royal Society of London. Series B: Biological Sciences* **352**: 171–182. DOI: https://doi.org/10.1098/rstb.1997.0012.

Read, KA, **Lewis, AC**. 2007. Dataset record: Leeds GC-FID non-methane hydrocarbons (NMHC) data at Halley Bay Station for the CHABLIS Campaign (2004–2005). Available at https://catalogue.ceda.ac.uk/uuid/fba1e1091d4dc630c8e89d940c7c43e7/. Accessed January 14, 2026.

Read, KA, **Lewis, AC**, **Bauguitte, S**, **Rankin, AM**, **Salmon, RA**, **Wolff, EW**, **Saiz-Lopez, A**, **Bloss, WJ**, **Heard, DE**, **Lee, JD**, **Plane, JMC.** 2008. DMS and MSA measurements in the Antarctic boundary layer: Impact of BrO on MSA production. *Atmospheric Chemistry and Physics* **8**: 2985–2997. DOI: https://doi.org/10.5194/acp-8-2985-2008.

Regayre, LA, **Schmale, J**, **Johnson, JS**, **Tatzelt, C**, **Baccarini, A**, **Henning, S**, **Yoshioka, M**, **Stratmann, F**, **Gysel-Beer, M**, **Grosvenor, DP**, **Carslaw, KS.** 2020. The value of remote marine aerosol measurements for constraining radiative forcing uncertainty. *Atmospheric Chemistry and Physics* **20**: 10063–10072. DOI: https://doi.org/10.5194/acp-20-10063-2020.

Rempillo, O, **Seguin, AM**, **Norman, A-L**, **Scarratt, M**, **Michaud, S**, **Chang, R**, **Sjostedt, S**, **Abbatt, J**, **Else, B**, **Papakyriakou, T**, **Sharma, S**, **Grasby, S**, **Levasseur, M.** 2011. Dimethyl sulfide air-sea fluxes and biogenic sulfur as a source of new aerosols in the Arctic fall. *Journal of Geophysical Research: Atmospheres* **116**. DOI:https://doi.org/10.1029/2011JD016336.

Revell, LE, **Kremser, S**, **Hartery, S**, **Harvey, M**, **Mulcahy, JP**, **Williams, J**, **Morgenstern, O**, **McDonald, AJ**, **Varma, V**, **Bird, L**, **Schuddeboom, A.** 2019. The sensitivity of Southern Ocean aerosols and cloud microphysics to sea spray and sulfate aerosol production in the HadGEM3-GA7.1 chemistry–climate model. *Atmospheric Chemistry and Physics* **19**: 15447–15466. DOI: https://doi.org/10.5194/acp-19-15447-2019.

Ridley, JK, **Ringer, MA**, **Sheward, RM.** 2016. The transformation of Arctic clouds with warming. *Climatic Change* **139**: 325–337. DOI: https://doi.org/10.1007/s10584-016-1772-4.

Roach, LA, **Dörr, J**, **Holmes, CR**, **Massonnet, F**, **Blockley, EW**, **Notz, D**, **Rackow, T**, **Raphael, MN**, **O'Farrell, SP**, **Bailey, DA**, **Bitz, CM.** 2020. Antarctic sea ice area in CMIP6. *Geophysical Research Letters* **47**: e2019GL086729. DOI: https://doi.org/10.1029/2019GL086729.

Rolph, RJ, **Feltham, DL**, **Schröder, D.** 2020. Changes of the Arctic marginal ice zone during the satellite era. *The Cryosphere* **14**: 1971–1984. DOI: https://doi.org/10.5194/tc-14-1971-2020.

Roscoe, HK, **Jones, AE**, **Brough, N**, **Weller, R**, **Saiz-Lopez, A**, **Mahajan, AS**, **Schoenhardt, A**, **Burrows, JP**, **Fleming, ZL.** 2015. Particles and iodine compounds in coastal Antarctica. *Journal of Geophysical Research: Atmospheres* **120**: 7144–7156. DOI:https://doi.org/10.1002/2015JD023301.

Roth, CM, **Goss, K-U**, **Schwarzenbach, RP.** 2004. Sorption of diverse organic vapors to snow.

Environmental Science & Technology **38**: 4078–4084. DOI:https://doi.org/10.1021/es0350684.

Rovelli, G, **Jacobs, MI**, **Willis, MD**, **Rapf, RJ**, **Prophet, AM**, **Wilson, KR.** 2020. A critical analysis of electrospray techniques for the determination of accelerated rates and mechanisms of chemical reactions in droplets. *Chemical Science* **11**: 13026–13043. DOI: https://doi.org/10.1039/D0SC04611F.

Ruiz-González, C, **Galí, M**, **Sintes, E**, **Herndl, GJ**, **Gasol, JM**, **Simó, R.** 2012. Sunlight effects on the osmotrophic uptake of DMSP-sulfur and leucine by polar phytoplankton. *PLOS ONE* **7**: e45545. DOI: https://doi.org/10.1371/journal.pone.0045545.

Saiz-Lopez, A, **Mahajan, AS**, **Salmon, RA**, **Bauguitte, SJ-B**, **Jones, AE**, **Roscoe, HK**, **Plane, JMC.** 2007. Boundary layer halogens in coastal Antarctica. *Science* **317**: 348–351. DOI:https://doi.org/10.1126/science.1141408.

Sander, R. 2023. Compilation of Henry's law constants (version 5.0.0) for water as solvent. *Atmospheric Chemistry and Physics* **23**: 10901–12440. DOI: https://doi.org/10.5194/acp-23-10901-2023.

Schmale, J, **Arnold, SR**, **Law, KS**, **Thorp, T**, **Anenberg, S**, **Simpson, WR**, **Mao, J**, **Pratt, KA.** 2018. Local Arctic air pollution: A neglected but serious problem. *Earth's Future* **6**: 1385–1412. DOI: https://doi.org/10.1029/2018EF000952.

Schmale, J, **Baccarini, A.** 2021. Progress in unraveling atmospheric new particle formation and growth across the Arctic. *Geophysical Research Letters* **48**: e2021GL094198. DOI: https://doi.org/10.1029/2021GL094198.

Schmale, J, **Baccarini, A**, **Thurnherr, I**, **Henning, S**, **Efraim, A**, **Regayre, L**, **Bolas, C**, **Hartmann, M**, **Welti, A**, **Lehtipalo, K**, **Aemisegger, F**, **Tatzelt, C**, **Landwehr, S**, **Modini, RL**, **Tummon, F**, **Johnson, JS**, **Harris, N**, **Schnaiter, M**, **Toffoli, A**, **Derkani, M**, **Bukowiecki, N**, **Stratmann, F**, **Dommen, J**, **Baltensperger, U**, **Wernli, H**, **Rosenfeld, D**, **Gysel-Beer, M**, **Carslaw, KS.** 2019. Overview of the Antarctic Circumnavigation Expedition: Study of Preindustrial-Like Aerosols and their Climate Effects (ACE-SPACE). *Bulletin of the American Meteorological Society* **100**(11): 2260–2283. DOI:https://doi.org/10.1175/BAMS-D-18-0187.1.

Schmale, J, **Sharma, S**, **Decesari, S**, **Pernov, J**, **Massling, A**, **Hansson, H-C**, **von Salzen, K**, **Skov, H**, **Andrews, E**, **Quinn, PK**, **Upchurch, LM**, **Eleftheriadis, K**, **Traversi, R**, **Gilardoni, S**, **Mazzola, M**, **Laing, J**, **Hopke, P.** 2022. Pan-Arctic seasonal cycles and long-term trends of aerosol properties from 10 observatories. *Atmospheric Chemistry and Physics* **22**: 3067–3096. DOI: https://doi.org/10.5194/acp-22-3067-2022.

Schmale, J, **Zieger, P**, **Ekman, AML.** 2021. Aerosols in current and future Arctic climate. *Nature Climate Change* **11**: 95–105. DOI: https://doi.org/10.1038/s41558-020-00969-5.

Schnack-Schiel, SB, **Haas, C**, **Michels, J**, **Mizdalski, E**, **Schünemann, H**, **Steffens, M**, **Thomas, DN.** 2008. Copepods in sea ice of the western Weddell Sea during austral spring 2004. *Deep Sea Research Part II: Topical Studies in Oceanography* **55**: 1056–1067. DOI: https://doi.org/10.1016/j.dsr2.2007.12.014.

Schönhardt, A, **Begoin, M**, **Richter, A**, **Wittrock, F**, **Kaleschke, L**, **Gómez Martín, JC**, **Burrows, JP.** 2012. Simultaneous satellite observations of IO and BrO over Antarctica. *Atmospheric Chemistry and Physics* **12**: 6565–6580. DOI: https://doi.org/10.5194/acp-12-6565-2012.

Sciare, J, **Mihalopoulos, N.** 2000. A new technique for sampling and analysis of atmospheric dimethylsulfoxide (DMSO). *Atmospheric Environment* **34**: 151–156. DOI:https://doi.org/10.1016/S1352-2310(99)00214-9.

Séférian, R, **Nabat, P**, **Michou, M**, **Saint-Martin, D**, **Voldoire, A**, **Colin, J**, **Decharme, B**, **Delire, C**, **Berthet, S**, **Chevallier, M**, **Sénési, S**, **Franchisteguy, L**, **Vial, J**, **Mallet, M**, **Joetzjer, E**, **Geoffroy, O**, **Guérémy, J-F**, **Moine, M-P**, **Msadek, R**, **Ribes, A**, **Rocher, M**, **Roehrig, R**, **Salas-y-Mélia, D**, **Sanchez, E**, **Terray, L**, **Valcke, S**, **Waldman, R**, **Aumont, O**, **Bopp, L**, **Deshayes, J**, **Éthé, C**, **Madec, G.** 2019. Evaluation of CNRM Earth System Model, CNRM-ESM2-1: Role of Earth system processes in present-day and future climate. *Journal of Advances in Modeling Earth Systems* **11**: 4182–4227. DOI:https://doi.org/10.1029/2019MS001791.

Seguin, AM, **Norman, A-L**, **Eaton, S**, **Wadleigh, M.** 2011. Seasonality in size segregated biogenic, anthropogenic and sea salt sulfate aerosols over the North Atlantic. *Atmospheric Environment* **45**: 6947–6954. DOI: https://doi.org/10.1016/j.atmosenv.2011.09.033.

Sellegri, K, **Barthelmeß, T**, **Trueblood, J**, **Cristi, A**, **Freney, E**, **Rose, C**, **Barr, N**, **Harvey, M**, **Safi, K**, **Deppeler, S**, **Thompson, K**, **Dillon, W**, **Engel, A**, **Law, C.** 2023. Quantified effect of seawater biogeochemistry on the temperature dependence of sea spray aerosol fluxes. *Atmospheric Chemistry and Physics* **23**: 12949–12964. DOI: https://doi.org/10.5194/acp-23-12949-2023.

Seo, S, **Richter, A**, **Blechschmidt, A-M**, **Bougoudis, I**, **Burrows, JP.** 2020. Spatial distribution of enhanced BrO and its relation to meteorological parameters in Arctic and Antarctic sea ice regions. *Atmospheric Chemistry and Physics* **20**: 12285–12312. DOI: https://doi.org/10.5194/acp-20-12285-2020.

Sharma, S, **Barrie, LA**, **Magnusson, E**, **Brattström, G**, **Leaitch, WR**, **Steffen, A**, **Landsberger, S.** 2019. A factor and trends analysis of multidecadal lower tropospheric observations of Arctic aerosol composition, black carbon, ozone, and mercury at Alert, Canada. *Journal of Geophysical Research: Atmospheres* **124**: 14133–14161. DOI: https://doi.org/10.1029/2019JD030844.

Shaw, DK, **Sekar, J**, **Ramalingam, PV.** 2022. Recent insights into oceanic dimethylsulfoniopropionate

biosynthesis and catabolism. *Environmental Microbiology* **24**: 2669–2700. DOI: https://doi.org/10.1111/1462-2920.16045.

Shen, J, **Scholz, W**, **He, X-C**, **Zhou, P**, **Marie, G**, **Wang, M**, **Marten, R**, **Surdu, M**, **Rörup, B**, **Baalbaki, R**, **Amorim, A**, **Ataei, F**, **Bell, DM**, **Bertozzi, B**, **Brasseur, Z**, **Caudillo, L**, **Chen, D**, **Chu, B**, **Dada, L**, **Duplissy, J**, **Finkenzeller, H**, **Granzin, M**, **Guida, R**, **Heinritzi, M**, **Hofbauer, V**, **Iyer, S**, **Kemppainen, D**, **Kong, W**, **Krechmer, JE**, **Kürten, A**, **Lamkaddam, H**, **Lee, CP**, **Lopez, B**, **Mahfouz, NGA**, **Manninen, HE**, **Massabò, D**, **Mauldin, RL**, **Mentler, B**, **Müller, T**, **Pfeifer, J**, **Philippov, M**, **Piedehierro, AA**, **Roldin, P**, **Schobesberger, S**, **Simon, M**, **Stolzenburg, D**, **Tham, YJ**, **Tomé, A**, **Umo, NSS**, **Wang, D**, **Wang, Y**, **Weber, SK**, **Welti, A**, **Wollesen de Jonge, R**, **Wu, Y**, **Zauner-Wieczorek, M**, **Zust, F**, **Baltensperger, U**, **Curtius, J**, **Flagan, RC**, **Hansel, A**, **Möhler, O**, **Petäjä, T**, **Volkamer, R**, **Kulmala, M**, **Lehtipalo, K**, **Rissanen, M**, **Kirkby, J**, **El-Haddad, I**, **Bianchi, F**, **Sipilä, M**, **Donahue, NM**, **Worsnop, DR.** 2022. High gas-phase methanesulfonic acid production in the OH-Initiated oxidation of dimethyl sulfide at low temperatures. *Environmental Science & Technology* **56**: 13931–13944. DOI: https://doi.org/10.1021/acs.est.2c05154.

Shiraiwa, M, **Ammann, M**, **Koop, T**, **Pöschl, U.** 2011. Gas uptake and chemical aging of semisolid organic aerosol particles. *Proceedings of the National Academy of Sciences* **108**: 11003–11008. DOI: https://doi.org/10.1073/pnas.1103045108.

Shiraiwa, M, **Li, Y**, **Tsimpidi, AP**, **Karydis, VA**, **Berkemeier, T**, **Pandis, SN**, **Lelieveld, J**, **Koop, T**, **Pöschl, U.** 2017. Global distribution of particle phase state in atmospheric secondary organic aerosols. *Nature Communications* **8**: 15002. DOI:https://doi.org/10.1038/ncomms15002.

Sieg, K, **Starokozhev, E**, **Schmidt, MU**, **Püttmann, W.** 2009. Inverse temperature dependence of Henry's law coefficients for volatile organic compounds in supercooled water. *Chemosphere* **77**: 8–14. DOI: https://doi.org/10.1016/j.chemosphere.2009.06.028.

Siegel, K, **Gramlich, Y**, **Haslett, SL**, **Freitas, G**, **Krejci, R**, **Zieger, P**, **Mohr, C.** 2023. Arctic observations of hydroperoxymethyl thioformate (HPMTF)—Seasonal behavior and relationship to other oxidation products of dimethyl sulfide at the Zeppelin Observatory, Svalbard. *Atmospheric Chemistry and Physics* **23**: 7569–7587. DOI:https://doi.org/10.5194/acp-23-7569-2023.

Simó, R. 2001. Production of atmospheric sulfur by oceanic plankton: Biogeochemical, ecological and evolutionary links. *Trends in Ecology & Evolution* **16**: 287–294. DOI:https://doi.org/10.1016/S0169-5347(01)02152-8.

Simó, R, **Dachs, J.** 2002. Global ocean emission of dimethylsulfide predicted from biogeophysical data. *Global Biogeochemical Cycles* **16**: 26-1–26-10. DOI: https://doi.org/10.1029/2001GB001829.

Simó, R, **Vila-Costa, M.** 2006. Ubiquity of algal dimethylsulfoxide in the surface ocean: Geographic and temporal distribution patterns. *Marine Chemistry* **100**: 136–146. DOI:https://doi.org/10.1016/j.marchem.2005.11.006.

Simpson, WR, **Brown, SS**, **Saiz-Lopez, A**, **Thornton, JA**, **von Glasow, R.** 2015. Tropospheric halogen chemistry: Sources, cycling, and impacts. *Chemical Reviews* **115**: 4035–4062. DOI: https://doi.org/10.1021/cr5006638.

Sipilä, M, **Sarnela, N**, **Jokinen, T**, **Henschel, H**, **Junninen, H**, **Kontkanen, J**, **Richters, S**, **Kangasluoma, J**, **Franchin, A**, **Peräkylä, O**, **Rissanen, MP**, **Ehn, M**, **Vehkamäki, H**, **Kurten, T**, **Berndt, T**, **Petäjä, T**, **Worsnop, D**, **Ceburnis, D**, **Kerminen, V-M**, **Kulmala, M**, **O'Dowd, C.** 2016. Molecular-scale evidence of aerosol particle formation via sequential addition of HIO_3. *Nature* **537**: 532–534. DOI: https://doi.org/10.1038/nature19314.

Smith, MM, **Angot, H**, **Chamberlain, EJ**, **Droste, ES**, **Karam, S**, **Muilwijk, M**, **Webb, AL**, **Archer, SD**, **Beck, I**, **Blomquist, BW**, **Bowman, J**, **Boyer, M**, **Bozzato, D**, **Chierici, M**, **Creamean, J**, **D'Angelo, A**, **Delille, B**, **Fer, I**, **Fong, AA**, **Fransson, A**, **Fuchs, N**, **Gardner, J**, **Granskog, MA**, **Hoppe, CJM**, **Hoppema, M**, **Hoppmann, M**, **Mock, T**, **Muller, S**, **Müller, O**, **Nicolaus, M**, **Nomura, D**, **Petäjä, T**, **Salganik, E**, **Schmale, J**, **Schmidt, K**, **Schulz, K**, **Shupe, MD**, **Stefels, J**, **Thielke, L**, **Tippenhauer, S**, **Ulfsbo, A**, **van Leeuwe, M**, **Webster, M**, **Yoshimura, M**, **Zhan, L.** 2023. Thin and transient meltwater layers and false bottoms in the Arctic sea ice pack—Recent insights on these historically overlooked features. *Elementa: Science of the Anthropocene* **11**: 00025. DOI: https://doi.org/10.1525/elementa.2023.00025.

Sokol, AB, **Storelvmo, T.** 2024. The spatial heterogeneity of cloud phase observed by satellite. *Journal of Geophysical Research: Atmospheres* **129**: e2023JD039751. DOI: https://doi.org/10.1029/2023JD039751.

Sotiropoulou, G, **Sedlar, J**, **Tjernström, M**, **Shupe, MD**, **Brooks, IM**, **Persson, POG.** 2014. The thermodynamic structure of summer Arctic stratocumulus and the dynamic coupling to the surface. *Atmospheric Chemistry and Physics* **14**: 12573–12592. DOI:https://doi.org/10.5194/acp-14-12573-2014.

Spiese, CE, **Kieber, DJ**, **Nomura, CT**, **Kiene, RP.** 2009. Reduction of dimethylsulfoxide to dimethylsulfide by marine phytoplankton. *Limnology and Oceanography* **54**: 560–570. DOI: https://doi.org/10.4319/lo.2009.54.2.0560.

Stanley, RHR, **Bell, TG.** 2025. Air-sea gas exchange and marine gases, in Anbar, A, Weis, D eds., *Treatise on geochemistry. 3rd ed.* Oxford: Elsevier: 53–83. DOI: https://doi.org/10.1016/B978-0-323-99762-1.00055-3.

Stark, H, **Brown, SS**, **Goldan, PD**, **Aldener, M**, **Kuster, WC**, **Jakoubek, R**, **Fehsenfeld, FC**, **Meagher, J**, **Bates, TS**, **Ravishankara, AR.** 2007. Influence of nitrate radical on the oxidation of dimethyl sulfide

in a polluted marine environment. *Journal of Geophysical Research: Atmospheres* **112**. DOI: https://doi.org/10.1029/2006JD007669.

Stefels, J. 2000. Physiological aspects of the production and conversion of DMSP in marine algae and higher plants. *Journal of Sea Research* **43**: 183–197. DOI: https://doi.org/10.1016/S1385-1101(00)00030-7.

Stefels, J, **Carnat, G**, **Dacey, JWH**, **Goossens, T**, **Elzenga, JTM**, **Tison, J-L.** 2012. The analysis of dimethylsulfide and dimethylsulfoniopropionate in sea ice: Dry-crushing and melting using stable isotope additions. *Marine Chemistry* **128–129**: 34–43. DOI:https://doi.org/10.1016/j.marchem.2011.09.007.

Stefels, J, **Steinke, M**, **Turner, S**, **Malin, G**, **Belviso, S.** 2007. Environmental constraints on the production and removal of the climatically active gas dimethylsulphide (DMS) and implications for ecosystem modelling. *Biogeochemistry* **83**: 245–275. DOI: https://doi.org/10.1007/s10533-007-9091-5.

Stefels, J, **van Leeuwe, MA**, **Jones, EM**, **Meredith, MP**, **Venables, HJ**, **Webb, AL**, **Henley, SF.** 2018. Impact of sea-ice melt on dimethyl sulfide (sulfoniopropionate) inventories in surface waters of Marguerite Bay, West Antarctic Peninsula. *Philosophical Transactions of the Royal Society A: Mathematical, Physical and Engineering Sciences* **376**: 20170169. DOI: https://doi.org/10.1098/rsta.2017.0169.

Steiner, N, **Deal, C**, **Lannuzel, D**, **Lavoie, D**, **Massonnet, F**, **Miller, LA**, **Moreau, S**, **Popova, E**, **Stefels, J**, **Tedesco, L.** 2016. What sea-ice biogeochemical modellers need from observers. *Elementa: Science of the Anthropocene* **4**: 000084.

Steiner, N, **Denman, K.** 2008. Parameter sensitivities in a 1-D model for DMS and sulphur cycling in the upper ocean. *Deep Sea Research Part I: Oceanographic Research Papers* **55**: 847–865. DOI: https://doi.org/10.1016/j.dsr.2008.02.010.

Stone, D, **Whalley, LK**, **Heard, DE.** 2012. Tropospheric OH and HO_2 radicals: Field measurements and model comparisons. *Chemical Society Reviews* **41**: 6348–6404. DOI:https://doi.org/10.1039/C2CS35140D.

Stroeve, JC, **Kattsov, V**, **Barrett, A**, **Serreze, M**, **Pavlova, T**, **Holland, M**, **Meier, WN.** 2012. Trends in Arctic sea ice extent from CMIP5, CMIP3 and observations. *Geophysical Research Letters* **39**. DOI: https://doi.org/10.1029/2012GL052676.

Su, H, **Cheng, Y**, **Pöschl, U.** 2020. New multiphase chemical processes influencing atmospheric aerosols, air quality, and climate in the Anthropocene. *Accounts of Chemical Research* **53**: 2034–2043. DOI: https://doi.org/10.1021/acs.accounts.0c00246.

Sumner, AL, **Shepson, PB.** 1999. Snowpack production of formaldehyde and its effect on the Arctic troposphere. *Nature* **398**: 230–233. DOI: https://doi.org/10.1038/18423.

Sun, J, **Todd, JD**, **Thrash, JC**, **Qian, Y**, **Qian, MC**, **Temperton, B**, **Guo, J**, **Fowler, EK**, **Aldrich, JT**, **Nicora, CD**, **Lipton, MS**, **Smith, RD**, **De Leenheer, P**, **Payne, SH**, **Johnston, AWB**, **Davie-Martin, CL**, **Halsey, KH**, **Giovannoni, SJ.** 2016. The abundant marine bacterium Pelagibacter simultaneously catabolizes dimethylsulfoniopropionate to the gases dimethyl sulfide and methanethiol. *Nature Microbiology* **1**: 1–5. DOI: https://doi.org/10.1038/nmicrobiol.2016.65.

Swanson, WF, **Holmes, CD**, **Simpson, WR**, **Confer, K**, **Marelle, L**, **Thomas, JL**, **Jaeglé, L**, **Alexander, B**, **Zhai, S**, **Chen, Q**, **Wang, X**, **Sherwen, T.** 2022. Comparison of model and ground observations finds snowpack and blowing snow aerosols both contribute to Arctic tropospheric reactive bromine. *Atmospheric Chemistry and Physics* **22**: 14467–14488. DOI: https://doi.org/10.5194/acp-22-14467-2022.

Tashmim, L, **Porter, WC**, **Bertram, TH**, **Kilgour, DB**, **Rollins, A.** 2025. Global impacts of marine methanethiol emissions and chemistry in the atmosphere. *Environmental Science & Technology* **59**(38): 20421–20428. DOI: https://doi.org/10.1021/acs.est.5c02019.

Tashmim, L, **Porter, WC**, **Chen, Q**, **Alexander, B**, **Fite, CH**, **Holmes, CD**, **Pierce, JR**, **Croft, B**, **Ishino, S.** 2024. Contribution of expanded marine sulfur chemistry to the seasonal variability of dimethyl sulfide oxidation products and size-resolved sulfate aerosol. *Atmospheric Chemistry and Physics* **24**: 3379–3403. DOI: https://doi.org/10.5194/acp-24-3379-2024.

Tatzelt, C, **Henning, S**, **Welti, A**, **Baccarini, A**, **Hartmann, M**, **Gysel-Beer, M**, **van Pinxteren, M**, **Modini, RL**, **Schmale, J**, **Stratmann, F.** 2022. Circum-Antarctic abundance and properties of CCN and INPs. *Atmospheric Chemistry and Physics* **22**: 9721–9745. DOI: https://doi.org/10.5194/acp-22-9721-2022.

Teng, Z-J, **Qin, Q-L**, **Zhang, W**, **Li, J**, **Fu, H-H**, **Wang, P**, **Lan, M**, **Luo, G**, **He, J**, **McMinn, A**, **Wang, M**, **Chen, X-L**, **Zhang, Y-Z**, **Chen, Y**, **Li, C-Y.** 2021. Biogeographic traits of dimethyl sulfide and dimethylsulfoniopropionate cycling in polar oceans. *Microbiome* **9**: 207. DOI: https://doi.org/10.1186/s40168-021-01153-3.

Tesdal, J-E, **Christian, JR**, **Monahan, AH**, **von Salzen, K.** 2015. Evaluation of diverse approaches for estimating sea-surface DMS concentration and air–sea exchange at global scale. *Environmental Chemistry* **13**: 390–412. DOI: https://doi.org/10.1071/EN14255.

Theys, N, **Van Roozendael, M**, **Hendrick, F**, **Yang, X**, **De Smedt, I**, **Richter, A**, **Begoin, M**, **Errera, Q**, **Johnston, PV**, **Kreher, K**, **De Mazière, M.** 2011. Global observations of tropospheric BrO columns using GOME-2 satellite data. *Atmospheric Chemistry and Physics* **11**: 1791–1811. DOI: https://doi.org/10.5194/acp-11-1791-2011.

Thomas, JL, **Stutz, J**, **Frey, MM**, **Bartels-Rausch, T**, **Altieri, K**, **Baladima, F**, **Browse, J**, **Dall'Osto, M**, **Marelle, L**, **Mouginot, J**, **Murphy, JG**, **Nomura, D**, **Pratt, KA**, **Willis, MD**, **Zieger, P**, **Abbatt, J**, **Douglas, TA**, **Facchini, MC**, **France, J**, **Jones, AE**,

Kim, K, **Matrai, PA**, **McNeill, VF**, **Saiz-Lopez, A**, **Shepson, P**, **Steiner, N**, **Law, KS**, **Arnold, SR**, **Delille, B**, **Schmale, J**, **Sonke, JE**, **Dommergue, A**, **Voisin, D**, **Melamed, ML**, **Gier, J.** 2019. Fostering multidisciplinary research on interactions between chemistry, biology, and physics within the coupled cryosphere-atmosphere system. *Elementa: Science of the Anthropocene* **7**: 58. DOI: https://doi.org/10.1525/elementa.396.

Thomas, JL, **Stutz, J**, **Lefer, B**, **Huey, LG**, **Toyota, K**, **Dibb, JE**, **von Glasow, R.** 2011. Modeling chemistry in and above snow at Summit, Greenland—Part 1: Model description and results. *Atmospheric Chemistry and Physics* **11**: 4899–4914. DOI: https://doi.org/10.5194/acp-11-4899-2011.

Thomas, MA, **Suntharalingam, P**, **Pozzoli, L**, **Rast, S**, **Devasthale, A**, **Kloster, S**, **Feichter, J**, **Lenton, TM.** 2010. Quantification of DMS aerosol-cloud-climate interactions using the ECHAM5-HAMMOZ model in a current climate scenario. *Atmospheric Chemistry and Physics* **10**: 7425–7438. DOI: https://doi.org/10.5194/acp-10-7425-2010.

Thompson, CR, **Shepson, PB**, **Liao, J**, **Huey, LG**, **Apel, EC**, **Cantrell, CA**, **Flocke, F**, **Orlando, J**, **Fried, A**, **Hall, SR**, **Hornbrook, RS**, **Knapp, DJ**, **Mauldin, RL III**, **Montzka, DD**, **Sive, BC**, **Ullmann, K**, **Weibring, P**, **Weinheimer, A.** 2015. Interactions of bromine, chlorine, and iodine photochemistry during ozone depletions in Barrow, Alaska. *Atmospheric Chemistry and Physics* **15**: 9651–9679. DOI: https://doi.org/10.5194/acp-15-9651-2015.

Thornhill, G, **Collins, W**, **Olivié, D**, **Skeie, RB**, **Archibald, A**, **Bauer, S**, **Checa-Garcia, R**, **Fiedler, S**, **Folberth, G**, **Gjermundsen, A**, **Horowitz, L**, **Lamarque, J-F**, **Michou, M**, **Mulcahy, J**, **Nabat, P**, **Naik, V**, **O'Connor, FM**, **Paulot, F**, **Schulz, M**, **Scott, CE**, **Séférian, R**, **Smith, C**, **Takemura, T**, **Tilmes, S**, **Tsigaridis, K**, **Weber, J.** 2021. Climate-driven chemistry and aerosol feedbacks in CMIP6 Earth system models. *Atmospheric Chemistry and Physics* **21**: 1105–1126. DOI: https://doi.org/10.5194/acp-21-1105-2021.

Thume, K, **Gebser, B**, **Chen, L**, **Meyer, N**, **Kieber, DJ**, **Pohnert, G.** 2018. The metabolite dimethylsulfoxonium propionate extends the marine organosulfur cycle. *Nature* **563**: 412–415. DOI: https://doi.org/10.1038/s41586-018-0675-0.

Tilgner, A, **Schaefer, T**, **Alexander, B**, **Barth, M**, **Collett, JLJr**, **Fahey, KM**, **Nenes, A**, **Pye, HOT**, **Herrmann, H**, **McNeill, VF.** 2021. Acidity and the multiphase chemistry of atmospheric aqueous particles and clouds. *Atmospheric Chemistry and Physics* **21**: 13483–13536. DOI: https://doi.org/10.5194/acp-21-13483-2021.

Tison, J-L, **Brabant, F**, **Dumont, I**, **Stefels, J.** 2010. High-resolution dimethyl sulfide and dimethylsulfoniopropionate time series profiles in decaying summer first-year sea ice at Ice Station Polarstern, western Weddell Sea, Antarctica. *Journal of Geophysical Research: Biogeosciences* **115**. DOI: https://doi.org/10.1029/2010JG001427.

Toole, DA, **Siegel, DA.** 2004. Light-driven cycling of dimethylsulfide (DMS) in the Sargasso Sea: Closing the loop. *Geophysical Research Letters* **31**. DOI: https://doi.org/10.1029/2004GL019581.

Toyota, K, **McConnell, JC**, **Lupu, A**, **Neary, L**, **McLinden, CA**, **Richter, A**, **Kwok, R**, **Semeniuk, K**, **Kaminski, JW**, **Gong, S-L**, **Jarosz, J**, **Chipperfield, MP**, **Sioris, CE.** 2011. Analysis of reactive bromine production and ozone depletion in the Arctic boundary layer using 3-D simulations with GEM-AQ: Inference from synoptic-scale patterns. *Atmospheric Chemistry and Physics* **11**: 3949–3979. DOI: https://doi.org/10.5194/acp-11-3949-2011.

Tremblay, S, **Picard, J-C**, **Bachelder, JO**, **Lutsch, E**, **Strong, K**, **Fogal, P**, **Leaitch, WR**, **Sharma, S**, **Kolonjari, F**, **Cox, CJ**, **Chang, RY-W**, **Hayes, PL.** 2019. Characterization of aerosol growth events over Ellesmere Island during the summers of 2015 and 2016. *Atmospheric Chemistry and Physics* **19**: 5589–5604. DOI: https://doi.org/10.5194/acp-19-5589-2019.

Trevena, AJ, **Jones, GB.** 2006. Dimethylsulphide and dimethylsulphoniopropionate in Antarctic sea ice and their release during sea ice melting. *Marine Chemistry* **98**: 210–222. DOI: https://doi.org/10.1016/j.marchem.2005.09.005.

Tuckermann, M, **Ackermann, R**, **Gölz, C**, **Lorenzen-Schmidt, H**, **Senne, T**, **Stutz, J**, **Trost, B**, **Unold, W**, **Platt, U.** 1997. DOAS-observation of halogen radical-catalysed arctic boundary layer ozone destruction during the ARCTOC campaigns 1995 and 1996 in Ny-Ålesund, Spitsbergen. *Tellus B: Chemical and Physical Meteorology* **49**. DOI: https://doi.org/10.3402/tellusb.v49i5.16005.

Turner, J, **Bracegirdle, TJ**, **Phillips, T**, **Marshall, GJ**, **Hosking, JS.** 2013. An initial assessment of Antarctic sea ice extent in the CMIP5 Models. *Journal of Climate* **26**: 1473–1484. DOI: https://doi.org/10.1175/JCLI-D-12-00068.1.

Turnipseed, AA, **Barone, SB**, **Ravishankara, AR.** 1996. Reaction of OH with dimethyl sulfide. 2. Products and mechanisms. *The Journal of Physical Chemistry* **100**: 14703–14713. DOI: https://doi.org/10.1021/jp960867c.

Tyndall, GS, **Ravishankara, AR.** 1991. Atmospheric oxidation of reduced sulfur species. *International Journal of Chemical Kinetics* **23**: 483–527. DOI: https://doi.org/10.1002/kin.550230604.

Uhlig, C, **Damm, E**, **Peeken, I**, **Krumpen, T**, **Rabe, B**, **Korhonen, M**, **Ludwichowski, K-U.** 2019. Sea ice and water mass influence dimethylsulfide concentrations in the central Arctic Ocean. *Frontiers in Earth Science* **7**. DOI: https://doi.org/10.3389/feart.2019.00179.

van Leeuwe, MA, **Fenton, M**, **Davey, E**, **Rintala, J-M**, **Jones, EM**, **Meredith, MP**, **Stefels, J.** 2022. On the phenology and seeding potential of sea-ice microalgal species. *Elementa: Science of the Anthropocene* **10**: 00029. DOI: https://doi.org/10.1525/elementa.2021.00029.

van Leeuwe, MA, **Tedesco, L**, **Arrigo, KR**, **Assmy, P**, **Campbell, K**, **Meiners, KM**, **Rintala, J-M**, **Selz, V**, **Thomas, DN**, **Stefels, J.** 2018. Microalgal community structure and primary production in Arctic and Antarctic sea ice: A synthesis. *Elementa: Science of the Anthropocene* **6**: 4. DOI: https://doi.org/10.1525/elementa.267.

Vancoppenolle, M, **Meiners, KM**, **Michel, C**, **Bopp, L**, **Brabant, F**, **Carnat, G**, **Delille, B**, **Lannuzel, D**, **Madec, G**, **Moreau, S**, **Tison, J-L**, **van der Merwe, P.** 2013. Role of sea ice in global biogeochemical cycles: Emerging views and challenges. *Quaternary Science Reviews* **79**: 207–230. DOI: https://doi.org/10.1016/j.quascirev.2013.04.011.

Veres, PR, **Neuman, JA**, **Bertram, TH**, **Assaf, E**, **Wolfe, GM**, **Williamson, CJ**, **Weinzierl, B**, **Tilmes, S**, **Thompson, CR**, **Thames, AB**, **Schroder, JC**, **Saiz-Lopez, A**, **Rollins, AW**, **Roberts, JM**, **Price, D**, **Peischl, J**, **Nault, BA**, **Møller, KH**, **Miller, DO**, **Meinardi, S**, **Li, Q**, **Lamarque, J-F**, **Kupc, A**, **Kjaergaard, HG**, **Kinnison, D**, **Jimenez, JL**, **Jernigan, CM**, **Hornbrook, RS**, **Hills, A**, **Dollner, M**, **Day, DA**, **Cuevas, CA**, **Campuzano-Jost, P**, **Burkholder, J**, **Bui, TP**, **Brune, WH**, **Brown, SS**, **Brock, CA**, **Bourgeois, I**, **Blake, DR**, **Apel, EC**, **Ryerson, TB.** 2020. Global airborne sampling reveals a previously unobserved dimethyl sulfide oxidation mechanism in the marine atmosphere. *Proceedings of the National Academy of Sciences* **117**: 4505–4510. DOI: https://doi.org/10.1073/pnas.1919344117.

Vila-Costa, M, **Simó, R**, **Harada, H**, **Gasol, JM**, **Slezak, D**, **Kiene, RP.** 2006. Dimethylsulfoniopropionate uptake by marine phytoplankton. *Science* **314**: 652–654. DOI: https://doi.org/10.1126/science.1131043.

von Albedyll, L, **Hendricks, S**, **Hutter, N**, **Murashkin, D**, **Kaleschke, L**, **Willmes, S**, **Thielke, L**, **Tian-Kunze, X**, **Spreen, G**, **Haas, C.** 2024. Lead fractions from SAR-derived sea ice divergence during MOSAiC. *The Cryosphere* **18**: 1259–1285. DOI: https://doi.org/10.5194/tc-18-1259-2024.

von Glasow, R, **Crutzen, PJ.** 2004. Model study of multiphase DMS oxidation with a focus on halogens. *Atmospheric Chemistry and Physics* **4**: 589–608. DOI: https://doi.org/10.5194/acp-4-589-2004.

Walters, WW, **Michalski, G**, **Böhlke, JK**, **Alexander, B**, **Savarino, J**, **Thiemens, MH.** 2019. Assessing the seasonal dynamics of nitrate and sulfate aerosols at the South Pole utilizing stable isotopes. *Journal of Geophysical Research: Atmospheres* **124**: 8161–8177. DOI: https://doi.org/10.1029/2019JD030517.

Wang, C, **Yuan, T**, **Wood, SA**, **Goss, K-U**, **Li, J**, **Ying, Q**, **Wania, F.** 2017. Uncertain Henry's law constants compromise equilibrium partitioning calculations of atmospheric oxidation products. *Atmospheric Chemistry and Physics* **17**: 7529–7540. DOI: https://doi.org/10.5194/acp-17-7529-2017.

Wang, S, **Maltrud, ME**, **Burrows, SM**, **Elliott, SM**, **Cameron-Smith, P.** 2018. Impacts of shifts in phytoplankton community on clouds and climate via the sulfur cycle. *Global Biogeochemical Cycles* **32**: 1005–1026. DOI: https://doi.org/10.1029/2017GB005862.

Wang, S, **McNamara, SM**, **Moore, CW**, **Obrist, D**, **Steffen, A**, **Shepson, PB**, **Staebler, RM**, **Raso, ARW**, **Pratt, KA.** 2019a. Direct detection of atmospheric atomic bromine leading to mercury and ozone depletion. *Proceedings of the National Academy of Sciences* **116**: 14479–14484. DOI: https://doi.org/10.1073/pnas.1900613116.

Wang, W-L, **Song, G**, **Primeau, F**, **Saltzman, ES**, **Bell, TG**, **Moore, JK.** 2020. Global ocean dimethyl sulfide climatology estimated from observations and an artificial neural network. *Biogeosciences* **17**: 5335–5354. DOI: https://doi.org/10.5194/bg-17-5335-2020.

Wang, X, **Jacob, DJ**, **Eastham, SD**, **Sulprizio, MP**, **Zhu, L**, **Chen, Q**, **Alexander, B**, **Sherwen, T**, **Evans, MJ**, **Lee, BH**, **Haskins, JD**, **Lopez-Hilfiker, FD**, **Thornton, JA**, **Huey, GL**, **Liao, H.** 2019b. The role of chlorine in global tropospheric chemistry. *Atmospheric Chemistry and Physics* **19**: 3981–4003. DOI: https://doi.org/10.5194/acp-19-3981-2019.

Wanninkhof, R. 2014. Relationship between wind speed and gas exchange over the ocean revisited. *Limnology and Oceanography: Methods* **12**: 351–362. DOI: https://doi.org/10.4319/lom.2014.12.351.

Watanabe, E, **Jin, M**, **Hayashida, H**, **Zhang, J**, **Steiner, N.** 2019. Multi-model intercomparison of the Pan-Arctic ice-algal productivity on seasonal, interannual, and decadal timescales. *Journal of Geophysical Research: Oceans* **124**: 9053–9084. DOI: https://doi.org/10.1029/2019JC015100.

Watts, J, **Bell, TG**, **Anderson, K**, **Butterworth, BJ**, **Miller, S**, **Else, B**, **Shutler, J.** 2022. Impact of sea ice on air-sea CO_2 exchange—A critical review of polar eddy covariance studies. *Progress in Oceanography* **201**: 102741. DOI: https://doi.org/10.1016/j.pocean.2022.102741.

Watts, SF, **Brimblecombe, P.** 1987. The Henry's law constant of dimethyl sulphoxide. *Environmental Technology Letters* **8**: 483–486. DOI: https://doi.org/10.1080/09593338709384509.

Webb, AL, **van Leeuwe, MA**, **den Os, D**, **Meredith, MP**, **Venables, HJ**, **Stefels, J.** 2019. Extreme spikes in DMS flux double estimates of biogenic sulfur export from the Antarctic coastal zone to the atmosphere. *Scientific Reports* **9**: 2233. DOI: https://doi.org/10.1038/s41598-019-38714-4.

Weller, R, **Minikin, A**, **Wagenbach, D**, **Dreiling, V.** 2011a. Characterization of the inter-annual, seasonal, and diurnal variations of condensation particle concentrations at Neumayer, Antarctica. *Atmospheric Chemistry and Physics* **11**: 13243–13257. DOI: https://doi.org/10.5194/acp-11-13243-2011.

Weller, R, **Wagenbach, D**, **Legrand, M**, **Elsässer, C**, **Tian-Kunze, X**, **König-Langlo, G.** 2011b. Continuous 25-yr aerosol records at coastal Antarctica—I: Inter-annual variability of ionic compounds and links to climate indices. *Tellus B: Chemical and*

Physical Meteorology **63**: 901–919. DOI: https://doi.org/10.1111/j.1600-0889.2011.00542.x.

Wentworth, GR, **Murphy, JG**, **Croft, B**, **Martin, RV**, **Pierce, JR**, **Côté, J-S**, **Courchesne, I**, **Tremblay, J-É**, **Gagnon, J**, **Thomas, JL**, **Sharma, S**, **Toom-Sauntry, D**, **Chivulescu, A**, **Levasseur, M**, **Abbatt, JPD.** 2016. Ammonia in the summertime Arctic marine boundary layer: sources, sinks, and implications. *Atmospheric Chemistry and Physics* **16**: 1937–1953. DOI: https://doi.org/10.5194/acp-16-1937-2016.

Wex, H, **Eckermann, O**, **Jurányi, Z**, **Weller, R**, **Mangold, A**, **Van Overmeiren, P**, **Zeppenfeld, S**, **van Pinxteren, M**, **Dall'Osto, M**, **Henning, S.** 2025. Antarctica's unique atmosphere: Really low INP concentrations. *Geophysical Research Letters* **52**: e2024GL112583. DOI: https://doi.org/10.1029/2024GL112583.

Whaley, CH, **Law, KS**, **Hjorth, JL**, **Skov, H**, **Arnold, SR**, **Langner, J**, **Pernov, JB**, **Bergeron, G**, **Bourgeois, I**, **Christensen, JH**, **Chien, R-Y**, **Deushi, M**, **Dong, X**, **Effertz, P**, **Faluvegi, G**, **Flanner, M**, **Fu, JS**, **Gauss, M**, **Huey, G**, **Im, U**, **Kivi, R**, **Marelle, L**, **Onishi, T**, **Oshima, N**, **Petropavlovskikh, I**, **Peischl, J**, **Plummer, DA**, **Pozzoli, L**, **Raut, J-C**, **Ryerson, T**, **Skeie, R**, **Solberg, S**, **Thomas, MA**, **Thompson, C**, **Tsigaridis, K**, **Tsyro, S**, **Turnock, ST**, **von Salzen, K**, **Tarasick, DW.** 2023. Arctic tropospheric ozone: Assessment of current knowledge and model performance. *Atmospheric Chemistry and Physics* **23**: 637–661. DOI: https://doi.org/10.5194/acp-23-637-2023.

Williams, MB, **Campuzano-Jost, P**, **Bauer, D**, **Hynes, AJ.** 2001. Kinetic and mechanistic studies of the OH-initiated oxidation of dimethylsulfide at low temperature—A reevaluation of the rate coefficient and branching ratio. *Chemical Physics Letters* **344**: 61–67. DOI: https://doi.org/10.1016/S0009-2614(01)00764-3.

Williams, MB, **Campuzano-Jost, P**, **Cossairt, BM**, **Hynes, AJ**, **Pounds, AJ.** 2007. Experimental and theoretical studies of the reaction of the OH radical with alkyl sulfides: 1. Direct observations of the formation of the OH−DMS adduct−pressure dependence of the forward rate of addition and development of a predictive expression at low temperature. *The Journal of Physical Chemistry A* **111**: 89–104. DOI: https://doi.org/10.1021/jp063873+.

Williams, MB, **Campuzano-Jost, P**, **Hynes, AJ**, **Pounds, AJ.** 2009. Experimental and theoretical studies of the reaction of the OH radical with alkyl sulfides: 3. Kinetics and mechanism of the OH initiated oxidation of dimethyl, dipropyl, and dibutyl sulfides: Reactivity trends in the alkyl sulfides and development of a predictive expression for the reaction of OH with DMS. *The Journal of Physical Chemistry A* **113**: 6697–6709. DOI: https://doi.org/10.1021/jp9010668.

Williamson, CJ, **Kupc, A**, **Axisa, D**, **Bilsback, KR**, **Bui, T**, **Campuzano-Jost, P**, **Dollner, M**, **Froyd, KD**, **Hodshire, AL**, **Jimenez, JL**, **Kodros, JK**, **Luo, G**, **Murphy, DM**, **Nault, BA**, **Ray, EA**, **Weinzierl, B**, **Wilson, JC**, **Yu, F**, **Yu, P**, **Pierce, JR**, **Brock, CA.** 2019. A large source of cloud condensation nuclei from new particle formation in the tropics. *Nature* **574**: 399–403. DOI: https://doi.org/10.1038/s41586-019-1638-9.

Willis, MD, **Burkart, J**, **Thomas, JL**, **Köllner, F**, **Schneider, J**, **Bozem, H**, **Hoor, PM**, **Aliabadi, AA**, **Schulz, H**, **Herber, AB**, **Leaitch, WR**, **Abbatt, JPD.** 2016. Growth of nucleation mode particles in the summertime Arctic: A case study. *Atmospheric Chemistry and Physics* **16**: 7663–7679. DOI: https://doi.org/10.5194/acp-16-7663-2016.

Willis, MD, **Köllner, F**, **Burkart, J**, **Bozem, H**, **Thomas, JL**, **Schneider, J**, **Aliabadi, AA**, **Hoor, PM**, **Schulz, H**, **Herber, AB**, **Leaitch, WR**, **Abbatt, JPD.** 2017. Evidence for marine biogenic influence on summertime Arctic aerosol. *Geophysical Research Letters* **44**: 6460–6470. DOI: https://doi.org/10.1002/2017GL073359.

Willis, MD, **Lannuzel, D**, **Else, B**, **Angot, H**, **Campbell, K**, **Crabeck, O**, **Delille, B**, **Hayashida, H**, **Lizotte, M**, **Loose, B**, **Meiners, KM**, **Miller, L**, **Moreau, S**, **Nomura, D**, **Prytherch, J**, **Schmale, J**, **Steiner, N**, **Tedesco, L**, **Thomas, J.** 2023. Polar oceans and sea ice in a changing climate. *Elementa: Science of the Anthropocene* **11**: 00056. DOI: https://doi.org/10.1525/elementa.2023.00056.

Willis, MD, **Leaitch, WR**, **Abbatt, JPD.** 2018. Processes controlling the composition and abundance of Arctic aerosol. *Reviews of Geophysics* **56**: 621–671. DOI: https://doi.org/10.1029/2018RG000602.

Willmes, S, **Heinemann, G**, **Schnaase, F.** 2023. Patterns of wintertime Arctic sea-ice leads and their relation to winds and ocean currents. *The Cryosphere* **17**: 3291–3308. DOI: https://doi.org/10.5194/tc-17-3291-2023.

Wilson, KR, **Prophet, AM.** 2024. Chemical kinetics in microdroplets. *Annual Review of Physical Chemistry* **75**: 185–208. DOI: https://doi.org/10.1146/annurev-physchem-052623-120718.

Wohl, C, **Villamayor, J**, **Galí, M**, **Mahajan, AS**, **Fernández, RP**, **Cuevas, CA**, **Bossolasco, A**, **Li, Q**, **Kettle, AJ**, **Williams, T**, **Sarda-Esteve, R**, **Gros, V**, **Simó, R**, **Saiz-Lopez, A.** 2024. Marine emissions of methanethiol increase aerosol cooling in the Southern Ocean. *Science Advances* **10**: eadq2465. DOI: https://doi.org/10.1126/sciadv.adq2465.

Wolfe, GM, **Nicely, JM**, **St. Clair, JM**, **Hanisco, TF**, **Liao, J**, **Oman, LD**, **Brune, WB**, **Miller, D**, **Thames, A**, **González Abad, G**, **Ryerson, TB**, **Thompson, CR**, **Peischl, J**, **McKain, K**, **Sweeney, C**, **Wennberg, PO**, **Kim, M**, **Crounse, JD**, **Hall, SR**, **Ullmann, K**, **Diskin, G**, **Bui, P**, **Chang, C**, **Dean-Day, J.** 2019. Mapping hydroxyl variability throughout the global remote troposphere via synthesis of airborne and satellite formaldehyde observations. *Proceedings of the National Academy of Sciences* **116**: 11171–11180. DOI: https://doi.org/10.1073/pnas.1821661116.

Wollesen de Jonge, R, **Elm, J**, **Rosati, B**, **Christiansen, S**, **Hyttinen, N**, **Lüdemann, D**, **Bilde, M**, **Roldin, P.** 2021. Secondary aerosol formation from dimethyl

sulfide—Improved mechanistic understanding based on smog chamber experiments and modelling. *Atmospheric Chemistry and Physics* **21**: 9955–9976. DOI: https://doi.org/10.5194/acp-21-9955-2021.

Woodhouse, MT, **Carslaw, KS**, **Mann, GW**, **Vallina, SM**, **Vogt, M**, **Halloran, PR**, **Boucher, O.** 2010. Low sensitivity of cloud condensation nuclei to changes in the sea-air flux of dimethyl-sulphide. *Atmospheric Chemistry and Physics* **10**: 7545–7559. DOI: https://doi.org/10.5194/acp-10-7545-2010.

Woodhouse, MT, **Mann, GW**, **Carslaw, KS**, **Boucher, O.** 2013. Sensitivity of cloud condensation nuclei to regional changes in dimethyl-sulphide emissions. *Atmospheric Chemistry and Physics* **13**: 2723–2733. DOI: https://doi.org/10.5194/acp-13-2723-2013.

World Meteorological Organization (WMO). 2025. State of the Global Climate 2024. Available at https://library.wmo.int/idurl/4/69455. Accessed January 14, 2026.

Wu, R, **Wang, S**, **Wang, L.** 2015. New mechanism for the atmospheric oxidation of dimethyl sulfide. The importance of intramolecular hydrogen shift in a CH_3SCH_2OO radical. *The Journal of Physical Chemistry A* **119**: 112–117. DOI: https://doi.org/10.1021/jp511616j.

Xu, W, **Ovadnevaite, J**, **Fossum, KN**, **Lin, C**, **Huang, R-J**, **Ceburnis, D**, **O'Dowd, C.** 2022. Sea spray as an obscured source for marine cloud nuclei. *Nature Geoscience* **15**: 282–286. DOI: https://doi.org/10.1038/s41561-022-00917-2.

Yamagami, Y, **Watanabe, M**, **Mori, M**, **Ono, J.** 2022. Barents-Kara sea-ice decline attributed to surface warming in the Gulf Stream. *Nature Communications* **13**: 3767. DOI: https://doi.org/10.1038/s41467-022-31117-6.

Yang, CA, **Diao, M**, **Shi, Y**, **Liu, X.** 2025. Hemispheric asymmetry of phase partition in mixed-phase clouds based on near global-scale airborne observations. *Geophysical Research Letters* **52**: e2025GL115946. DOI: https://doi.org/10.1029/2025GL115946.

Yang, M, **Blomquist, BW**, **Huebert, BJ.** 2009. Constraining the concentration of the hydroxyl radical in a stratocumulus-topped marine boundary layer from sea-to-air eddy covariance flux measurements of dimethylsulfide. *Atmospheric Chemistry and Physics* **9**: 9225–9236. DOI: https://doi.org/10.5194/acp-9-9225-2009.

Yang, X, **Frey, MM**, **Rhodes, RH**, **Norris, SJ**, **Brooks, IM**, **Anderson, PS**, **Nishimura, K**, **Jones, AE**, **Wolff, EW.** 2019. Sea salt aerosol production via sublimating wind-blown saline snow particles over sea ice: Parameterizations and relevant microphysical mechanisms. *Atmospheric Chemistry and Physics* **19**: 8407–8424. DOI: https://doi.org/10.5194/acp-19-8407-2019.

Ye, Q, **Goss, MB**, **Isaacman-VanWertz, G**, **Zaytsev, A**, **Massoli, P**, **Lim, C**, **Croteau, P**, **Canagaratna, M**, **Knopf, DA**, **Keutsch, FN**, **Heald, CL**, **Kroll, JH.** 2021. Organic sulfur products and peroxy radical isomerization in the OH oxidation of dimethyl sulfide. *ACS Earth and Space Chemistry* **5**: 2013–2020. DOI: https://doi.org/10.1021/acsearthspacechem.1c00108.

Ye, Q, **Goss, MB**, **Krechmer, JE**, **Majluf, F**, **Zaytsev, A**, **Li, Y**, **Roscioli, JR**, **Canagaratna, M**, **Keutsch, FN**, **Heald, CL**, **Kroll, JH.** 2022. Product distribution, kinetics, and aerosol formation from the OH oxidation of dimethyl sulfide under different RO_2 regimes. *Atmospheric Chemistry and Physics* **22**: 16003–16015. DOI: https://doi.org/10.5194/acp-22-16003-2022.

Yeager, SG, **Karspeck, AR**, **Danabasoglu, G.** 2015. Predicted slowdown in the rate of Atlantic sea ice loss. *Geophysical Research Letters* **42**: 10,704–10,713. DOI: https://doi.org/10.1002/2015GL065364.

Zavarsky, A, **Goddijn-Murphy, L**, **Steinhoff, T**, **Marandino, CA.** 2018. Bubble-mediated gas transfer and gas transfer suppression of DMS and CO_2. *Journal of Geophysical Research: Atmospheres* **123**: 6624–6647. DOI: https://doi.org/10.1029/2017JD028071.

Zemmelink, HJ, **Dacey, JWH**, **Houghton, L**, **Hintsa, EJ**, **Liss, PS.** 2008a. Dimethylsulfide emissions over the multi-year ice of the western Weddell Sea. *Geophysical Research Letters* **35**. DOI: https://doi.org/10.1029/2007GL031847.

Zemmelink, HJ, **Houghton, L**, **Dacey, JWH**, **Stefels, J**, **Koch, BP**, **Schröder, M**, **Wisotzki, A**, **Scheltz, A**, **Thomas, DN**, **Papadimitriou, S**, **Kennedy, H**, **Kuosa, H**, **Dittmar, T.** 2008b. Stratification and the distribution of phytoplankton, nutrients, inorganic carbon, and sulfur in the surface waters of Weddell Sea leads. *Deep Sea Research Part II: Topical Studies in Oceanography* **55**: 988–999. DOI: https://doi.org/10.1016/j.dsr2.2007.12.011.

Zemmelink, HJ, **Houghton, L**, **Dacey, JWH**, **Worby, AP**, **Liss, PS.** 2005. Emission of dimethylsulfide from Weddell Sea leads. *Geophysical Research Letters* **32**. DOI: https://doi.org/10.1029/2005GL024242.

Zhao, J, **Ma, W**, **Bilsback, KR**, **Pierce, JR**, **Zhou, S**, **Chen, Y**, **Yang, G**, **Zhang, Y.** 2022. Simulating the radiative forcing of oceanic dimethylsulfide (DMS) in Asia based on machine learning estimates. *Atmospheric Chemistry and Physics* **22**: 9583–9600. DOI: https://doi.org/10.5194/acp-22-9583-2022.

Zheng, G, **Su, H**, **Cheng, Y.** 2023. Role of carbon dioxide, ammonia, and organic acids in buffering atmospheric acidity: The distinct contribution in clouds and aerosols. *Environmental Science & Technology* **57**: 12571–12582. DOI: https://doi.org/10.1021/acs.est.2c09851.

Zhou, L, **Booge, D**, **Zhang, M**, **Marandino, CA.** 2022. Winter season Southern Ocean distributions of climate-relevant trace gases. *Biogeosciences* **19**: 5021–5040. DOI: https://doi.org/10.5194/bg-19-5021-2022.

Zhu, L, **Nicovich, JM**, **Wine, PH.** 2003. Temperature-dependent kinetics studies of aqueous phase reactions of SO_4^- radicals with dimethylsulfoxide, dimethylsulfone, and methanesulfonate. *Journal of Photochemistry and Photobiology A: Chemistry* **157**: 311–319. DOI: https://doi.org/10.1016/S1010-6030(03)00064-9.

How to cite this article: Ishino, S, Willis, MD, Angot, H, Bartels-Rausch, T, Crabeck, O, Delille, B, Dunne, E, Franklin, E, Haddon, A, Hayashida, H, Joge, SD, Lapere, R, Lim, H-G, Mahajan, AS, Mallet, MD, Manville, G, Marelle, L, Nomura, D, Pratt, KA, Peeken, I, Price, R, Simó, R, Stefels, J, Thomas, JL, Zang, CL, Steiner, N. 2026. The biogenic sulfur cycle in the coupled ocean-sea ice-atmosphere system. *Elementa: Science of the Anthropocene* 14(1). DOI: https://doi.org/10.1525/elementa.2025.00067

Domain Editor-in-Chief: Detlev Helmig, Boulder AIR LLC, Boulder, CO, USA

Associate Editor: Byron W. Blomquist, Research Scientist III, Cooperative Institute for Research in Environmental Sciences, University of Colorado, Boulder, CO, USA

Knowledge Domain: Atmospheric Science

Part of an Elementa Special Feature: Coupling of Ocean-Ice-Atmosphere Processes: From Sea-Ice Biogeochemistry to Aerosols and Clouds (CIce2Clouds)

Published: February 16, 2026 **Accepted:** November 6, 2025 **Submitted:** June 6, 2025

ELEMENTA Science of the Anthropocene

Elem Sci Anth is a peer-reviewed open access journal published by University of California Press.

OPEN ACCESS